1. Blasting covering experience from projects

Lisbon Conference Proceedings 2011, R. Holmberg et al

Vibrations and concrete behaviour

T. Lewandowski
Enviro Strata Consulting Pty Ltd, NSW, Australia

K. Nguyen
Muswellbrook Coal, NSW, Australia

S. Wylie & T. Campbell
Xstrata Coal (NSW) Pty Ltd, NSW, Australia

ABSTRACT: The paper is designed to assess issues related to concrete breakage during ground vibration exposure from blasting. A systematic approach was undertaken by exposing various concrete structures to variable levels of vibrations. The impact of vibrations was assessed using a number of techniques ranging from vibration to displacement and other methods.

The study revealed that a number of factors need to be considered before the commencement of blasting and high ground vibration exposure. Besides the strength of the concrete structure, other factors to consider include:

- the rock strata conditions,
- the depth of foundations,
- the age and state of the structure,
- the elevation of the structure above ground level,
- the possible/combined effect of other factors and vibration impacts.

A practical example (breakage of a concrete water tank) of the combined effect of vibration and other forces is presented below with special emphasis on a holistic approach rather than on vibration assessment only.

1. INTRODUCTION

The article presented below includes an assessment of blast impacts on concrete structures, namely concrete water tanks. Based on open cut mining industry experience, the probability of damage to concrete structures from blast impacts is typically assessed purely from a vibration point of view. However, this is a rather simplistic approach and quite often will not provide a full picture in regards to potential structural damage.

Generally, the assessing engineer relies on an assumption that the concrete elements comprising the structure are of uniform strength and composition, which very often is not entirely true. It should be understood that any given structure is usually full of defects / deficiencies, or has deteriorated with time due to environmental factors such as wind, water or others. Rather than assuming structural and material uniformity therefore, a more appropriate approach would be to undertake a detailed assessment process. This should provide a more objective

assessment of the state of the structure which will then assist in better recognition of any potential future issues related to high vibration levels.

It is imperative that any high vibration study should cover the following points:

- assessment on the general state of the structure/structure conditions
- assessment of the strength of the material and/or variation in strength
- identification of major/minor faults, which could play a role in the structure's response when exposed to high vibration levels
- assessment of underlying geology/structural foundations

The postulated approach will rely on collecting any piece of information prior to blasting. The collected data will form the basis of a more scientific approach to properly addressing the blast impacts.

The paper presented below provides a number of case studies undertaken in 2008/2009 at Muswellbrook Coal (Australia). The studies were instigated due to close range blasting to various infrastructure including concrete water tanks. Two redundant water tanks were designated to the study to investigate effect of blasting including tank rupture.

In summary, the proposed methodology relies on a holistic approach of complete assessment, not only the strength of the structure itself but a collection of other relevant data. This in turn will provide a basis for more accurate assessment of structural response to vibrations.

2. CONCRETE DAMAGE – INDICATIVE LEVELS

When considering house structures it is important to understand that there is a possibility of low level cracking (i.e. cosmetic cracking), which potentially can occur at lower levels of vibrations. The indicative levels of the first occurrence of cosmetic cracking (i.e. based on the USBM research) are highly dependent upon generated frequencies. The indicative vibration levels of hairline cracking are 15 mm/s at 4 Hz increasing to 20 mm/s at 15 Hz and 50 mm/s at 40Hz. It should be noted that these numbers apply to relatively weak structures such as residential buildings.

It should also be understood that for stronger types of structures including concrete, steel and reinforced concrete, these vibration limits do not apply. For these structures, higher levels of vibrations are applicable. In Australia the indicative and postulated limit in the ACARP report (no. C14057) is 100 mm/s. The limit also follows the Australian Standard AS 2187.2-2006, where 100 mm/s is recommended as a safe level to prevent damage. Also, the authors of the ACARP study postulate that higher levels may be allowed depending on the results of a more detailed investigation of PPV (ground vibrations) combined with frequency analysis and direct strain measurements.

Considering the high demand for coal in the world, it is quite common for open cut operators to undertake relatively large-scale blasting operations near concrete/steel industrial structures such as coal silos, water towers, head-frame towers and tall smoke stacks. Based on industry experience, generally it could be said that for structures of heavy steel construction with strong foundations, ground vibrations are generally of no concern. Although, it should be said that concrete or masonry structures are more susceptible to blast induced damage. The important factors to consider include the shape of the structure, response (to the ground motion), frequency and duration of the ground motion, and the natural frequency and damping of the structure or its contents.

In general it can be said that for a tall, large industrial structure:

- in the case of low frequency ground motions, there is an expectation of an amplified response (4-8 times that of the ground),
- in the case of high frequency ground motions, there is an expectation of no amplified response.

Prior to providing some explanatory notes in regards to infrastructure damage, it should be understood that generally there are two possible mechanisms for inducing damage to infrastructure from blasting / vibration impacts. Usually, concrete elements such as foundations are in direct contact with rock strata or soil. For such a structure, the damage can be induced in two possible ways, i.e.

- via densification of soils or similar phenomena, or
- via delivering substantial energy exceeding the strength of the material.

The most obvious includes phenomena caused by soil densification or liquefaction, which directly impact on the concrete foundation of a given structure. As a result, a major shift in stresses can potentially result in concrete material failure. The other

possible mechanism can be related to damage of the rock strata which forms a base for any infrastructure placed on it. In essence, when sufficient energy is delivered to rock strata (i.e. a level exceeding rock strata strength) then rock strata damage occurs. This can be manifested in physical displacement and/or movement of the rock strata. As a consequence, this could impact on the infrastructure foundations and subsequently induce cracks and/or minor/major damage to the infrastructure itself. Obviously this will apply to weak strata layers, possibly also affected by water action or other external factors.

The second possible damage mechanism is a direct mechanism and is related to the excessive strain delivered during the blasting process to the infrastructure. This mechanism is mainly driven by generated displacement, which is a function of vibration levels and generated frequencies.

It is important to understand that the damage to a concrete structure or concrete elements can occur only when substantial vibration levels are generated. This is due to the fact that the strength of concrete is substantially higher than, for example, plasterboard or similar construction materials.

Considering earthquake exposure, Siskind (2005) for example, indicates that cracks in underlying concrete would not be expected to occur unless extensive damage to the structure itself was also to occur. Also, based on Siskind, some indicative vibration levels for damage to occur for some cracks in ordinary non-reinforced masonry concrete irrigation ditches need to be in the order of 3.6 in/s (i.e. equivalent to 91.4 mm/s), which is equivalent to Intensity VII on the Mercalli scale. Also, below ground damage, for example, for underground water pipes is listed for Intensity IX, which is in the order of 7.2 in/s, which is equivalent to 182.9 mm/s.

Obviously one should understand that there are certain frequency differences between earthquake induced vibration and that generated by blasting so it is highly likely that the above mentioned levels do not exactly apply.

Considering blast vibration exposure one of the most comprehensive overviews of issues related to concrete cracking / breakage was compiled by Oriard (1998, 2002) and included a review of various projects related to concrete crack formation, chipping and concrete damage.

Oriard (2002) provides a number of case studies related to the assessment of the impact of vibrations on a variety of infrastructure constructed of concrete, steel and bricks. Based on the compiled data, one can conclude that various concrete structures (i.e. in good overall condition) can be exposed to relatively high vibration levels before any onset of damage.

Some indicative vibration levels following Oriard's tests on a Mississippi river construction works (navigational lock wall) indicated the following:

- 100 in/s (i.e. 254 mm/s) - spalling of the poorly bonded grout
- 200 in/s (i.e. 508 mm/s) - spalling of the deteriorated surface skin
- 375 in/s (i.e. 9525 mm/s) - cracking in old concrete
- 600 in/s (i.e. 15240 mm/s) - formation of a small crater

It is important to stress that the above quoted observation applied to an old concrete structure.

2.1 Concrete Pads, Driveways and Walkways

As indicated by Siskind (2005), these types of structures are restrained by the ground therefore higher levels of vibrations are required to induce any damage. The indicative, although speculative, number is in the order of > 100 in/s (i.e. > 254 mm/s). Although, the author indicates that there were no instances of cracks observed in any of the mining blast studies of the USBM

2.2 Masonry Foundations

As indicated by Siskind (2005), there were some observations for freestanding walls of crack occurrence at 6 - 11 in/s (i.e. equivalent to 152.4 – 279.4 mm/s). Also, it is indicated that the masonry foundations / concrete block walls considered here are either freestanding or in direct contact with the soil.

Svinkin (2007) provided a comprehensive summary on the current state regarding the assessment of safe ground and structure vibration from blasting including concrete material. The author postulates that the most sensible approach is to utilise existing vibration limit criteria supported by vibration measurements and structural response study. This should also be complemented by observation of results of dynamic effects of blasting.

Overall, there is no doubt that the impact of vibration will have some effect on any considered structure. However, it is stressed that the magnitude of vibration alone is not indicative of the resulting damage level. It is believed that any damage caused during vibration is mostly

driven by generated displacement, which is a function of vibration and generated frequency.

In addition to this, it should be remembered that the state of the structure, age of the structure and material strength all play an important part when considering the allowable vibration limits. This will be discussed in the following sections of this paper.

3. EXAMPLES OF PRACTICAL STRUCTURAL ASSESSMENTS

In any vibration study it is imperative to undertake an initial detailed assessment of any concrete or similar structures prior to their exposure to high vibration levels. Such an assessment if properly undertaken will provide clues in regards to potential future behaviour of any given structure.

Ideally, an assessment should cover a whole range of data gathering including geotechnical, foundation, structural and design issues. Unfortunately, in real life such information is often not readily available or accessible. To overcome this lack of technical details an assessing officer can undertake an alternative, but detailed, structural survey of the structure, which if correctly compiled and analysed will provide potential tell-tale signs in regards to structural integrity of the structure and /or potential ongoing damage issues or minor defects.

The first step in the assessment process applies to a review of any available technical information in regards to structure positioning and / or structural assessment.

The second step applies to observations of any structural defects in the existing structure and drawing appropriate conclusions. Ideally, this should be done prior to high vibration exposure. In the example used here Figure 1 indicates the presence of cracks in the concrete area adjacent to the pool structure.

This type of information is extremely important to any structural engineer as the lack of expansion joints in the concrete itself has the potential to create problems down the track. For comparison purposes, one can undertake a similar photo survey for newly constructed pools and surrounding areas. Basically, modern construction methods will include the presence of a high number of expansion joints for

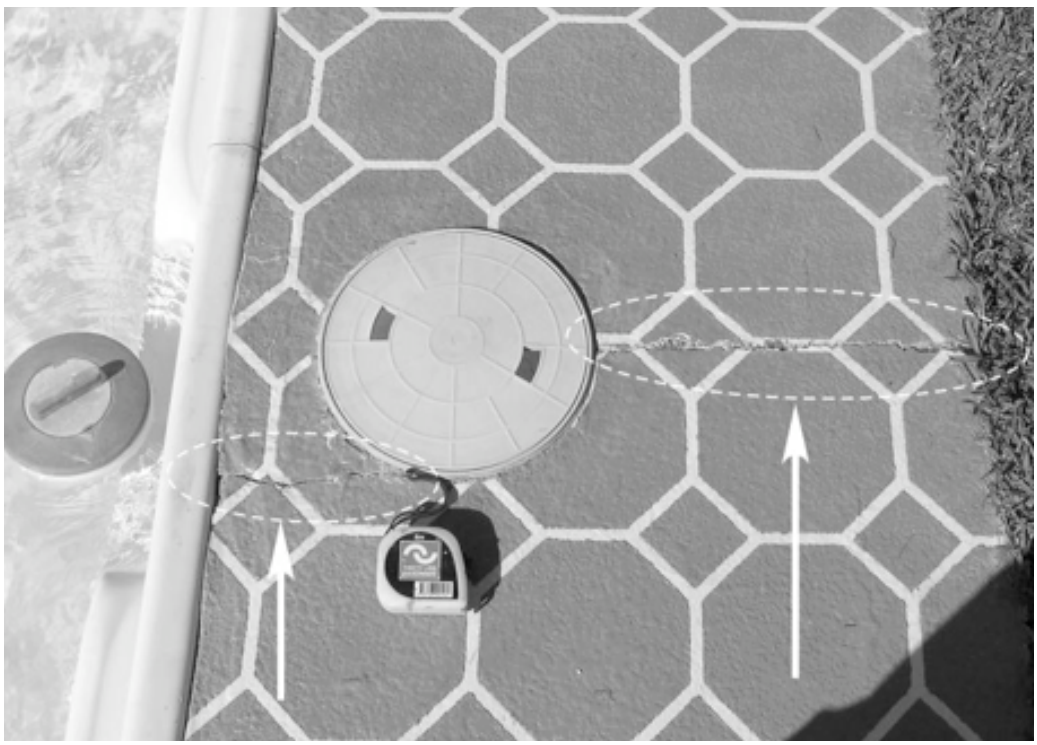

Figure 1. Photo survey showing concrete and pool cracking.

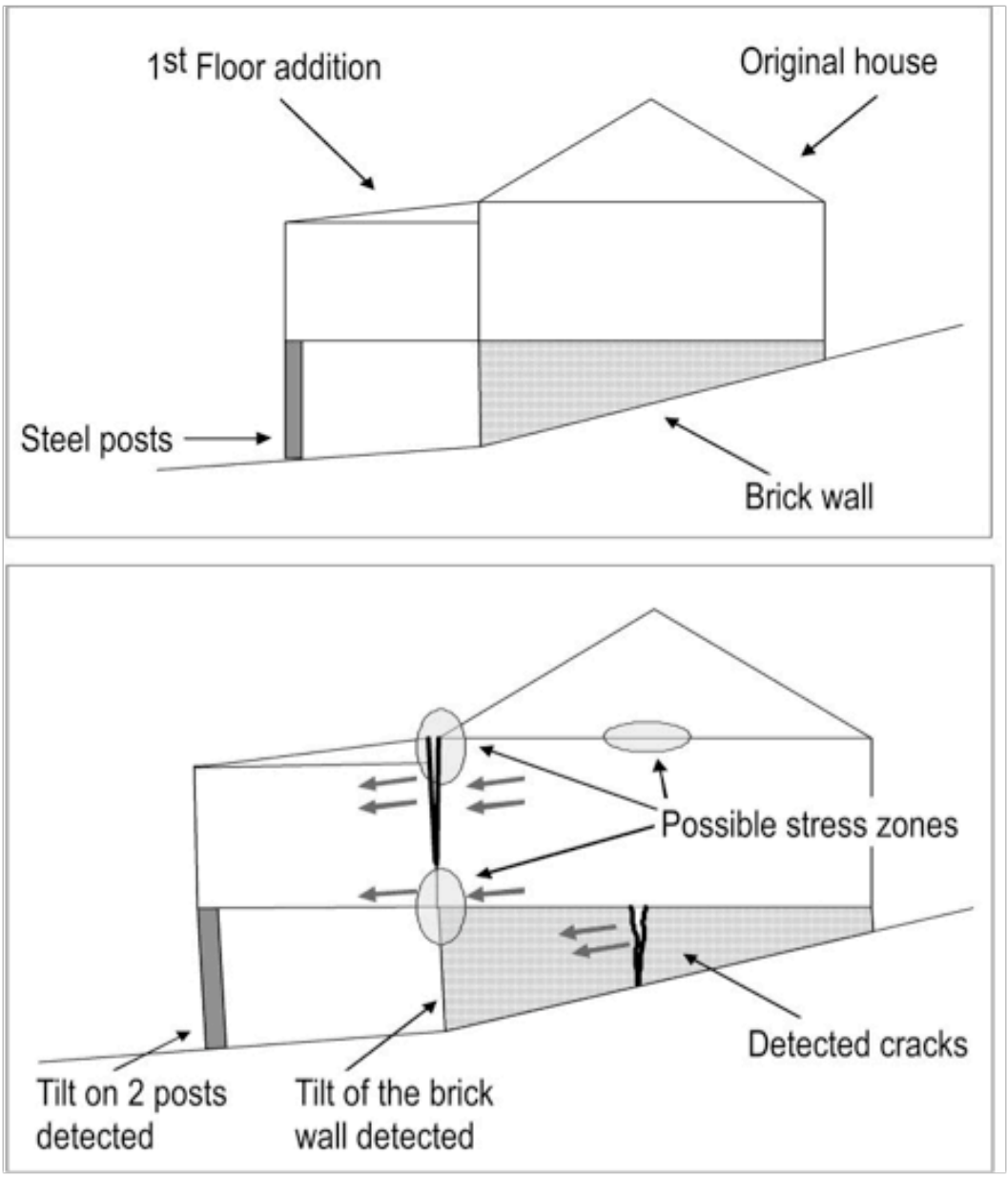

Figure 2. Schematic representation of the house and probable stressed zones.

the concrete areas. This piece of information is critical in discrediting potential future damage claims due to blasting, and will be sufficient in providing a short but adequate explanation to interested parties.

Other sources of information are any geotechnical / geological data sets (if available). Basically, the knowledge of underlying geology, the presence of any rock strata weaknesses and/ or the presence of fill material are usually critical in making assessments and conclusions about possible causes of existing damage to a structure or identifying underlying issues.

Another example presented here reveals a house

structure positioned on a slope. In this particular case it was alleged that damage caused by the separation of the first floor extension occurred due to apparent vibration exposure. It should also be noted that there was no additional information provided in relation to the building design, underlying rock strata or strength of the materials used for construction. The only available tool was a detailed structural damage assessment and scattered information that related to the first floor extension to the building structure. As observed, besides the first floor detachment, there were other tell-tale signs of underlying and ongoing damage problems caused by the inferred issue of the house's positioning on the slope.

The undertaken assessment revealed other major cracking on both sides of the house structure. The assessment revealed the appearance of old cracks. The cracking occurs in the brickwork on both sides of the house, which is shown in Figure 2. Such findings are indications of a significant stability issue. Among many causes of such behaviour the detected cracking could be due to the following factors:

- Slope stability issues
- Insufficient foundations
- Variation in clay component due to different slope exposure, where each part of the structure responds differently (i.e. according to different clay layers) resulting in a highly variable stress regime for the house structure.

The characteristics of the detected cracking are such that these cracks are wider in the top part of the brick work than at the bottom part. Consequently, such a pattern indicates tilting in the top part of the house. The tilting side of the house is adjacent to the 1st floor extension. As a result it is most likely that the pressure of the tilting wall is transferred onto the adjacent extension causing cracking between the house wall and the extension.

It appears that the cracking in the house walls and cracking between the house and the extension are related to each other subsequently producing stresses in the upper section of the house, i.e. on the junction of the new addition and the old house structure. The schematic of the described behaviour is presented in Figure 2. The figure helps to visualise the described findings and possible mechanism behind the reported cracking.

In addition to the detected cracking there are other symptoms of important structural problems. These include:

- Tilting of the bottom brick wall, which is part of the support for the first floor extension
- Tilting on at least two steel posts (the posts supporting the first floor extension)

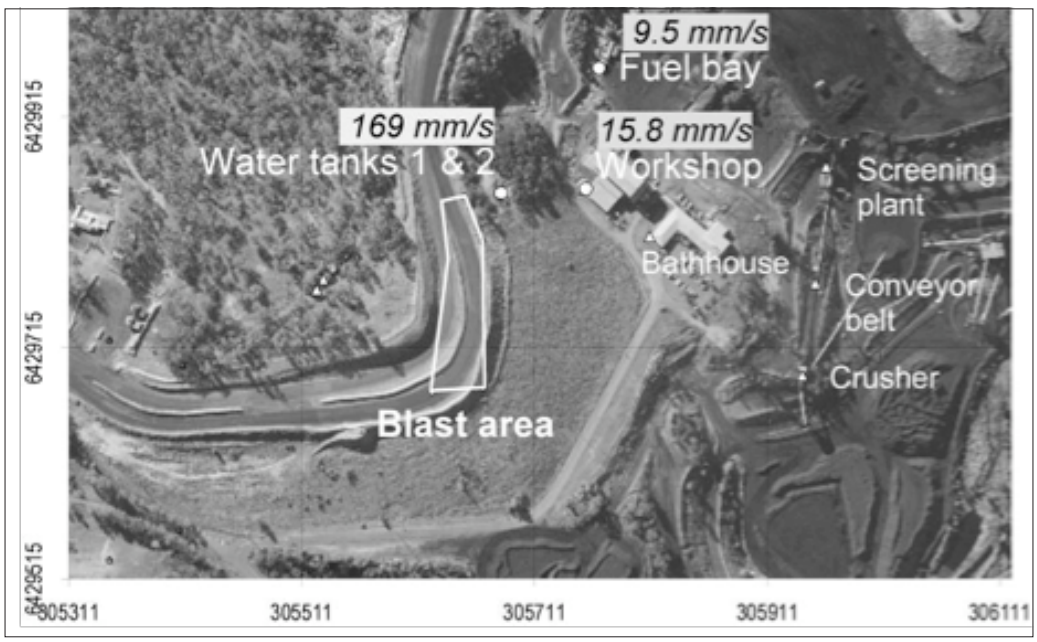

Figure 3. Location of concrete water tanks and blast location.

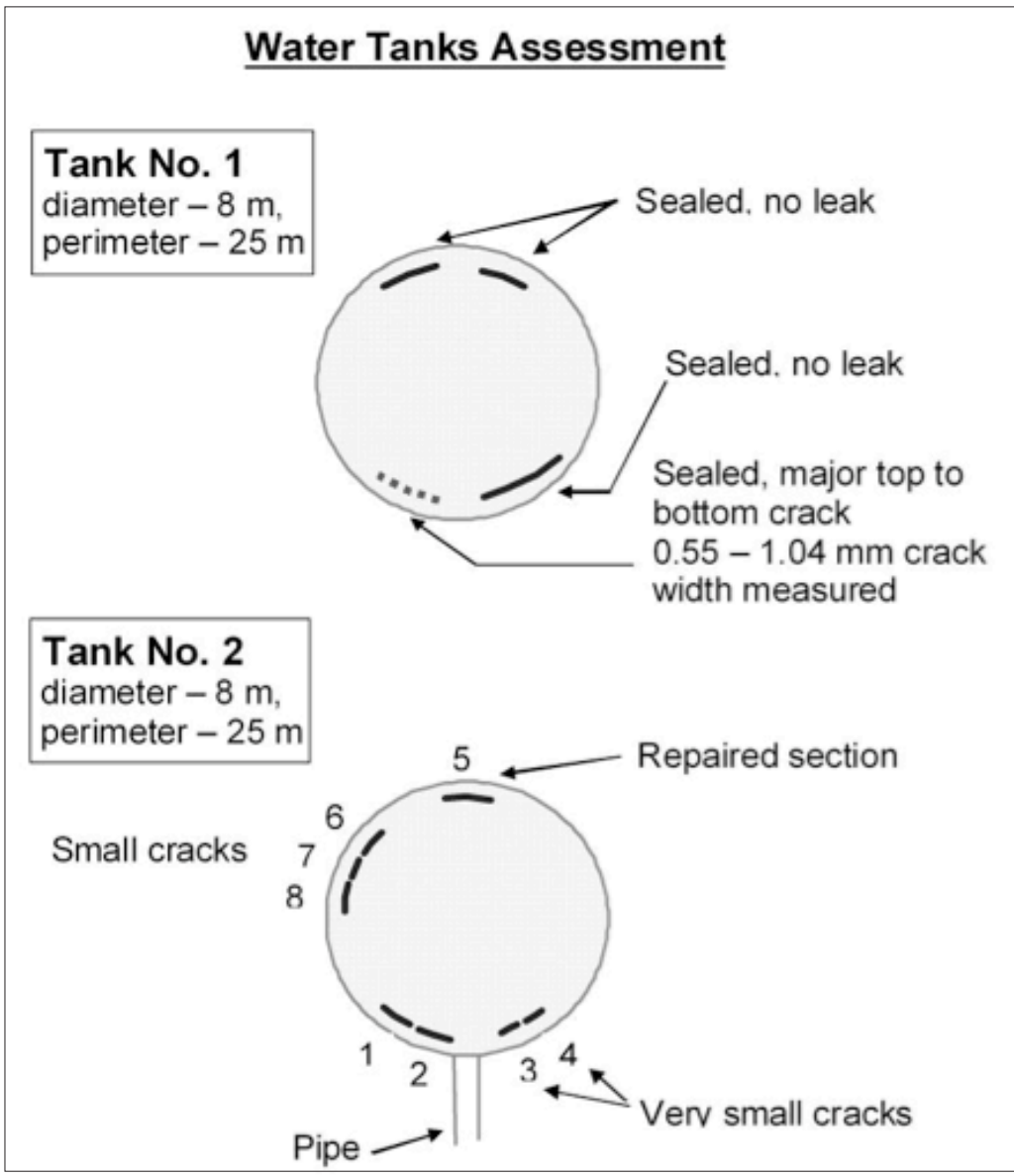

Figure 4. Schematic of crack damage assessment for water tanks no. 1 and 2.

− Concrete cracking around the above mentioned posts

As shown, simple assessment techniques such as spirit level measurement, crack mapping and photo surveying can lead to very different and more scientific conclusions than that reported in the first instance which attributed the cause of the damage to vibration exposure.

In summary, as shown based on the samples provided above, it is imperative to collect any piece of information which can complement the vibration monitoring study. Also, as pointed out this holistic approach should generally provide scientific proof of the actual causes of structural damage to any

Figure 5. View of major crack – tank no. 1.

concrete or similar structures.

4. CONCRETE WATER TANKS (NO. 1 AND 2) STUDY

This example presents the detailed assessment of a concrete structure's response to high vibration levels. The assessment included the following:

- Pre-blast survey
- Vibration and displacement monitoring
- Post-blast survey

The assessment of the concrete water tank was undertaken prior to close range blasting. This included a detailed pre-blast survey of the concrete structure including detailed crack mapping and concrete strength measurements.

As blasting was planned to be undertaken in the immediate vicinity of the concrete water tanks, a detailed blast impact study was undertaken. The approximate location of the blasting area and concrete water tanks is presented in Figure 3.

The inspection revealed that there are two tanks of concern; namely two concrete cylinder tanks. Each tank is 8 metres in diameter. The water tanks are of older origin and have a number of cracks as described below.

Schematics of the observations made during the damage inspection are presented in Figures 4 - 6. The results of the damage inspection are summarised as follows:

- Water tank no. 1 – the number of cracks is limited to approximately four and all of the cracks appear to be sealed. Out of the four cracks, only one crack is classified as a major crack. This crack extends from ground level to the top of the tank (i.e. through the whole height of the tank) and potentially can affect the strength of the entire structure. The measured width of this crack ranged from 0.55 mm to 1.04 mm. The remaining cracks are small in length and therefore are expected to have limited impact when exposed to blast vibrations.
- Water tank no. 2 – the total number of observed cracks is eight. None of the cracks are classified as major, i.e. that could affect

Figure 6. View of small cracks (cracks no 1 and 2) – tank no. 2.

Table 1. Summary of concrete strength results using Schmidt Hammer test.

Infrastructure	Measured UCS (MPa)	Estimated Average UCS (MPa)
Tank No. 1	24.1, 32.4, 20.0, 12.4, 20.0, 37.9, 32.4	25.6
Tank No. 2	30.3, 24.8, 10.3, 35.9, 35.9, 35.4, 24.8, 13.8	26.4

the infrastructure behaviour. All of the cracks are relatively small and do not present a potential hazard issue. It is inferred that if such cracks are exposed to substantial vibration levels the damage will be limited. It is assumed that the cracks can undergo certain elongation or crack expansion without significant impact on the tank integrity. It is highly unlikely therefore that these cracks could cause structural damage.

In addition to the above assessment, to gauge the strength of the infrastructure of concern a non-destructive test of concrete strength was carried out using a Schmidt hammer. It should be understood that a Schmidt hammer test is considered an indicative type of test only. The results of the assessment are summarised in Table 1. Note that the estimated UCS values for each tank represent average numbers calculated from samples of several readings.

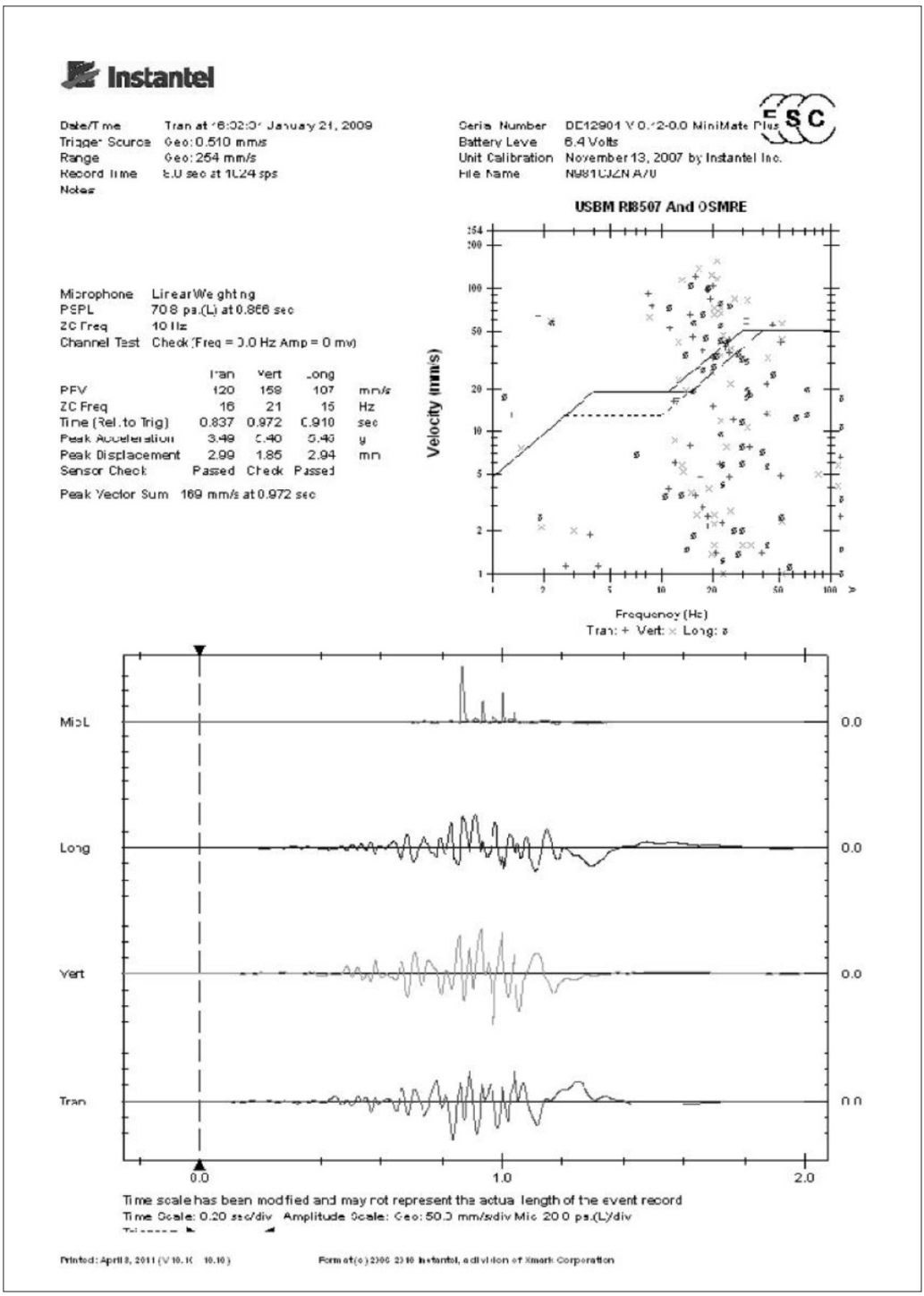

Figure 7. Vibration monitoring result – water tank.

In general, the state of tanks 1 and 2 was described as satisfactory. This is based on a direct comparison of the condition of the other tanks (3 and 4) discussed in the following section. There was however a 'top to bottom' crack observed on tank no.1 posing a degree of concern. Overall, the state of both concrete tanks (1 and 2) was of better condition than the state of the other two tanks discussed in the next section.

Also, the estimated strength of the concrete (approx. 25 MPa) is believed to be sufficient to undergo relatively high vibration impact. However, it should be remembered that it is the presence of major cracks (and not the strength of the concrete) that is ultimately responsible for the water tanks behaviour when exposed to high levels of vibrations.

The approximate location of the blast fired in the vicinity of the tanks is shown above in Figure 3. The expected ground vibration levels for the two water tanks were in the order of 225 mm/s for 200 kg MIC fired within a distance of 35 metres. In addition, the tanks were located on the side of a hill.

The subsequent blast exposure of these particular tanks (no. 1 and 2) revealed that the tanks were exposed to a level of vibrations in the order of 169 mm/s, see Figure 7. Frequencies generated by the blast were highly variable (i.e. 0 – 30 Hz range with dominant frequencies of 1.38, 11.1 and 22.6 Hz for longitudinal, transverse and vertical channels respectively). The generated displacement levels were moderate and were in the order of 2.94, 2.99 and 1.85 mm, for longitudinal, transverse and vertical channels respectively.

Also, the post-blast assessment did not reveal any damage to the tank structures. The post-blast crack survey did not reveal any increase in crack size or crack elongation which could otherwise negatively impact on the future stability of the tank structures.

5. CONCRETE WATER TANKS (NO. 3 AND 4) STUDY

The other two concrete water tanks marked here as tanks no. 3 and 4 were assessed in a similar fashion to the previously described tanks no. 1 and 2. The study revealed the following state of the tanks:

- The tanks represent an older type of structure than the previously analysed tanks 1 and 2.
- The general state of tanks 3 and 4 was described as significantly worse than the previously described tanks 1 and 2.
- Tanks 3 and 4 presented with a series of major cracks across the body of the

Figure 8. General condition of tank no. 3.

Figure 9. General condition of tank no. 4.

containers, which could pose a major concern.

- Both tanks will be exposed to a series of high levels of vibrations due to the close proximity of blasting (i.e. 4 blasts with high charge masses).
- The underlying rock strata was assumed to be virgin, however following the first blast it was discovered that the underlying r rock strata consisted of a fill material.

It ought to be noted that a pre-blast inspection of the water tanks revealed a high number of pre-existing cracks vertical as well as horizontal (i.e. 0.5 m – 3 m long). The cracks represent localised material failure (see Figures 8 - 9).

The inspection also revealed an absence of critical cracks. Most of the cracks were of limited length. A critical crack in this case is specified as passing through the whole wall of the tank vertically or around the tank. Nevertheless, the detected cracks were classified as major.

The tanks were exposed to four close range blasts. The locations of the tanks and the four blast areas are shown in Figure 10.

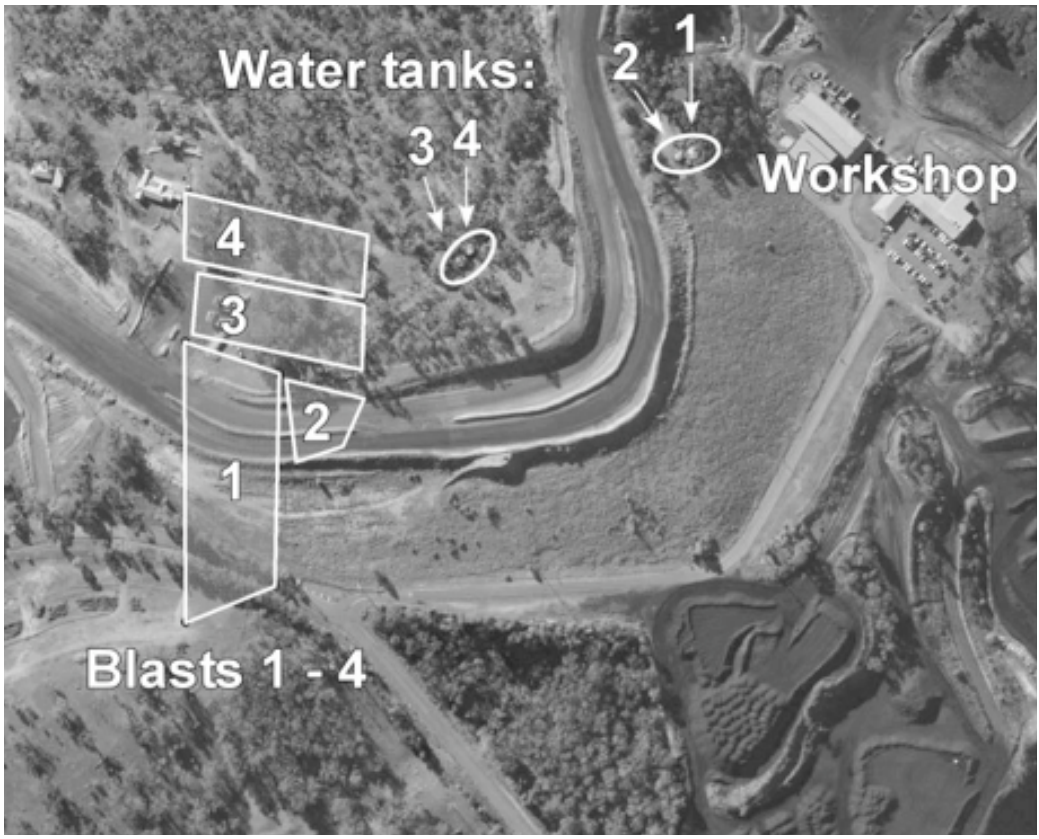

Figure 10. Location of tanks no. 3 and 4, and the four blast areas.

Table 2. Blast parameters.

Parameters	Blast 1	Blast 2	Blast 3	Blast 4
Blast ID	S10-240-01	S10-240-02	S10-240-03	S10-240-04
MIC (kg)	900	1000	1000	1000
Initiation Sequence (ms)	17 x 100	17 x 100	17 x 100	17 x 100
No. of Holes	175	53	105	113
Burden/Spacing (m)	7 x 8	7 x 8.5	7 x 8.5	7 x 8.5
Average depth (m)	26	28	29	28
Stemming (m)	5	5	5	5

The design parameters for each blast are summarized in Table 2.

The distance estimations and vibration predictions for each of the four blasts are presented in Table 3.

5.1 Blast no.1

The predicted vibration levels for the water tanks were in the order of 70 - 78 mm/s, while for the workshop they were in the order of 15 mm/s.

Table 3. Ground vibration predicted and measured values.

Monitoring Point	Distance (m)	MIC (kg)	Predicted Gr. Vibr. (mm/s)	Measured Gr. Vibr. (mm/s)
Blast 1: S10-240-01 9.05.08				
Water Tank 3	131	900	78.2	74
Water Tank 4	140	900	70.2	69.3
Workshop station	366	900	15.1	20.6
Blast 2: S10-240-02 20.06.08				
Water Tank 3	99	1000	132.9	-
Water Tank 4	110	1000	112.3	-
Workshop station	327	1000	19.6	-
Blast 3: S10-240-03 15.08.08				
Water Tank 3	63	1000	273.9	-
Water Tank 4*	71	1000	226.2	-
Workshop station	299	1000	22.7	-
Blast 4: S10-240-04 29.08.08				
Water Tank 3	63	1000	273.9	-
Water Tank 4	70	1000	231.4	-
Workshop station	284	1000	24.6	19.8

** Water tank rupture*

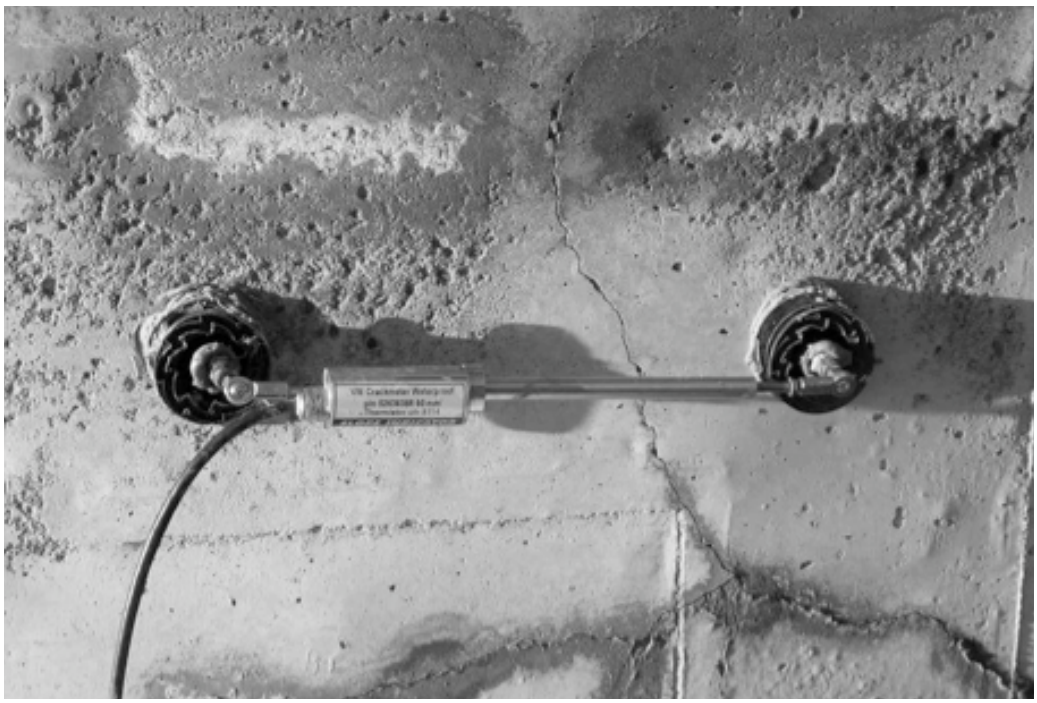

Figure 11A. VW crack meter against vertical crack.

In addition to vibration measurements, a number of displacement measurements were taken. A summary of the monitoring results, including vibration measurements for the first blast, are presented in Table 3.The analysis revealed that the first blast fired in the vicinity of the water tanks induced vibration levels between 69.3 and 74.0 mm/s. This correlates to approximately 1.28 – 1.35 mm of displacement generated at the ground level of the water tanks.

In addition to measuring the response of the water tanks due to induced ground vibrations, a VW crack meter was installed across a vertical crack on the wall of the water tank no. 4, see Figures 11A-B. The VW crack meter is a high-resolution instrument used to measure crack response to movement or induced vibrations. The induced permanent displacement measured during the basting period was in the order of 0.05 mm, refer to Figure 11B.

In addition, three sets of displacement targets across the existing vertical and horizontal cracks were glued to the water tanks. The targets were used to measure change in displacement in the existing vertical and horizontal cracks. The targets confirmed an absence of significant permanent displacement induced by the first blast. The measured changes in displacement were less than 0.1 mm.

In summary, the blast did not produce any significant displacement or tilt to the water tank structures. The induced crack displacement measured by the VW crack meter was in the order of 0.05 mm. This value is considered to have a limited impact on the existing localised concrete failure. The crack measurements using a calliper technique revealed that the measurements were within the instrument tolerance. In essence, no significant displacement was measured.

5.2 Blast no. 2 and 3 performance and blast outcomes

The vibration monitoring was not undertaken for blasts no. 2 and 3. However, based on the predictive model the following ground vibration levels were deduced for the considered water tanks i.e.

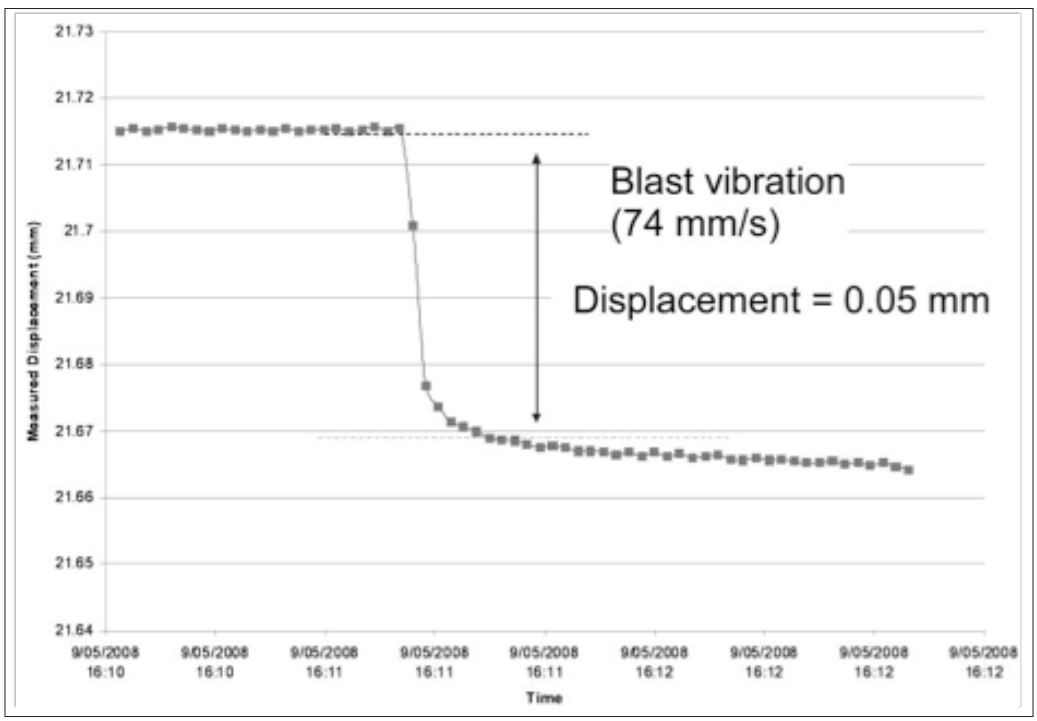

Figure 11B. Displacement monitoring results – VW crack meter.

- Blast no 2 – 112 - 133 mm/s for 99 - 110 m distance (using MIC of 1000 kg)
- Blast no 3 – 226 - 274 mm/s for 63 - 71 m distance (using MIC of 1000 kg)

This is based on the provided blast design parameters and distance estimations.

It is important to state that water was present in both tanks (which were filled to approximately 75% capacity) during blasts no. 1, 2, and 3. Although blast no. 2 was not monitored it should be noted that the visual inspection of the water tanks following this blast did not reveal any distinguished marks or tale-tale signs of induced damage or tank deterioration (water leakage etc.).

Blast no. 3 however caused water tank no. 4 to rupture. As reported by the blast engineer immediately following the described blast there was a huge amount of water cascading down the hill. An immediate inspection of the tanks revealed that tank no. 4 had ruptured. Basically, the water tank was ruptured along the middle section of the tank, refer to Figures 12 - 17. In this particular case the previously observed crack along the middle section of the tank was split open (i.e. resulting in connecting number of cracks) causing the bottom part of the tank to detach completely, while the top part of the tank fell onto the ground. This is for the north-westerly part of the tank, while for the north-

Figure 12. Extent of cracking.

Figure 13. Extent of cracking.

Figure 14. Extent of cracking.

Figure 15. Extent of cracking.

Figure 16. Extent of cracking.

Figure 17. Extent of cracking.

easterly part of the tank there was a slightly different mechanism, where the whole section from the top to bottom was pushed away. In this particular case it can be deduced that the damage was caused by the weight of the water pushing on the whole section of concrete and causing a physical detachment from the rest of the tank.

There is no doubt that the observed water tank rupture was a combination of vibration exposure for the concrete structure as well as the motion of water caused by induced ground vibration and passing ground vibration waves. This combined effect produced a lethal force, which culminated in the spectacular destruction of the water tank.

Also, it should be said that water tank no. 3 was able to sustain the induced vibration exposure, despite shorter distance to the blast and probably higher vibration effect.

Following this observed behaviour one can only speculate that different behaviour would have been observed if the water tank was exposed to the same vibration levels but without any water present. Also, another speculation can be made considering, for example, a reinforced water tank exposure had the tank been reinforced with bracing prior to blasting.

All in all it has been undoubtedly shown that the state of the structure, and not the strength of the structure itself, is one of detrimental factors when considering high vibration exposure for any structure. Also, from parallel study the author can draw the same conclusion would apply to underground workings where, for example, a roof with UCS of 20 MPa can be exposed to substantially higher vibration levels in comparison to a roof with the same strength of 20 MPa but high density jointing (i.e. comparable to high structural defects).

5.3 Blast no. 4

The vibration monitoring for Blast no. 4 was only undertaken at the workshop area and was in the order of 19.8 mm/s. Based on the predictive model, the following ground vibration levels were estimated for the considered water tanks, i.e.

− Blast no. 4 – 231 - 274 mm/s for 63 - 70

distance (using MIC of 1000 kg)

No visual damage to the remaining tank no. 3 was observed following this blast.

6 CONCLUSIONS

In 2008/2009 a number of detailed blast vibration impact studies were undertaken by Muswellbrook Coal with the assistance of Enviro Strata Consulting. The studies included detailed assessment of blast impacts on infrastructure including a number of concrete water tanks. In addition to vibration monitoring, the studies included structural surveys, detailed assessment of structural integrities, as well as crack displacement monitoring.

The studies confirmed that significantly higher vibration exposure is required to induce damage in concrete structures exposed to vibration impacts from open cut blasting. This is in comparison to materials used for building house structures. This finding is in line with other studies, briefly discussed in this paper.

The findings of this paper can be summarized as follows:

- The paper includes practical examples of structural surveys, which can assist mining engineers in assessing a structure's integrity. The assessment, if undertaken properly, should include a whole range of data gathering including geological/geotechnical assessment, structural survey (including crack mapping, photographic evidence) and any other available data.
- The paper summarises vibration monitoring pre and post blast survey studies undertaken on four different concrete water tanks. The tanks showed variable degrees of deficiencies including cracking, repaired sections and others. These tanks were exposed to various levels of vibrations, culminating in the rupture of one of the concrete water tanks when exposed to one of the blasts.
- The distances between the blasting area and the water tanks ranged between 35 metres up to 140 metres. The MIC for the undertaken blasts ranged from 200 kg up to 1000 kg.
- The paper included one case of water tank rupture when exposed to one of the blasts. It appears that the observed water tank rupture was a combination of vibration exposure of the concrete structure, as well as the motion of the water caused by induced ground vibration and passing ground vibration waves. This combined effect resulted in the destruction of the concrete water tank no 4. The blast was located approximately 71 metres from the water tank with a nominal charge mass of 1000 kg. The estimated vibration exposure generated by this blast was in the order of 226 mm/s.
- The ruptured tank had already developed a series of major cracks prior to blasting. As such, the pre-blast survey identified this tank as one of two tanks with a major underlying issue in regards to overall structural integrity. This can be described as a potential existing issue (i.e. presence of major cracks observed), which can produce serious problems when exposed to high vibration levels.
- The estimated blast exposure of the remaining three concrete water tanks ranged between 70 and 274 mm/s. The tanks were not negatively affected by high vibration exposure, i.e. no damage detected.
- The paper identified that overall structural integrity is one of the most important parameters which governs structural behaviour during high vibration exposure. The strength of the material alone is not the ultimate factor, but one of many.

The paper also presents details of a comprehensive approach which is recommended when undertaking close range blasting, including high vibration exposure. Overall, based on the presented studies the following recommendations can be made:

- The mere assessment of material strength and vibration monitoring is considered a simplistic approach, and in many cases is insufficient to predict potential structure behaviour when exposed to high vibration levels.
- The detailed pre-blast structural survey of a structure exposed to high vibration levels is essential in predicting potential structure behaviour during vibration exposure. The survey, if properly undertaken, should include crack mapping, assessment of the strength of the material, assessment of foundations and / or underlying geology, photography and others. The pre-blast survey is essential in assessing the integrity of the structure and better prediction of structural behaviour.
- The proposed holistic approach should

- The proposed holistic approach should generally provide scientific proof and better understanding of the existing issues (if any) and potential indication in regards to future behaviour and / or current causes behind existing damage (if any).

7 ACKNOWLEDGEMENTS

The authors gratefully acknowledge the permission of Muswellbrook Coal Management to present the results described in this paper.

REFERENCES

ACARP report no C 14057 “Effect of blasting on Infrastructure” 2008, Australia.

Australian Standard AS 2187.2-2006.

Oriard, L.L. 1998. Blasting Specifications for Concrete. J. International Society of Explosives Engineers, July/August, pp 40-45.

Oriard, L.L. 2002. Explosive Engineering, Construction Vibrations and Geotechnology. Int. Soc. Of Explosives Engineers, Cleveland, Ohio.

Siskind, D.E. 2005. Vibration from blasting. International. Society of Explosives Engineers, Cleveland, Ohio.

Svinkin, M.R. 2007. Assessment of safe ground and structure vibrations from blasting. In Proc. Fourth EFEE World Conference on Explosives and Blasting, Vienna.

Lisbon Conference Proceedings 2011, R. Holmberg et al

Seismic measurements of bench blasting operations in Slovakia

V. Bauer, M. Beňovský & B. Pandula
Technical University of Košice, Fakulty BERG, Slovakia
Authors are members of Slovak Society of Blasting & Drilling, Banská Bystrica, Slovakia

ABSTRACT: The paper deals with the safety and environmental aspects of bench blasting in open pits and quarries in Slovakia. In order to control and minimize ground vibrations generated by the production blasts, seismic measurements have been performed and analysed for two rounds. The evaluated results from the two blasts were used for assuring that the ground vibrations reaching nearby structures would fall below the damage criteria given by the Slovak standard STN 73 0036. Furthermore the results were used for establishing the benchmark for blasting operations in the Slovak quarry Brezina-Sokolec. The methods for seismic measurements and analysis and the methodology for calculating the blasting parameters are presented in this case study. The case study presented is typical for establishing blasting operations in Slovakia. The results from the two blasts show that ground vibrations emitted were well below the criteria for causing any damage to surrounding structures.

1. TECHNICAL CONDITIONS FOR BENCH BLASTING

Bore holes are mostly drilled in three rows with slightly inclined parallel bore-holes in open pit productions in Slovakia. Stable and secure quarry benches are projected to be 15 – 20 meters high. Usually the burden for the front row is 25% larger than for the second and third row. The hole diameter is 95–115 mm. In hard rock the spacing is about 80-130% of the maximal burden (W_{max}). The burden is calculated by blasting engineers through well known and tested methods formulated by multiple authors (Beňovský (2002), Bauer (2006), Dojčár *et al*. (1996), Langefors & Kihlström (1978), Müncner *et al*. (2000). There are mobile and easy to operate drilling rigs with outstanding technical specifications used in most open pits.

The drill and blast patterns are based on theoretical calculations and are adjusted with regard to achieved blasting results in the quarry. Drilling patterns and specific charges for various drill diameters is done by a standardised process used for the suggested type of industrial explosive. All operational technical parameters are determined by calculations and documented in the blasting

project. The calculation is performed by highly qualified professionals (technical construction engineer) separately for each blast. The technical project of bench blasting includes detailed calculations of;

a) Concentration of borehole charge,
b) Specific charge,
c) Maximum and practical burden,
d) Borehole spacing,
e) Horizontal maximal burden for the front row,
f) Horizontal maximal burden for the 2nd and 3rd rows
g) Subdrilling,
h) Stemming height,
i) Total charge weight per hole,
j) Delay time between individual charges.

A planning tool is developed by the Institute of Mining and Environmental Protection, Faculty BERG in technical university Kosice. Technical engineers also evaluate the economical parameters of it at the same time, Expressed in [€/ton]; [€/m^3]

- The explosive cost (C_E)
- Detonators cost (C_D)
- Cord cost (C_C)
- Drilling cost (CD_R)
- Blasting cost (C_B)
- Primers cost (C_P)
- Cost for secondary blasting (C_{SB})

In a technical documentation of each bench blasting project a prediction is also made of possible ground vibrations that may cause damage to building facilities and construction objects. The following is considered;

a) Protection of buildings and plant facilities from direct impact of seismic waves.
b) Safety for people with regards to blast vibrations.

The most reliable way to define intensity of blast vibrations is to directly measure seismic effects on structures of concern for a known quantity of test charge, (Olofsson, 1990).

2. BENCH BLASTING TECHNICAL PARAMETERS CALCULATION

Bench blasting represents a very effective way of breaking and fragmenting rock if the blasting is performed in a constant controlled way with the right delay times.

The calculation of bench blasting parameters is given by:

- Theoretical principles of the rock breaking process done by explosives
- Methods and techniques used in the explosion process
- Results acquired by practical tests

While calculating bench blasting parameters, the technical engineer must consider environmental, technological, technical, and operational factors, which are parts of two important technical projects of mining operations:

a) General technical project – plan of opening a quarry, preparation, and mining, which represents a plan of deposit extraction for several years to come.
b) Technical project GTP – general technical project of bench blasting for huge explosion works.

The calculation of bench blasting parameters takes into account the following:

- Preparation process and realisation of bench blasting
- Determination of permitted extent of blasting
- Maximum explosive charge fired simultaneously (at the same time)
- The total quantity of explosives needed for a blast

The maximum amount of an explosive charge to be used is estimated through calculations, but also verified and adjusted through test blasts and monitoring of environmental disturbances from emitted noise, air blasts and ground vibrations.

3. SEISMIC MEASUREMENTS

Due to the increasing conflicts of interest and environmental issues, regular seismic measurements are performed on site. Measuring devices like geophones and microphones are located on the foundations of surveyed objects and particle velocities and predominant wave frequencies are recorded and documented (Pandula and Kondela, 2010).

A modified Koch formula (STN 73 0036) is used for a rough preliminary estimate of the seismic impact at a nearby building structure.

$$v = K.\frac{\sqrt{Q_{ev}}}{l} \quad (1)$$

where,

v seismic wave speed oscillation [mm/s]
Q_{ev} equivalent explosive charge in one interval number [kg]
L distance from the blast [m]

K index characterizing energy transmission through the rock environment

The coefficient of energy transfer K varies depending on the type of rock. The Slovak Technical Standard (STN 73 0036) defines the vibration-proof object categories based on the acceptable degree of damage. In this case, the safety distance of the building structure from the blast place will be approximately:

$$l = k_1 . Q_{ev}^{k_2} \quad (2)$$

where,

k_1 category construction index (degree of building damage related to the equivalent explosive charge)

k_2 coefficient depending from equivalent explosive charge Q_{ev}

Q_{ev} equivalent explosive charge [kg]

The criteria for possible damage to civil engineering structures, depending on the speed of vibration (v) is characterised according to the standard STN 73 0036. Types of damages are divided into light, moderate and severe damages and partial collapse of buildings. For the purpose of technical seismicity evaluation the standard determines the degrees of damage depending on the maximum speed of vibration respectively oscillation frequency *(f_k)* – [f_k <10 Hz; 10 Hz < f_k < 50 Hz; f_k > 50 Hz;], depending on the facility construction type and on the foundation soil category (three categories).

Degree of damage is estimated by maximum particle velocity (v_{max}), type of building construction and geology from 2 to 400 mm/s. The effects of seismic vibrations at particle velocities above the limit of 400 mm/s are very harmful and can cause severe damage to buildings.

The peak particle velocity, PPV, is the highest value of the three components measured.

In conformity with standards and based on ground vibration measurements in open pit mines throughout Slovakia, it is possible to accept the following criteria for damage to a brick building structure.

v = 0–10 mm/s – there is no fear of damage
v = 10–30 mm/s ¬– possibility for the first degree damage
v = 30–60 mm/s – possibility for slight damage

4. PRACTICAL CASE FOR ESTABLISHING A BLASTING OPERATION

The blasting work in several quarries in Slovakia is carried out by the company LUVEMA, spol. s r.o. Nová Baňa. A practical case for establishing the blasting operations in quarry Brezina – Sokolec is presented here.

Two bench blasts – BB no.14 and BB no.17, were performed in the quarry. See Figure 1 for layout and place where the monitoring of the ground vibrations took place. Sensors were mounted on the concrete foundation of the quarry - administration building.

For the bench blasting operation a cartridged dynamite Supergel 30 with a diameter of 90 mm was used as a toe charge (~1/3 of the loaded bore hole) and a bulk powder explosive DAP was used in the column.

Calculation of the technical parameters for drilling and blasting was carried out under the current methodology, that the company LUVEMA and others have used for a long time. For a series of bench blasting rounds the chosen drill hole diameter was d = 115 mm. The calculation was performed in the following sequence (Table 1);

$$p = V_v \times \rho_{Tr} \times K_n \quad (3)$$

where,

p linear charge concentration in bore hole [kg/m]

V_v borehole volume per meter of length [m³]

ρ_{Tr} density of explosive [kg/m³]

K_n explosive degree of packing in the borehole

$$q = f_p \times s \times v \frac{e}{k} . u \quad (4)$$

where,

q specific explosive charge [kg/ m³]

f_p rock strength coefficient acc. to Protodyakonov

s rock structure coefficient

v rock fastening coefficient

e brisance coefficient (Tritol=1, Supergel 30 =1.2)

u stemming coefficient

k coefficient for explosive filling degree of borehole

$$W_{max} = \left(\frac{p}{q \times m} \right)^{\frac{1}{2}} \quad (5)$$

where,

p linear charge concentration in borehole [kg/m]

W_{max} maximal horizontal burden [m]

q specific explosive charge [kg/m³]

m explosive charge approximation coefficient

$$X = \frac{\left(0.5 \times p^2 \times sin^2\alpha_v + 4 \times q \times p \times \sin\alpha_v \times H \times L\right)^{0.5} - \mathbf{0.71} \times p \times \sin\alpha_v}{\left(2 \times q \times m \times H \times \sin\alpha_v\right)} \quad (6)$$

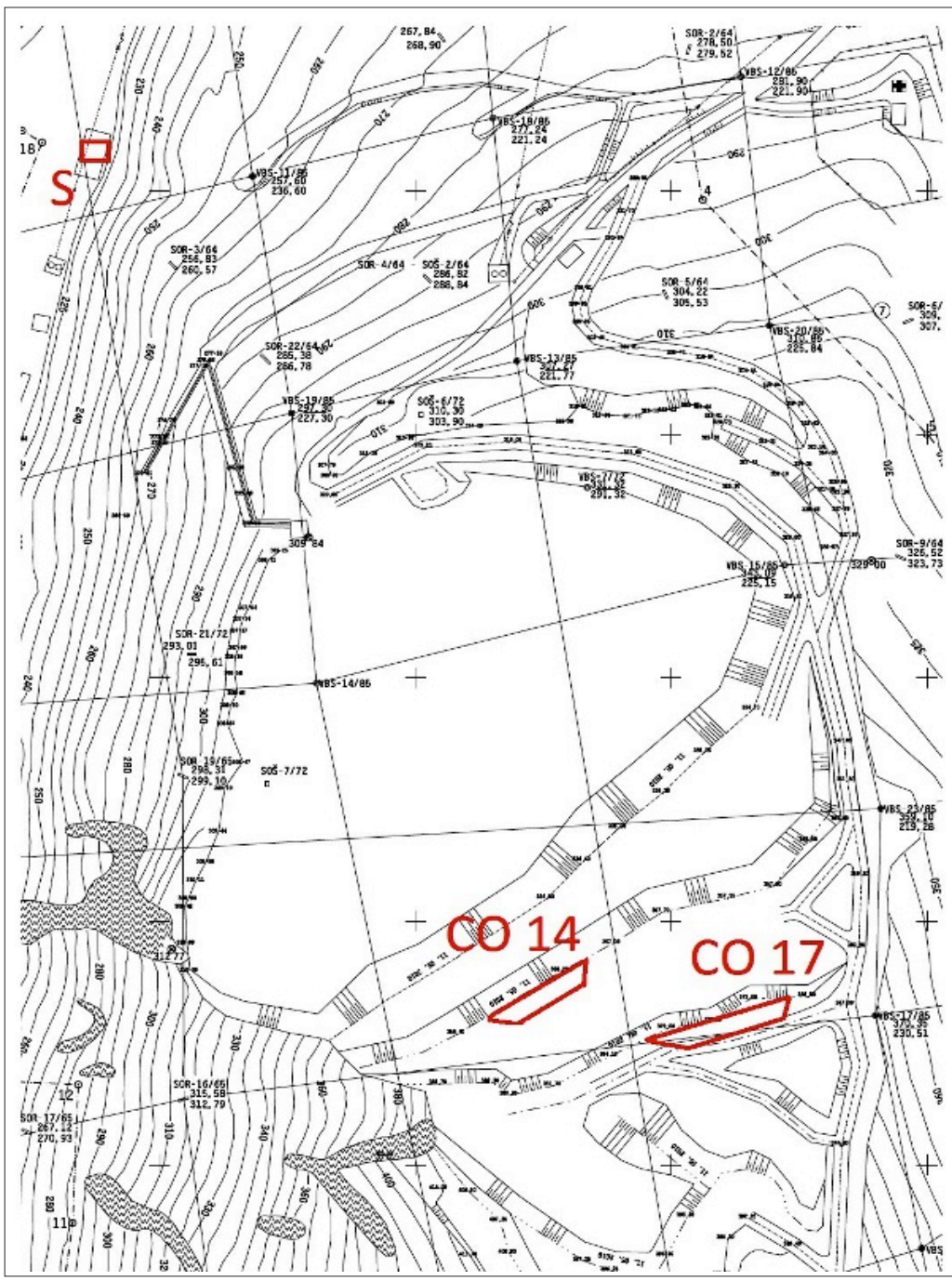

Figure 1. Layout of the rounds #14 and #17 in the quarry Bzenica-Sokolec. The measuring position is marked with S.

Table 1. Technical parameters for the rounds BB No. 14 and BB No. 17. H =20 m. L=21.3 m.

Technical parameters	Computed values	Additional conditions values
1. Linear charge concentration (p)	*Supergel30* *9.8 kg/m* *DAP* *8.89 kg/m*	*(d) = 115 mm* *(Kn) = 0.65 Supergel 30, ø 90 mm* *(Kn) = 0.95 DAP* *(ρtr) = 1450 kg/m3 Supergel 30* *(ρtr) = 900 kg/m3 DAP*
2. Specific explosive charge (q)	*0.501 kg/m3*	*essential coefficients* *fp=0.7 ; s=1.0; v=0.85;* *u=1.0; e =0.8; k=0.95*
3. Maximal Burden Front row (W_{max}) *2nd and 3rd row ($W_{max\ 2,3}$)*	*3.76 m*	*4.71 m p=8.89 for DAP* *$W_{max\ 2,3} = 0.8W_{max}$*
4. Borehole spacing (a)	*3.76 m*	*m = 0.8; a = mW_{max}*
5. Horizontal maximal burden (X) row 1	*3.76 m*	*□$_v$ = 70 °, H = 20 m*
6. Horizontal practical burden (X2) and (X3) rows 2 and 3	*4.22 m*	*K = 0.05; X2=X3= X - K H*
7. Subdrilling (lp)	*1.36 m*	*lp = 0.29 W_{max}*
8. Boreholes stemming (lu)	*3.3 m*	*lu = 0.7 W_{max}*
9. Maximal charge weight per borehole (Qv)	*172 kg*	*Qv max = p (L + lp - lu), L=21.3m*

where,
X denotes horizontal burden [m]
αv ; borehole inclination [°]
H; bench height [m]
L; borehole length without sub drilling [m]

$$X2 = X - K_v \times H \quad (7)$$

where,
K_v: drill hole deviation coefficient [m/m]

$$Q_v = p \times (L + lp - lu) \quad (8)$$

where,
Q_v: maximal column weight charge of individual borehole [kg]
lp: subdrilling [m]
lu: stemming length [m]

$$lp = 0.29 W_{max} \quad (9)$$

$$lu = 0.7\ W_{max} \quad (10)$$

Part of the methodology of calculation is the basic calculation of the blasting effects on the immediate vicinity and the nearby building objects to be protected against the adverse effects of blasting.

5. SEISMIC MEASUREMENTS

Two rounds No.14 and No.17 were blasted and monitored. The instrument used for monitoring the vibrations was Instantel - BE15324 V 10.06-8.17 MiniMate Plus. Figure 1 shows the layout of the rounds and the measuring position. Results of the performed monitoring are given in the Table 2. The MiniMate Plus calculates the Peak Particle Velocity, Zero Crossing Frequency, Peak Acceleration, and Peak Displacement for each of the transverse, vertical, and longitudinal axes. Peak Particle Velocity (PPV) indicates the maximum speed particles travel, resulting from a ground vibration event. The MiniMate Plus calculates the PPV for each geophone. The Zero Crossing Frequency (CZ Frec) calculates the event waveforms frequency at the largest peak.

Table 2. Seismic measuring by use of the MiniMate Plus instrument.

Bench blast #	Mini Mate Plus	Measured values		
BB 14/2010	*PPV [mm/s]*	*Tran*	*Vert*	*Long*
	ZC Freq [Hz]	*0.667*	*0.73*	*0.73*
		8.6	*13.2*	*21.1*
BB 17/2010	*PPV [mm/s]*	*Tran*	*Vert*	*Long*
	ZC Freq [Hz]	*1.03*	*0.667*	*0.81*
		10.3	*7.4*	*6.2*

Both rounds measured utilised electric initiation with a delay time of 0.25 seconds. The effect of seismic waves is evaluated according to STN 73 0036. Under this standard, when a delay time of a minimum of 0.25 seconds is used, each charge is considered separated.

During the risk analysis of the vibrations, the frequency is estimated with regards to the equivalent explosive charge used. See Table 3.

The PPV at the measured building objects can be estimated and based through a simple equation (See equation 11).

Blast place:	Quarry Bzenica - SOKOLEC
Place of measurement:	Concrete foundation
Measurements were made by:	Ing. Marian Benovsky

Table 3. Estimation of frequency.

Frequency (f)	*Equivalent explosive charge (Qev)*
$f < 10$ *Hz*	$2000\ kg < Qev$
$10 < f < 50$ *Hz*	$5\ kg < Qev < 2000\ kg$
$50 < f$ *Hz*	$Qev < 5\ kg$

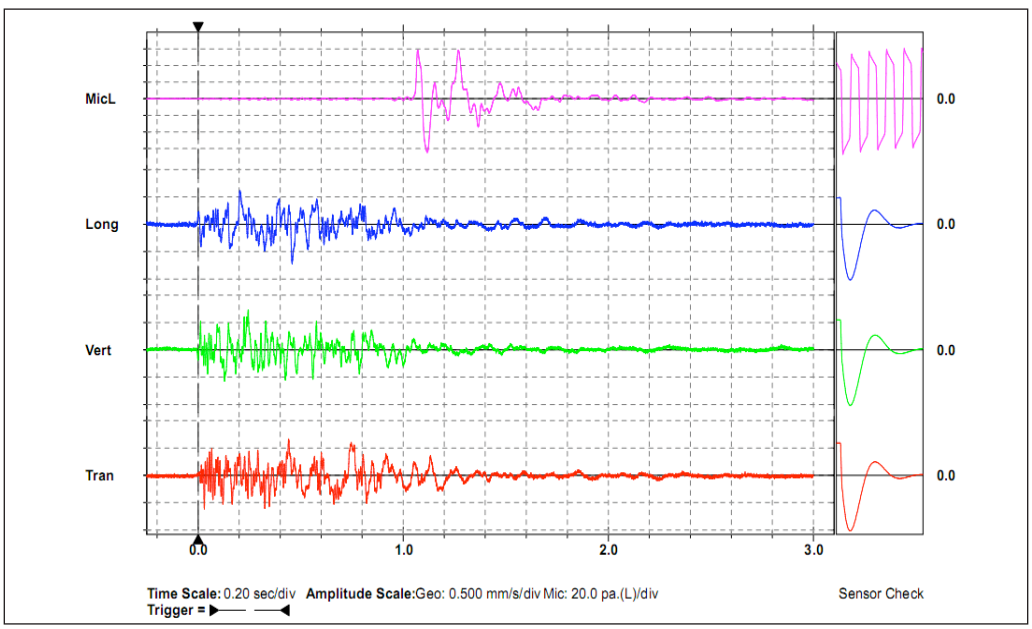

Figure 2. Seismogram after blasting BB No.14.

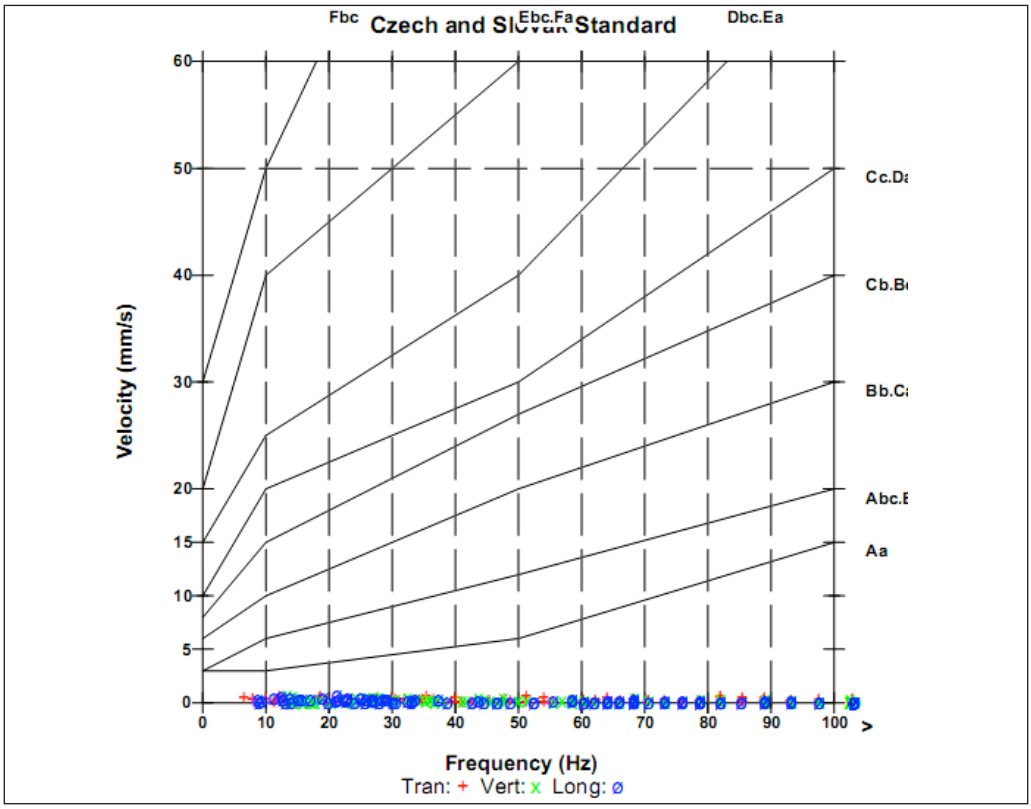

Figure 3. Frequencies range pointing BB No.14.

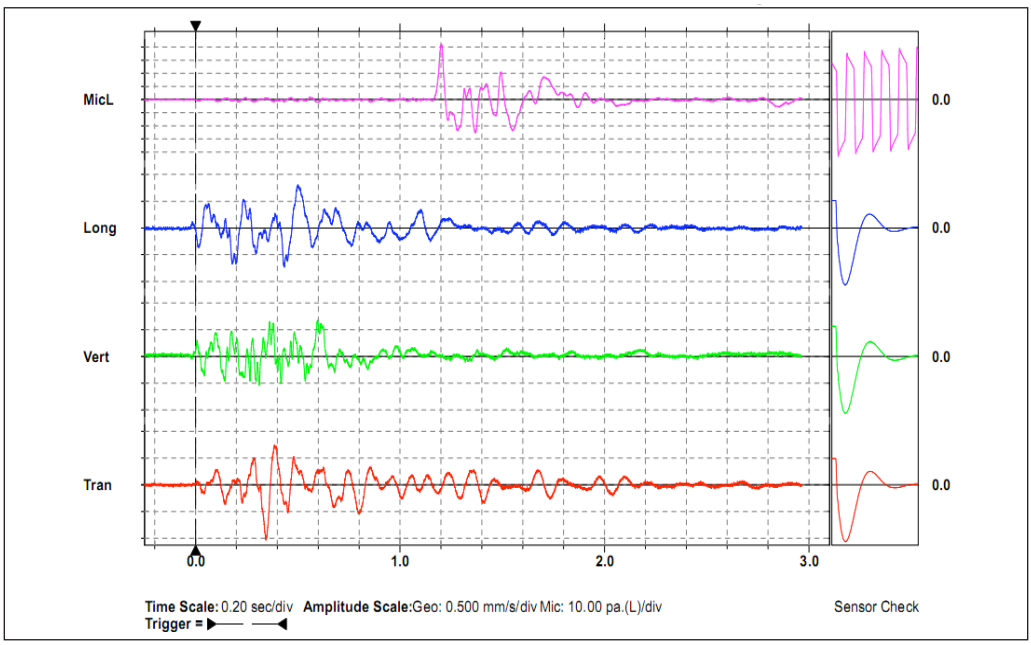

Figure 4. Seismogram after blasting BB No.17.

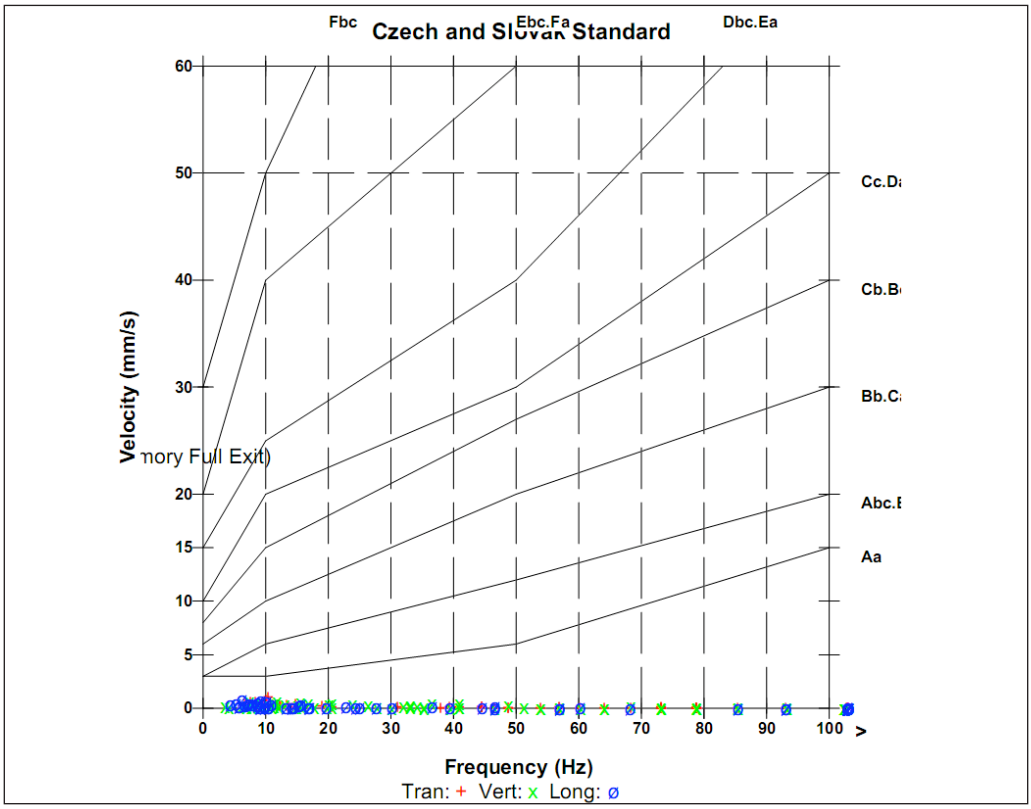

Figure 5. Frequencies range pointing BB No.17.

$$v = K\frac{Q_{ev}^{-2}}{1000 \times L_{SV}} \qquad (11)$$

where,

v denotes the PPV [mm/s]

K : energy transmission coefficient depending on geology and attenuation

Q_{ev}: equivalent explosive charge [kg]

L_{sv} : distance from blast [m]

The effects of seismic waves in the building objects were assessed according to the Slovak standard STN 73 0036. The buildings were respectively situated at distances of 380 m and 450 m from the blasts. Calculated values of PPV were as follows:

- 380 m (BB14); PPV= 7.32 [mm/s]
- 450m (BB17); PPV= 6.18 [mm/s]

The measured values were

- 380 m (BB14); PPV=0.73 [mm/s], Frequency f=21.2 Hz
- 450 m (BB17); PPV=1.03 [mm/s], Frequency f = 10.3 Hz

The results compared to the calculated values indicate that the degree of damage is zero, which means safe blasting performance. The visual inspection of the buildings did not indicate that any structural or cosmetic damages had occurred. The measured values were well below the permitted value in the standard STN 73 0036 which is 10 mm/s.

CONCLUSION

The two rounds #14 and #17 observed, had a drill and blast pattern with three rows. When a delay time of 0.25 s was used this resulted in no negative impact on the building structures in the neighbourhood, due to a positive interference of seismic waves. Multi-parallel blasthole rounds are designed mainly to achieve a higher efficiency and performance of the blasting operation and for increased safety.

The tests have shown that the Slovak standard is

giving a good guidance and that the quarry is performing the blasting operation in a safe and economical way.

REFERENCES

Bauer, V. 2006. Drilling and blasting. *Lecture Workbook-CD. ES Košice*. p 95 (Prednáškové zošity).

Beňovský, M. 2002. Generally blasting plan in quarries. Technical report of Luvema, s.r.o. ((Technický projekt clonového odstrelu)).

Dojčár, O. Horký, J. & Kořínek, R. 1996. Blasting technique. Ostrava Montanex, 421 s. ISBN 80-85780-69-0.

Langefors, U. & Kihlström, B. 1978. *The Modern Technique of Rock Blasting*. Wiley, New York.

Müncner, E. & kol. 2000. *Handbook for construction engineers and tampers*. Slovak Society of Drilling and Blasting Works, STVP Banská Bystrica p 201 (Príručka pre strelmajstrov a TVO).

Olofsson, S.O. 1990. *Applied explosives §technology for construction and mining.* Ljungföretagen tryckeri AB, Örebro. p 342.

Pandula, B. & Kondela, J. 2010. *Methodology of blast works seismic*. Banská Bystrica, DEKI Design, s.r.o., p 156 (Metodika seizmiky trhacích prác).

STN 73 0036 (1997): Seismic loading of building construction. Office for normalization, metrology and tests SR, Bratislava 68 str. (Seizmické zaťaženia stavebných konštrukcií. Úrad pre normalizáciu, metrológiu a skúšobníctvo SR, Bratislava).

Lisbon Conference Proceedings 2011, R. Holmberg et al

Evaluation method of the effects of seismic blasting in Maglovec quarry

J. Kondela, B. Pandula & K. Pachocka
The Technical University, Faculty of BERG, Institute of Geo-sciences,
Park Komenského 15 of Košice, Slovakia.

ABSTRACT: Blasting has positive effects but may also have negative impacts causing damage to surrounding civil objects. The intensity of seismic waves' vibrations is proportional to the weight of the applied explosive. If the vibrations are sufficient in energy, surrounding buildings can be damaged or destroyed. Evaluating the negative effects of the blasting operations and quantification of the seismic safety is nowadays very actual and a challenging problem. The article presents the results of the analysis as well as an evaluation method of seismic safety of the objects during blasting work held by the seismic waves' attenuation law in Maglovec quarry. The results of the evaluation of seismic effects of blasting verified in a Maglovec quarry are the methodological base for evaluation of the effects of seismic blasting in all quarries in Slovakia.

The diorite porphyrite quarry in Maglovec is located in the northern part of Slanské vrchy Mts., approximately 35 km to the NW from Košice. In the vicinity of the quarry (approx 800 m to the SW) Vyšná Šebastová and Severná villages (SW) are situated. The monitoring of blasting operations in Maglovec quarry, as an example, enabled to describe seismic of blasting operations methodology (Podel 1980).

1. TRANSMITTING MEDIUM

The semi – intruded body of diorite porphyrite in Maglovec quarry is of Neogene age (Middle Sarmatian, 12+- 0.3 Ma) and intruded into the Neogene, Lower Miocene sediments. The intrusions of diorite porphyrite (laccoliths, sills) penetrated during Middle Sarmatian at the boundary of Lower Miocene and Lower Sarmatian volcanic complexes. The rocks are dark gray and light gray with distinctive dark minerals phenocrysts (Figure 1b). The phenocrysts most often are composed of plagioclase (An34-36), hypersthene, augite and amphibole. The structure is porphyric with holocrystalline, microallotriomorphic to hypidiomorphic grainy ground substance. The final structure is then amphibolic – pyroxene to pyroxene – amphibolic diorite porphyrite. (Kaličiak *et al*. 1991).

The thickness of mantle-rock varies from 5 m to 40 m. Progressing exploitation in the quarry revealed internal structure of diorite porphyrite body. The structure is much more difficult than it was expected during investigation based on borehole research. Due to the current mined part of deposit in Vyšná Šebastová there was identified the tectonic qwline with general trend NNE – SSW, with its origin

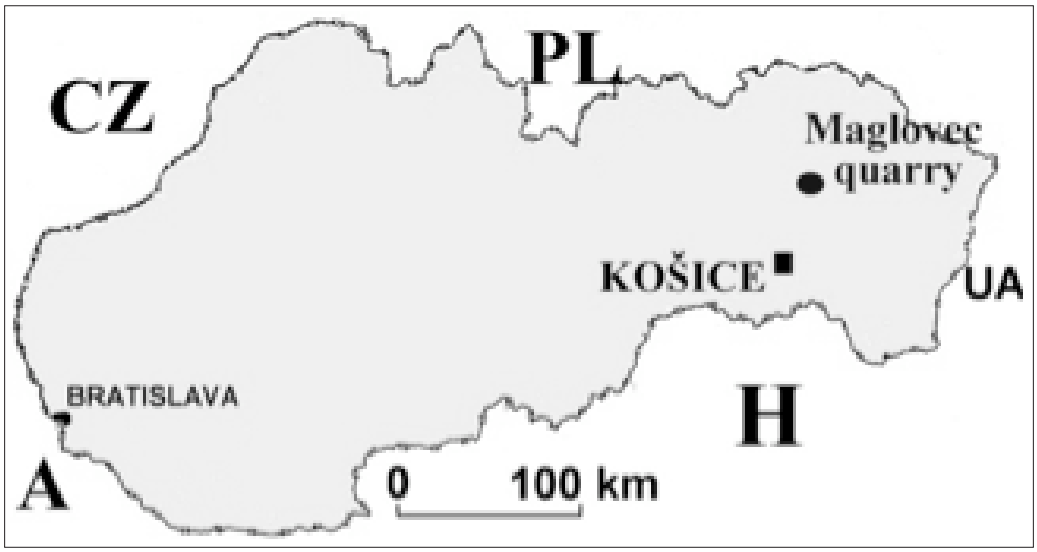

Figure 1a. Position of Maglovec quarry.

Figure 1b. Aerial view of Maglovec quarry.

genetically connected to consolidation of footwall clay sediments caused by load of solidified body. It is a failure zone, which destroys part of the deposit and divides the deposit into two parts (Figure 2).

1 *fluvial sediments: loams, sands, clays,*
2 *proluvial sediments: sandy gravels with loess loams regolith,*
3 *deluvial sediments: loamy – rocky undivided sediments,*
4 *mirkovske formation: monotonous, grey calcareous claystones,*
5 *kladzianske formation: greenish – grey claystones with beds of fine – grained sandstones,*
6 *zuberecke formation: alternation of sandstones, siltstones with interformation conglomerates, Mn carbonate ore and varicolored claystones,*

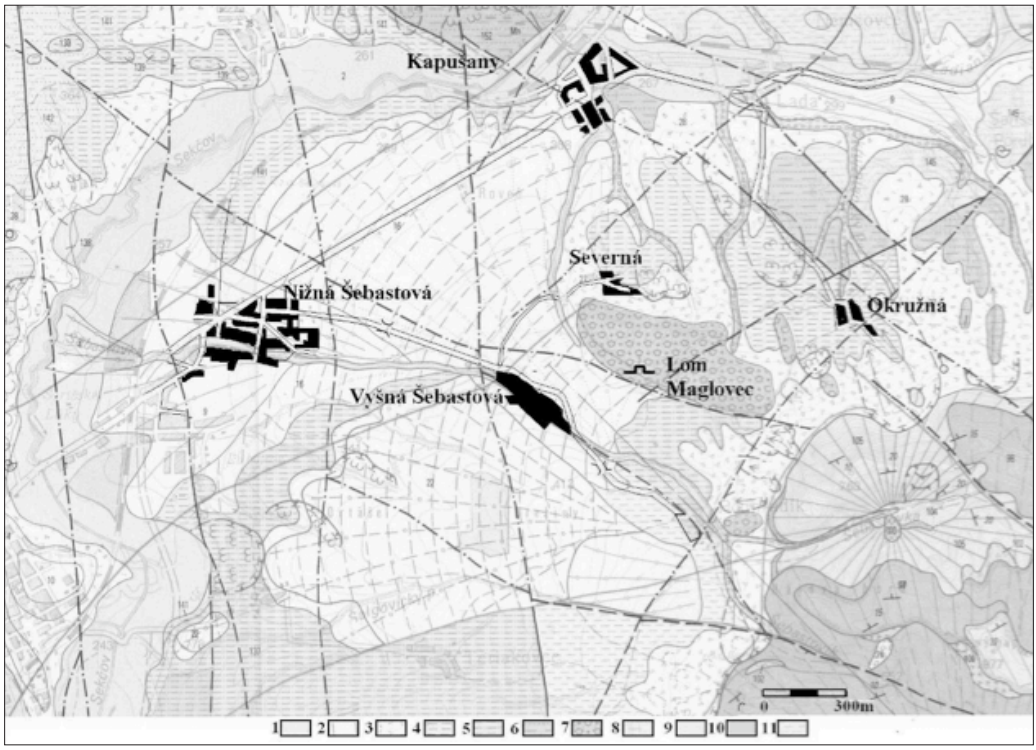

Figure 2. Geological map of Maglovec quarry with the nearest villages (Kaličiak et al. 1991) modified version.

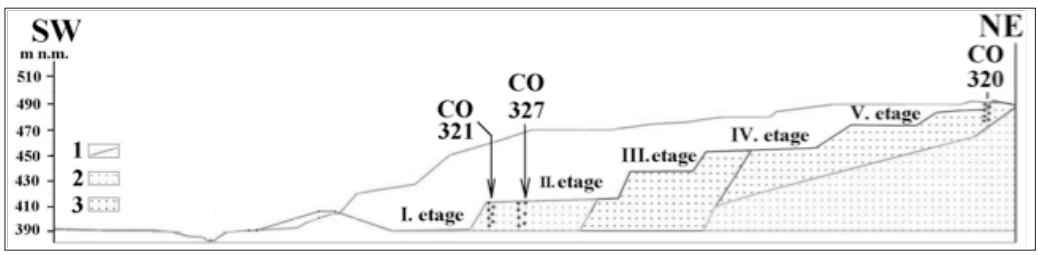

Figure 3. Schematic geological cross-section of Maglovec quarry with primary morphology of the surface, distinctive tectonic zone and blasting sites. 1 primary morphology of quarry, 2 slightly ruptured diorite porphyrite, 3 tectonic zone of intensively ruptured diorite porphyrite.

7 *intrusions of amphibolic pyroxene diorite porphyrite,*
8 *Čelovské formation: light grey siltstones to fine – grained sandstones,*
9 *Sebastovka formation: lava torrent of amphibolic pyroxene andesite,*
10 *Stavica formation: lava torrent of augite - hypesthenic andesite, hypesthenic – augite andesite, pyroxene andesite with different ratio of augite and hypesthene,*
11 *Čelovské formation: light grey greenish – grey micaous claystones,*

The blasting site CO 320 was situated at the highest, fifth etage 453 – 473 MASL, where solid rock mass is partly weathered. From tectonic failure point of view the solid rock mass is dominantly fractured in one direction (Figure. 4), but on the fifth etage (blasting site) the rock mass is omnidirectionally fractured. The direction of fracturing follows the direction of the main tectonic structure which separates the blasting site and Vyšná Šebastová. This means that the activated seismic wave has to pass the tectonic line before reaching the village.

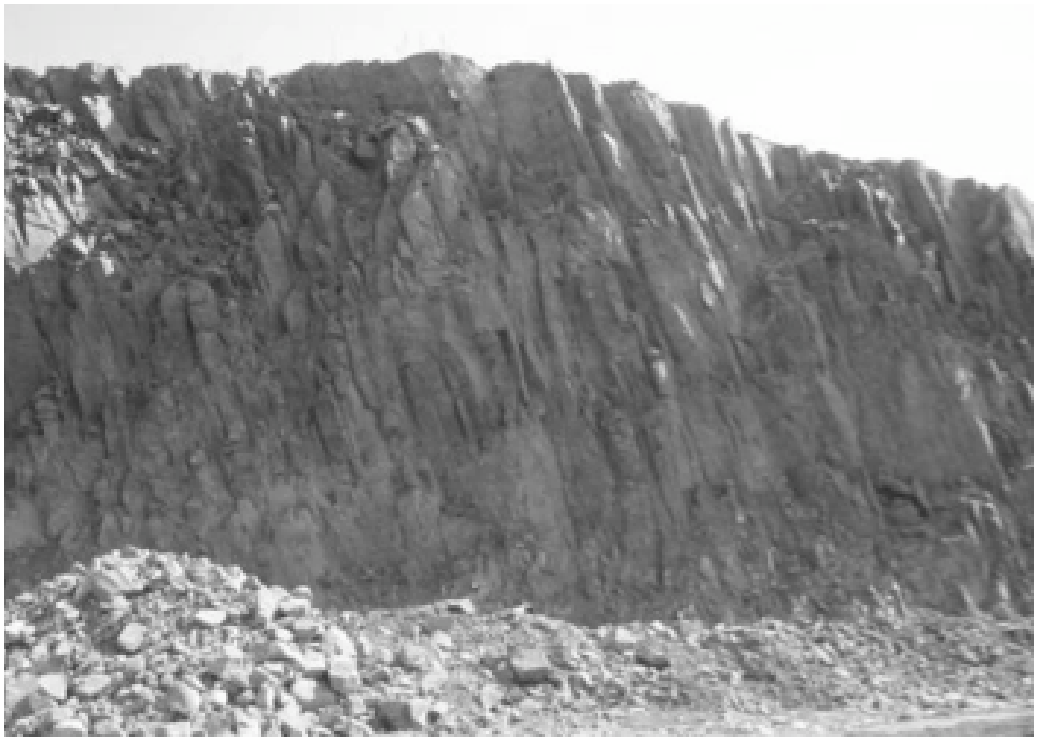

Figure 4a. Fissured solid rock mass at etage 453 – 473 MASL.

Figure 4b. Partly weathered diorite porphyrite at fifth etage.

2. SOURCE OF VIBRATIONS

The seismic vibrations' source was tristichous bench blasting (CO) 315, 320 and 321 (Figures 6 and 7). 100 boreholes were drilled, each of 26 m depth. One borehole contained 225 kg of Titan 1000 explosives. The total explosive charge in boreholes was 22.500 kg. To ignite, the following media were used: 367,5 kg of Austrogel explosive, 100 pieces of detonators Ms 475/27M, 100 pieces of detonators Ms 500/78M, 66 pieces of detonators Ms 42/4,8M, 30 pieces of detonators Ms 17/4,8M, 2 pieces of detonators Ms 25/4,8M and 2 pieces of detonators Ms 0/4,8M. Figure 5 shows the borehole distribution scheme and blasting timing.

3. EQUIPMENT APPLIED AND MEASUREMENT METHODOLOGY

The following seismic recording equipment, located on five standpoints was applied for the purpose of measuring seismic effects during 315 bench blasting (further only 315 CO): ZEB/SM-3C with seismodetector 3E by Orica Mining Services Company, SRN (Figure 8). The seismodetectors were set on support with sharp steel spikes, which assured continual contact with foot. The digital four – channel seismograph UVS 1504 and seismodetectors by the Swedish company Nitro Consult (Figure 4) were used for measurement of seismic effects at standpoint number 6. The seismograph provides digital and graphic records of all three vibration velocity components of medium elements, horizontal longitudinal– v_x, horizontal lateral– v_y, vertical -v_z. The Seismograph UVS 1504 works autonomously, it tests channels automatically without intervention and influence of operators on the measured and registered vibration characteristics. The equipment has an AD convertor with automatic 14 bit dynamic range of 0,05 ÷ 250 mm/s. For these measurements there were used electrodynamic UVS geophones with frequency range 1 ÷ 1000 Hz and responsiveness of 20 mV/mm.s^{-1}.

Figure 5a. Borehole distribution scheme during 315 bench blasting at etage 390-415 MASL.

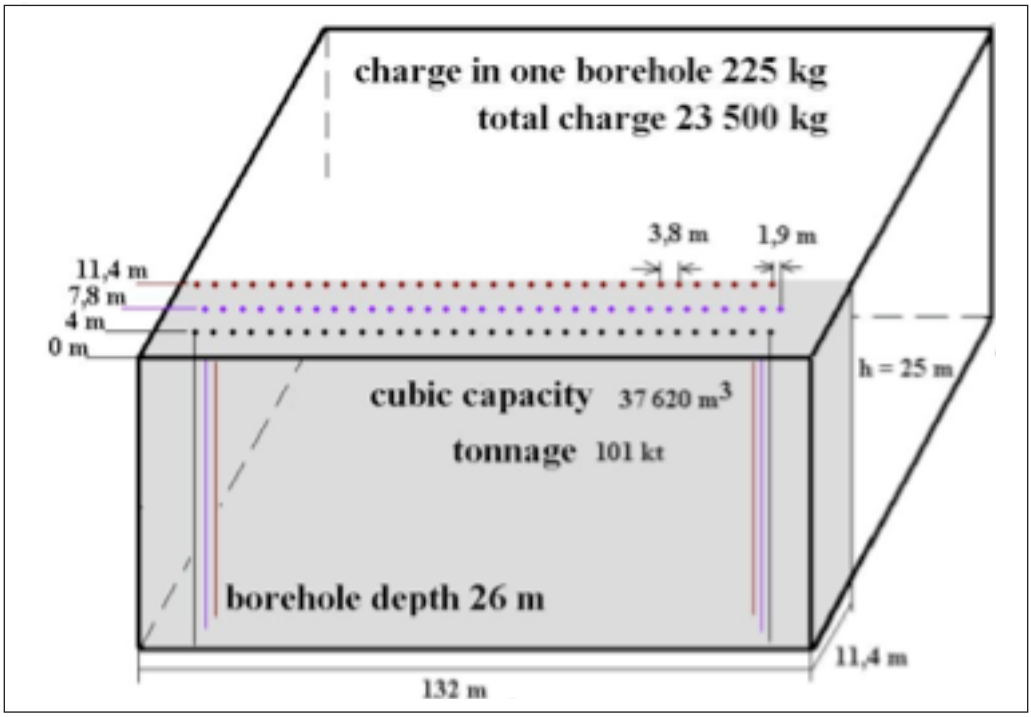

Figure 5b. Parameters of explosive charge during 315 bench blasting at etage 390-415 MASL.

Figure 6. The place of rock blast during CO 320 at etage 390 – 415 MASL.

Figure 7. The place of rock blast during CO 315 at etage 453-473 MASL.


Figure 8a. Standpoint 6 (hay-barn) – seismograph UVS 1504 and seismodetectors of the Swedish company Nitro Consult.

Figure 8b. Standpoint 2 (house Nr. 243. In Vyšná Šebastová village) with record seismic apparatus ZEB/SM – 3C and seismodetectors of Orica Mining Services, Germany.

4. CRITERIA FOR SEISMIC EFFECTS ON PARTICULAR RECEPTOR

The effects of so called technical seismicity, activated by blasting operations are measured and evaluated due to vibration velocity of medium's elements (velocity of amplitude) 'v' based on the maximum value of one of its three components x, y, z. The principle of seismic protection – seismic safety of building objects in face of the technical seismicity is expressed by the following relation: $\mathbf{v \leq v_d}$

where 'v' is the maximum value of component of vibration velocity activated by vibration source at reference standpoint of the protected object. The reference standpoint is the basement of the building. The 'v' value depends primarily on maximum weight of the explosion charge set off in one time stage Qc (kg), maximum distance from the source to the receptor of vibrations L (m) and properties of geological transmitting medium midst source and receptor of vibrations. The 'v' value cannot be determined in advance neither analytically nor empirically using contemporary knowledge. The staunchest way to determine 'v' is by measurement, as it is in our case.

Value '$\mathbf{v_d}$' is the maximum allowed (limiting) vibration velocity for the protected object. At this vibration velocity, no damage of objects will happen – level of damage is 0. Value '$\mathbf{v_d}$' is determined independently on rock blast (before the rock blast) based on practical skills according to different standards (e.g. STN 73 0036) or based on the expertise of specialists. The STN 73 0036 standard concerns relation between vibration intensity expressed by vibration velocity of individual components and possibility of building damage. In accordance with standard and skills acquired by measurement and evaluation of seismic effects in quarries in Slovakia, it is possible to apply the following criteria for brick civil buildings in particular constructional state:

- v = 0 – 10 mm/s
  - no danger of building damage

Table 1. Geodetic data about geophone position during individual rock blasts and characteristics of standpoints

Standpoint	Characteristics of standpoints				Distance from blast to standpoint (m)		note
		x	y	z	slant	horizontal	
0	etage 390-415	1206848,46	255243,2	391,15	0	0	CO 315
1	house. 167 VŠ	1206938,33	256064,22	379,54	832,11	832,02	
2	house. 243 VŠ	1206883,07	257025,57	347,94	1783,25	1782,71	
3	house. 205 VŠ	1207008,66	256593,69	360,20	1360,31	1359,96	
4	house. 178 S	1206203,42	256003,44	344,82	998,08	997,02	
5	house. 197 S	1206124,86	255467,73	370,15	757,92	757,63	
6	hay-barn JRD	1207398,85	255621,32	403,32	667,87	667,76	
0	etage 453- 473	1206842,10	255008,70	453	0	0	CO320
1	house. 255 VŠ	1207346,18	256026,65	381,51	1138,16	1135,92	69,8
2	house. 207 VŠ	1207132,80	256034,18	383,20	1068,17	1065,89	71,49
0	etage 390-415	1206848,46	255243,2	391,15	0	0	CO 321
1	house. 255 VŠ	1207346,18	256026,65	381,51	-	962	69,8

Table explanations: VŠ- Vyšná Šebastová, S-Severná

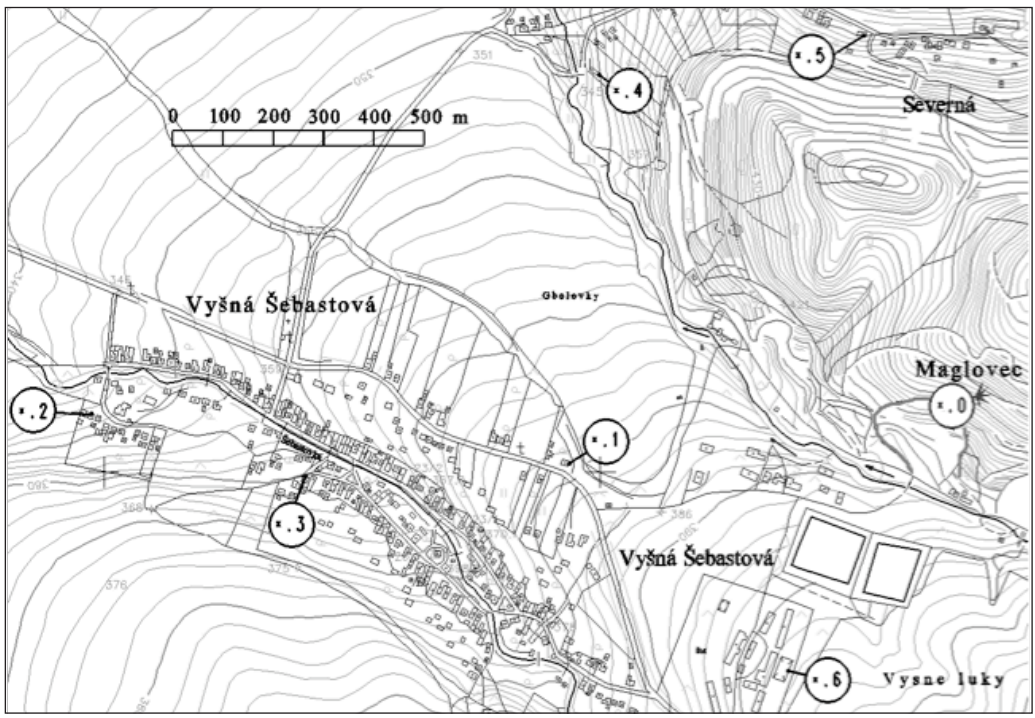

Figure 9. Distribution of six measuring standpoints map during CO 315 (black circles) and point of bench blasting (circle 0).

- v = 10 – 30 mm/s
  - possibility of first signs of damage
- v = 30 – 60 mm/s
  - possibility of slight damage

Based on mentioned facts, concerning a long-term character of rock blasts at the Maglovec deposit and taking into consideration the character of building objects, the maximum allowed vibration velocity for shooting by bench blasting at Maglovec deposit and for building objects in Vyšná

Table 2. Measured values of velocity and frequency during CO 315

standpoint	x Hz	y Hz	z Hz	standpoint	x mm/s	y mm/s	z mm/s
1 (h. 167)	11	7	18	h. 167	0,56	0,70	0,98
2 (h. 243)	-	-	-	h. 243	-	-	-
3 (h. 205)	4	5	42	h. 205	0,31	0,21	0,38
4 (h. 178)	2	3	3	h. 178	0,40	0,29	0,58
5 (h. 197)	5	7	8	h. 197	0,90	1,20	0,90
6 (hay-barn JRD)	11	10	13	hay-barn JRD	1,95	2,15	1,30

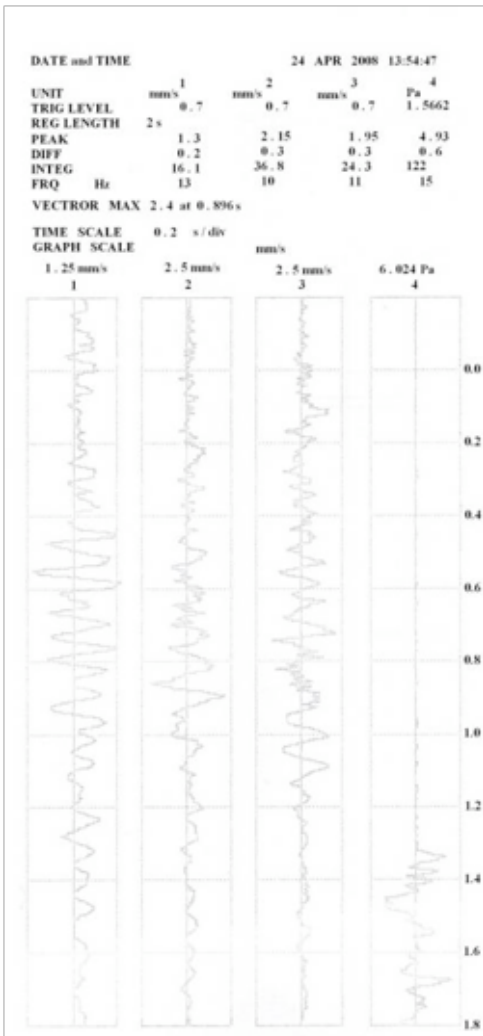

Figure 10a. Graphic records from measurement during CO 315, CO 321, CO 320.

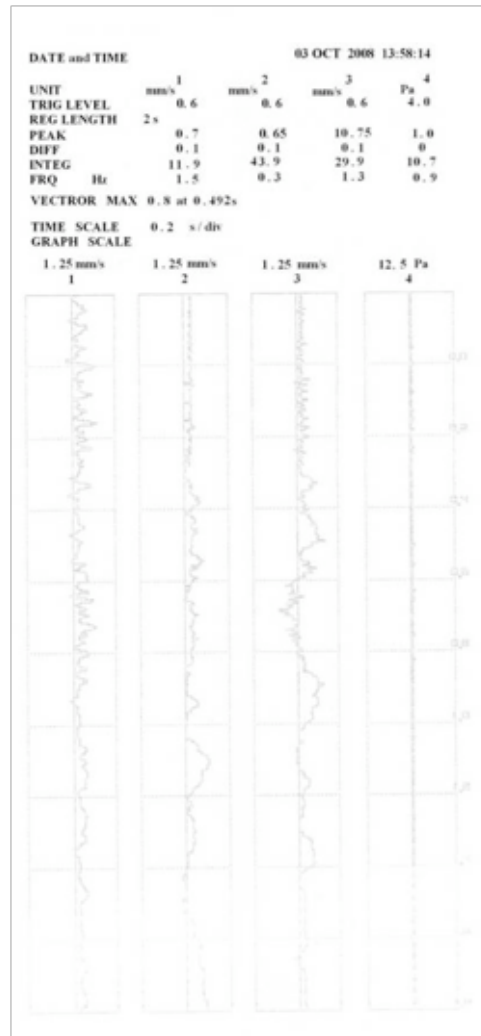

Figure 10b. Graphic records from measurement during CO 315, CO 321, CO 320.

Šebastová village is determined to $\mathbf{v_d} \leq 6$ mm/s.

5. MEASURED VALUES AND ANALYSIS

The maximum measured values of seismic effects activated by bench blasting and realized at the Maglovec quarry till now are mentioned below. These values provided a base for determination of principles for attenuation of seismic waves in the Maglovec quarry (Bartoš 1991, Pandula &

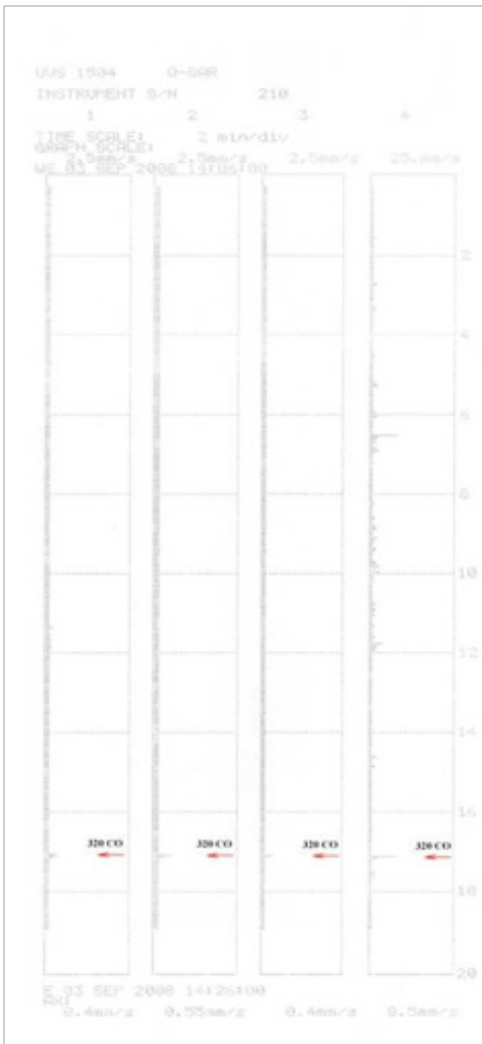

Figure 10c. Graphic records from measurement during CO 315, CO 321, CO 320.

Kondela 2010).

Apparatus set at individual standpoints were calibrated before measurements and responsivity was controlled. Values measured during rock blasts at different standpoints (Figure 10) are presented in Charts 1 - 4. At the standpoint number 6 the graphical trend of individual component of seismic oscillation was recorded. Log number 1 is component 'z', log number 2 is component 'y', log number 3 is component 'x' and log number 4 is recorded oscillation activated by rock blast.

Based on the data measured, a graphic relation of maximum components of vibration velocity on reduced distance during bench blasting was made. The graph in Figure 11 shows the so called principles of seismic waves attenuation for Maglovec quarry in which the value Q was used in form:

$$v = \left(\frac{L}{Q^{0,5}}\right) = K\left[\frac{L}{Q^{0,5}}\right]^{n}$$

where 'v' is maximum velocity of vibration (maximum component of vibration velocity) activated by the blast (mm/s),

- $L/Q^{0,5}$ denotes the reduced distance ($m/kg^{0,5}$)
- L is the distance from the vibration source
- receptor distance (m)
- Q is weight of explosive charge fired simultaneously (kg)
- K is coefficient dependent on conditions of rock blast, properties of transmission of rock environment, type of explosion,etc.
- N is index of seismic waves attenuation

From the principle of attenuation of seismic waves it is possible to determine the amount of explosive charge for a particular receptor for a known distance, under the condition that the maximum values of individual components of vibration velocity does not exceed the maximum determined vibration velocities (STN 730036,1997).

Due to the graphic trend of seismic waves' attenuation principle applied for the Maglovec quarry it follows that the allowed vibration

Table 3. Measured values of velocity and frequency during CO 320.

standpoint	**x Hz**	**y Hz**	**z Hz**	**x mm. s^{-1}**	**y mm. s^{-1}**	**z mm. s^{-1}**
č. 1- house 255	1,3	0,3	1,5	0,60	0,65	0,75

Table 4. Measured values of velocity during CO 321.

standpoint	**x mm/s**	**y mm/s**	**z mm/s**
č. 1- house 255	0,40	0,55	0,40

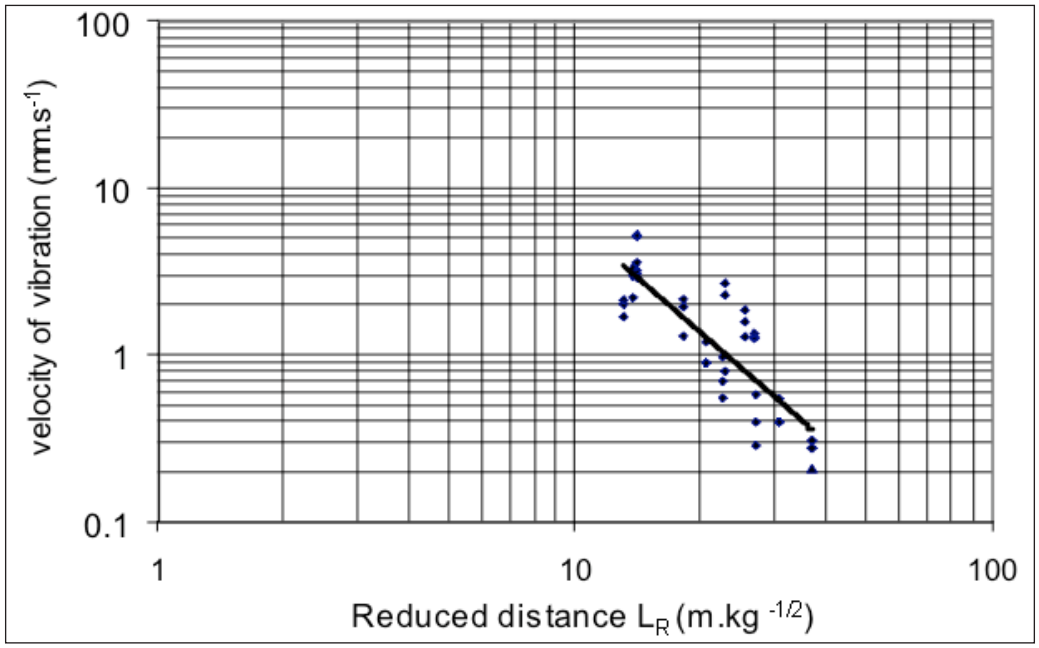

Figure 11. Graphic relation of maximum vibration velocity components at reduced distance during bench blasting in Maglovec quarry – seismic waves attenuation law.

velocity of 3 mm.s^{-1} for frequency lower than 50 Hz and higher than 10 Hz, at maximum allowed explosive charge of 2.440 kg for one time stage will not be exceeded to the distance of 1,150 m. The graph in Figure 11 shows measured values of vibration velocity during bench blasting 321 marked by a point. The lines are boundaries of maximum allowed vibration velocity for this type of foundation soil.

Figure 12 shows attenuation of seismic waves between source and receptor. Rock blasts in different geological media were sources of seismic waves. The parameters of source and receptor were identical in every case (tristichous bench blasting). The transmitting medium and distances between source and receptor were changing. In the first case (CO 315) the source of vibration was situated in unweathered and slightly ruptured environment of diorite porphyrite (I. etage).

In the second case (CO 321) the source was in identical rock environment, only the distance between source and receptor had changed. Both rock blasts CO 315 and CO 321 were located in a way that seismic waves incoming to receptor were not damped by tectonic rupture. The source of vibration in the third case (CO 320) was located in heavy weathered and ruptured diorite porphyrite behind the distinguished tectonic line separating a deposit, the result of which was damping of seismic waves. The measuring apparatus did not evaluate the graphic record of oscillation because the intensity of seismic waves was below the level of its responsivity. Because the frequency of seismic oscillation was not recorded during CO 320, it is probable that attenuation of seismic oscillation was stronger than it was in previous cases (rock blasts). Based on the measurements realized, there can be assumed significant influence of physically different lithologic environment (weathering zone) and tectonic line effects on vibration velocity and attenuation of seismic oscillation activated during blasting operations in the quarry.

After the evaluation of CO 315 (Figure 11), allowed vibration velocity $\mathbf{v_d}$ < 6 mm/s and safe distance source from receptor 750 m were determined.

The evaluation of CO 320 shows that there is a lithological environment in the Maglovec quarry within which attenuation of seismic waves is totally different as it was at CO 315. Therefore, further measurements are necessary to particularise the prediction of harmful effects of seismic waves during bench blasting in Maglovec quarry for surrounding build – up of Vyšná Šebastová village.

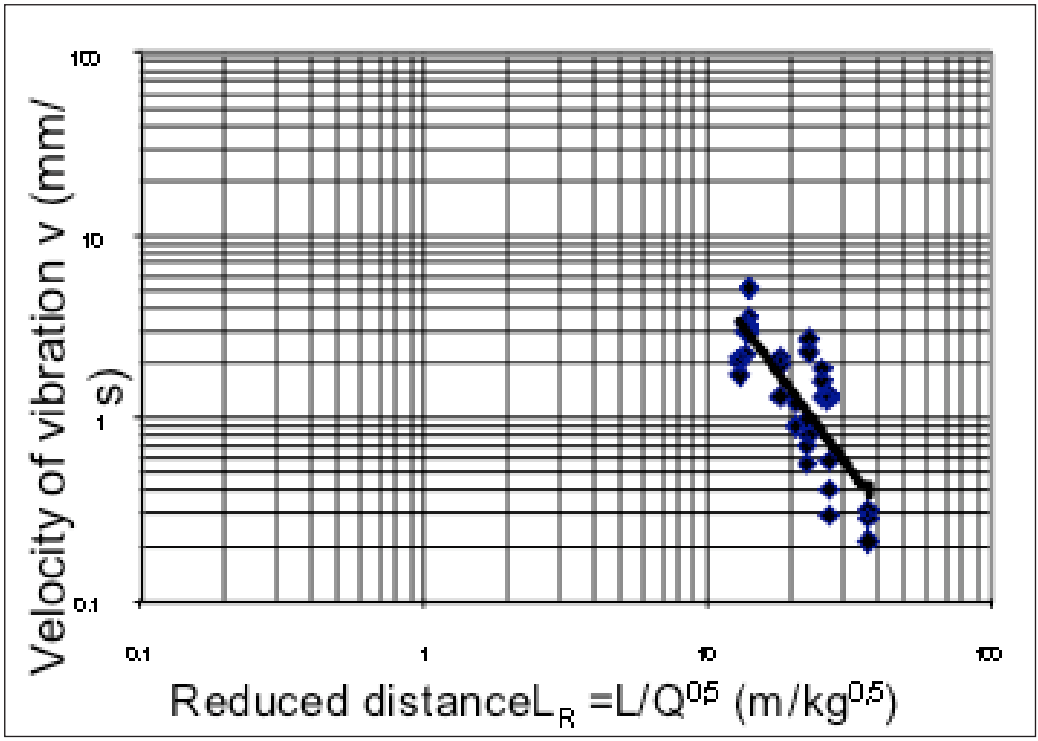

Figure 12a. Graphic relation of maximum vibration velocity components at reduced distance during CO 315 in Maglovec quarry.

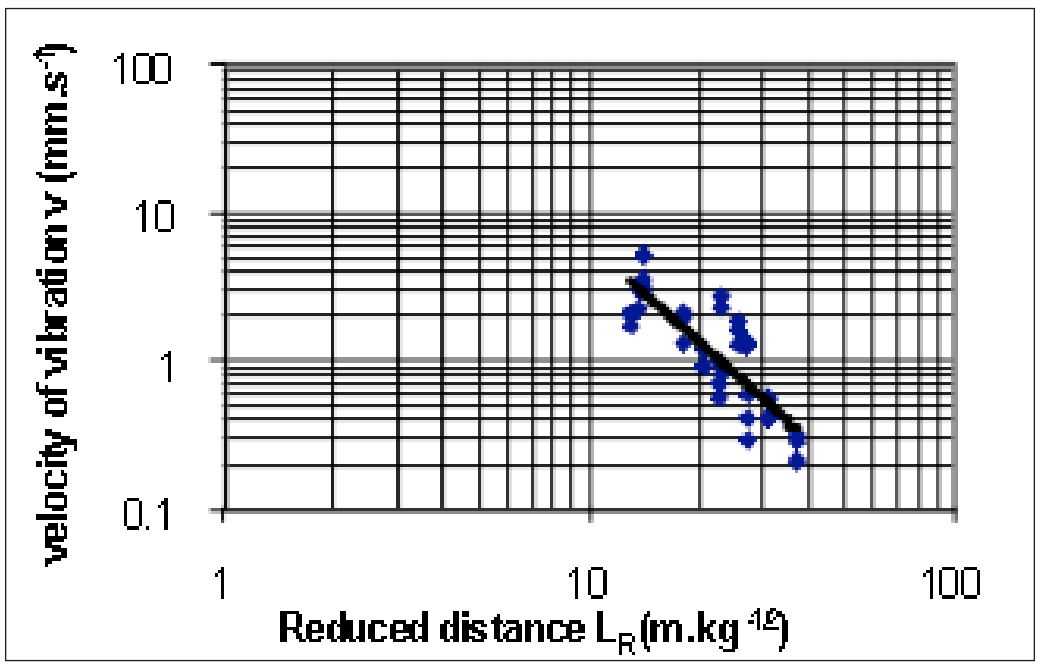

Figure 12b. Graphic relation of maximum vibration velocity components at reduced distance during CO 321 in Maglovec quarry.

After the evaluation of CO 321 (Figure 12) the allowed vibration velocity $\mathbf{v_d}$ < 3 mm/s and safe distance source from receptor 1150 m were determined, by keeping the same parameters of blasting operations.

6. CONCLUSION

Measurements during individual rock blasts CO 315, CO 320, CO 321 have shown significant effect of rupture stage and weathering of solid rock mass to the attenuation of seismic waves activated during blasting operations. It was found out that the attenuation principle for seismic waves formulated due to the only measurement does not take into account effects caused by heterogenity of rock environment.

In the rock environment with different lithology, even if the same parameters of source and receptor are preserved, more measurements are needed to predict negative effects of seismic waves, so that the heterogenity of rock environment is taken into account in attenuation principle of seismic waves.

7. ACKNOWLEDGEMENT

This article was supported by the Operational Programme ITMS 26220220031 Research and Development Grant project VEGA 1/0361/09.

REFERENCES

Bartoš, L. 1991. Zpráva o provedení seizmického merení pri 191. CO v lome Maglovec. Brno 1991, 9 p.

Kaličiak, M., Baňacký, V., Jacko, S., Janočko, J., Karoli, S., Molnár, J., Petro, Ľ., Priechodská, Z., Syčev, V., Škvarka, L., Vozár J., Zlinská, A. and Žec, B. 1991. Vysvetlivky ku geologickej mape severnej časti Slanských vrchov a Košickej kotliny. GÚDŠ, Bratislava, 231 p.

Pandula, B., Kondela, J. and Kotuľak, P. 2008. Meranie vplyvu technickej seizmicity v lome Maglovec na okolitú zástavbu obce Vyšná Šebastová. Výskumná správa ÚGV F BERG TU v Košiciach, Košice, 2008, 9 p.

Podel, R. 1980. Zpráva o provedení seizmického merení pri 60. CO v lome Maglovec. Brno 1980, 5 p.

Pandula, B. & Kondela, J. 2010. Metodológia seizmiky trhacích prác. SSTVP Banská Bystrica, 2010, 156 p.

STN 730036. 1997. Seizmické zaťaženie stavebných konštrukcii, Ústav pre normalizáciu, metrológiu a skúšobníctvo SR, Bratislava, 1977, 68 p.

Lisbon Conference Proceedings 2011, R. Holmberg et al
©2011 European Federation of Explosives Engineers, ISBN 978-0-9550290-3-5

Blasting 60 metres underwater in an environmentally challenging environment

J. Wallace
Wallace Technical Blasting, Inc.

J. Ventress & M. Langen
Global Diving & Salvage, Inc.

C. Breeds, PhD, PE
SubTerra, Inc.

ABSTRACT: The century-old Cheesman Dam on the South Platte River in the Rocky Mountains of Colorado, USA, is the major source of drinking water for 1.4 million people in the City of Denver. The original valves in the dam's three intake tunnels needed to be replaced, requiring drilling and blasting at depths of 18, 47 and 61 meters.

Pollutants of any type were prohibited. Precise final dimensions were required. Explosives and initiation selection were limited by the high water pressures at these depths. Strict overpressure limits were imposed to protect the old valves and to protect fish, resulting in restricted charge weights. The worksite was subject to almost daily lightning storms.

To protect the valves (some as near as 12 meters), inflatable airbags were deployed between the blasts and the valves and a bubble curtain was installed between the blasts and the airbags.

Underwater work was performed by divers using both surface and saturation diving procedures. In saturation diving, the divers remain under pressurized conditions continuously, 24 hours per day for up to 30 days. Measuring, surveying, installation of the drill template, drill operation, loading of explosives charges and mucking the material following the blasts were all accomplished mainly by hand, at depth. Interdisciplinary teamwork under extreme conditions resulted in successful completion of the project within schedule and budget.

1. INTRODUCTION

Cheesman Dam on the South Platte River in the east-central Rocky Mountains of Colorado, USA, was constructed as a water reservoir, beginning in 1898 and completed in 1905. The impoundment serves as a major source of drinking water for the City of Denver, Colorado, with approximately 1.4 million people depending upon Cheesman for their supply, Figure 1.

Figure 1. Cheesman Dam, South Platte River, Colorado. Work barge and crew.

2. THE CHALLENGES

Valves within the dam's intake tunnels had been installed during initial construction. These valves were now showing the effects of a century of operation and replacement was necessary. Due to the necessity to continue to supply water during all construction activities, the reservoir could not be drained. Both rock demolition and installation of the new valves had to take place within the full reservoir pool and intake tunnels. The three intake tunnels were: the Auxiliary Tunnel at a depth of 18 meters, the Mid Level Tunnel at a depth of 47 meters and the Low Level Tunnel at a depth of 61 meters.

The owner contracted with Global Diving & Salvage, Inc. (Global), Seattle, Washington office to perform the necessary work of removing overhanging rocks that threatened the work area, resizing the tunnel openings and installing the new valves. Resizing the portals required rock removal in close proximity to the existing worn and failing old valves, which could not be removed until the replacement valves were operational.

In order to protect the existing valves, Figure 2, a strict vibration limit of 50 mm/second was specified along with a maximum charge weight of 4.5 kg of explosives firing per 8 ms delay. Further a limit of 340 kPa at 20 meters on overpressure to protect the fish within the lake was also specified.

3. BLASTING OPTION SELECTED

Mechanical methods of rock removal were considered. Time and cost were serious issues with mechanical breakage. Blasting was considered but dependent upon resolution of several issues:

- Could a team be found with the varied expertise required to solve the challenges and devise a solution?
- Could a system be devised that would protect the nearby valves from damaging overpressures?
- Could charge weights sufficient to break the rock be used while still staying below the pressure and vibration limits?

Figure 2. Valve being installed during initial construction, 1899.

- Could drilling be accomplished under such adverse conditions within the critical accuracy necessary for both explosives confinement and construction tolerance?
- Could explosives products be found that would perform reliably at these depths and static pressures?
- Could explosives products be found that would perform reliably given the dynamic pressures that would result from firing in close proximity in a water environment?
- Could the charges be constructed on the surface in a fashion that would minimize work and risk for the divers?
- Could a safety program be designed to ensure safety for all, divers, fish and valves?
- Could an insurance company be found that was willing to insure the blasting option?

Global started by interviewing and selecting team members Wallace Technical Blasting, Inc. (WTB) as the blasting contractor and SubTerra, Inc. (STI) as the professional engineer. After careful consideration and calculation of the above challenges, tightly controlled drilling and blasting was selected as the best method to break the rock for removal.

4. THE ROCK

The quantities of rock to be blasted were small, approximately 100 cubic metres, however the type and location made blasting especially challenging. The rock consisted of large-grained granite, varying

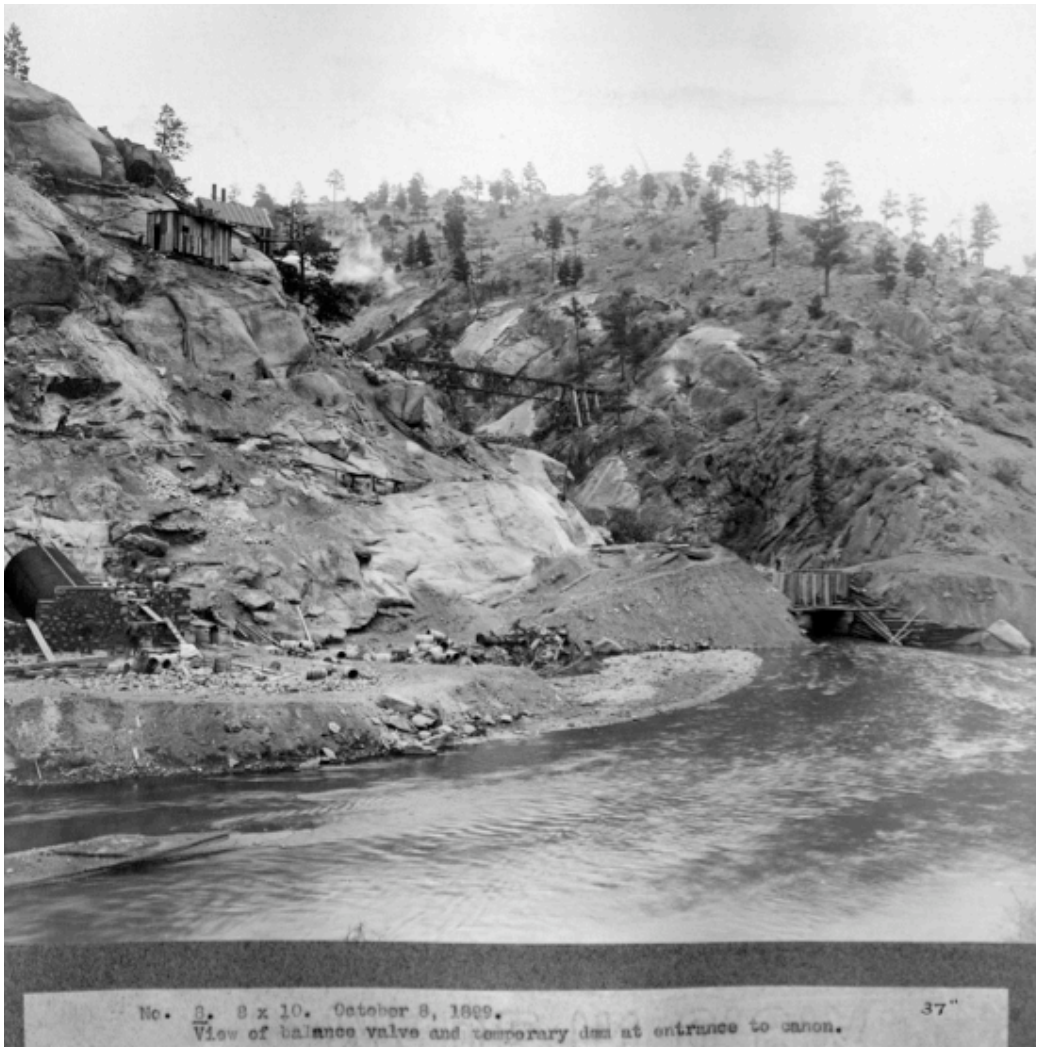

Figure 3. Representative geology of the site, taken during initial construction, now 60 meters underwater.

from massive to areas that were highly fractured by the original tunnel blasting, Figure 3. Rock to be blasted included overhangs above the tunnel portals and rock within the tunnels that encroached upon the space needed for the new valves. Excavation of the blasted material was complicated by the necessity to do most of the excavating manually with divers.

5. EXPLOSIVES SELECTION

Explosives selection was limited by both the work site conditions and contract specifications. These required written confirmation from the manufacturer that the products had been tested and proven to withstand 7 bar of static pressure. This was especially critical for the detonators. Water forcing its way past the boots could lead to misfires. One manufacturer was found who had tested and would certify a single type of their electronic detonators, the Orica i-kon to 10 bar of static pressure.

Small charge-weight cast boosters, 0.15 kg each, were chosen as the main charge. 10-grams per meter detonating cord was selected for threading each individual cast booster in a multiple booster charge and 40-grams per meter detonating cord was used for trim blasting and to

bring the charges up to their calculated full weights.

Long lead, 20 meter, non-electric detonators were selected as fish-scare charges.

6. DIVER CONSIDERATIONS, SURVEYING & LAYOUT

Prior to excavation operations, divers performed detailed surveys of each location to confirm rock geometry as well as establish a baseline for the measure and pay of the rock excavation. At the Auxiliary Level a rock outcropping which extended above the tunnel portal and interfered with the new gate and trashrack required removal. A concrete portal at the entrance to the tunnel which had been constructed in the dry some years previous provided a known datum point from which to perform the survey. Divers installed a fixed, structural steel measurement jig and performed physical measurements at predetermined increments in both the vertical and horizontal. Using these measurements the bathymetry of the outcropping was constructed and the required positioning of blast holes established.

Each slide gate assembly included a stainless steel spool (similar to a gate thimble) which provided a seal surface for the gate and served as a tunnel liner to provide shear resistance, additional tunnel brow support, and to lengthen potential seepage pathways from the reservoir to the tunnel. The portals of the Mid and Low level tunnels required widening in order to accommodate these spools. Divers installed a custom track set plumb and level along the floor of the existing tunnel and aligned with the centerline. A radial measuring jig was moved along the track in one foot increments and measurements taken every 15 degrees to determine the internal geometry of the tunnels. The track would later be used to guide the spool into proper alignment within the enlarged tunnel. Following excavation a final survey was performed to determine the quantity of rock removed at each of the locations.

7. DRILLING CHALLENGES

Accurate drilling was critical for both proper explosives confinement and for final dimensions on the tunnels so that the new spools could be installed properly. Variations in the geology of the rock surrounding each inlet and in the individual tunnel configurations required different drilling techniques for each elevation. Specialized equipment was designed and fabricated to assist divers in performing the work in a safe and efficient manner. Drill template assembly had to be customized for each tunnel, with drills capable of drilling accurately at the various required depths.

The first gate installed was at the Auxiliary Level, using surface diving operations. The relatively shallow water depth over the Auxiliary tunnel allowed use of a surface-deployed air track drill to drill holes for the demolition of the rock outcropping that extended above the tunnel portal. The initial plan was to mount, directly to the outcropping, a template designed to position and guide the drill bit. However, divers found the terrain too steep and rugged to mount the template, so a taut wire grid system was established to define locations of individual holes. Divers then mounted a guide, fabricated on the fly by support crews on the barge, at each location to align the drill bit.

Rock was excavated from the Mid and Low level tunnels by drilling horizontally along the tunnel alignment and placing explosives in the drilled holes. There was concern as to the ability to drill the horizontal holes within the critical accuracy necessary for explosives confinement. Specialized drill string was deployed to keep the drill bit centralized along the alignment of the hole. Several test holes were drilled which verified the ability to maintain accuracy of location along hole depths in excess of fifteen feet.

Horizontal holes were drilled using a TEI 300 hydraulic drifter on a purpose built drill jig and template. The drill jig mounted to the rock face outside the tunnel and provided horizontal and vertical movement so that the diver could precisely position the drill about the tunnel entry. Holes up to twelve feet deep were then drilled parallel to the tunnel alignment. For the Low level a considerable amount of rock and mortared rubble needed removal from around the entrance of the inlet. This required multiple blasts and an extensive vertical drilling program. A jig was designed and fabricated to accommodate the TEI 300 in a vertical orientation. Once again providing movement along two axis so that the diver could precisely position the drill, Figure 4.

Figure 4. Drill assembly with fabricated adjustable template.

8. VALVE PROTECTION BAGS

Guidelines developed by the Canadian Department of Fisheries (Wright and Hopky 1998) were used in conjunction with methods published by the US Army Corps of Engineers (Hempen *et al*. 2005, 2007) to predict overpressure and impulse for each proposed blast configuration and at each required blast location. Potential impacts were predicted and a combination of blast protection bags and an air bubble curtain were designed and used to mitigate impacts.

Inflatable blast protection bags were manufactured by Carter Lift Bag to fit the inside dimensions of each tunnel when expanded. Bags were made from heavy duty, vinyl coated polyester having a tensile strength of 550 kg/cm; this is the same material used to manufacture heavy lift bags used in diving salvage operations. Blast bag performance was analyzed by comparing the bag's load bearing resistance to the applied loads estimated from predicted water overpressures. Bag resistance was calculated from the inflation pressure and the area of the bag in contact with the tunnel perimeter assuming a friction coefficient of 0.3.

Bags were installed with 13 kPA (2-psi) overpressure valves to allow bleed off during ambient pressure reduction realizing that the spring loaded overpressure valve would probably not release given an expected impulse duration of less than one millisecond. One, two, or three blast protection bags were installed in series with a bubble curtain between the blast and the closest air bag for insurance.

The system performed as predicted with no impacts to the fragile downstream structures even though a blast overpressure over 690 kPA (100 psi), without mitigation, was predicted in the narrow submerged tunnels, Figure 5.

9. FISH CONSIDERATIONS

The reservoir is an important recreational trout fishery. The owner stipulated a maximum limit

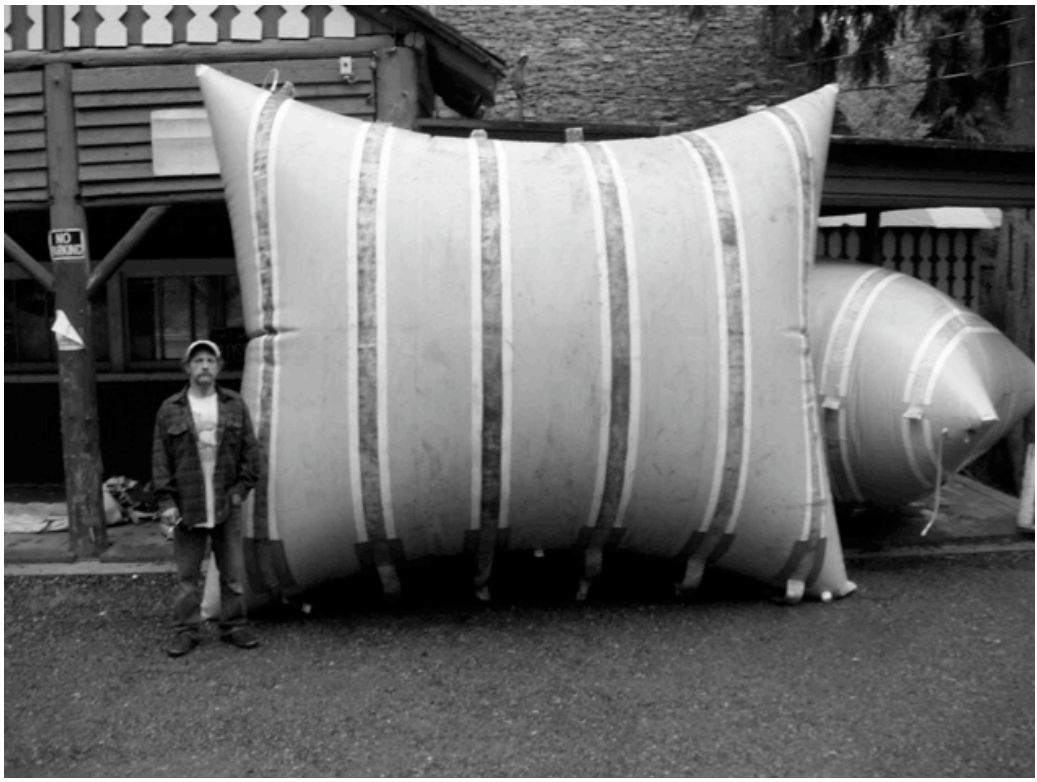

Figure 5. Air bags being tested on the surface prior to installation.

water over-pressure/under-pressure of 340 kPa at 20 meters. A single non electric detonator was fired 2 minutes prior to the main blast as a means to scare off any fish near the work area.

Additionally, due to the necessity to use small charge weights to protect the valves and that the charges were confined within stemmed drill holes for all blasting meant that this conservative fish protection limit was met on all blasts and no fish were injured by any blasts.

10. LIGHTNING ISSUES

Given the geographic jobsite location and the fact that the majority of the blasting took place during the summer meant that daily lightning storms could be expected, and did occur. One strike interfered with non-blasting work, damaging a submersible and injuring an employee of a subcontractor working with the dam itself. This incident heightened attention to the possibility of lightning damage.

Weather forecasts were monitored, and all blasting scheduled for mornings, prior to the typical mid to late afternoon arrival of lightning storms. Two lightning detectors were always aboard, one of which was worn personally by a member of the blasting crew.

Due to the long 29-hour time period necessary to load and fire the final blast, we did work during the hours that storms were most common. One storm approached to within range for concern so the divers were evacuated to the surface barge for approximately one hour during passage of the storm. Once conditions were deemed safe, the divers returned and completed the blasthole loading. Attention to a known hazard and following industry standard guidelines proved prudent.

11. DIVER CONSIDERATIONS FOR ROCK EXCAVATION

Since rock excavation would be done mainly by hand by the divers it was important that the fragmentation be small. Several factors worked to that result. The drill pattern was tight, 0.3 meters on the trim, and the charges were nearly full-

Figure 6. Prep bench with assembled individualised charges ready for lowering to divers.

column loads, albeit light. Problems arose with the quantity of muck produced by the blasts. Although the fragmentation was reasonable even small quantities of rock landing within the tunnels made for dangerous, time consuming work.

A cable blasting mat was installed within the tunnels prior to firing the blasts, the purpose of which was to allow the barge-mounted crane to pull the mat from within the tunnel while loaded with the blasted muck. This effort was only marginally successful due to weight, lifting limitations and friction along the tunnel. The divers ended up performing more hard physical work during the excavation than had been hoped for.

12. COMPILING THE PIECES OF THE SOLUTION

The keys to success on the project were teamwork and flexibility. Each tunnel presented unique challenges that the diving/general contractor had to solve. Those challenges included two different drilling methods, one from the surface on the shallower tunnel, and underwater drilling on the lower 2 tunnels. Drill templates had to be custom designed and constructed for each of the lower 2 tunnels.

Explosives, especially long legwire detonator, availability was also an issue. We ended up using every 80- meter legwire detonator to be found in North America. Following the change order for additional blasting at the Lower tunnel, the explosives supplier canvassed all known users and found just enough detonators to complete the job.

13. MAKING IT ALL WORK

Discussions on how to make the project work began prior to bid. Had the project team not felt we could perform the work safely and successfully, Global would not have presented a bid to the owner that included blasting.

Once the drilling challenges had been solved, it fell to the blasting crew to devise a method for

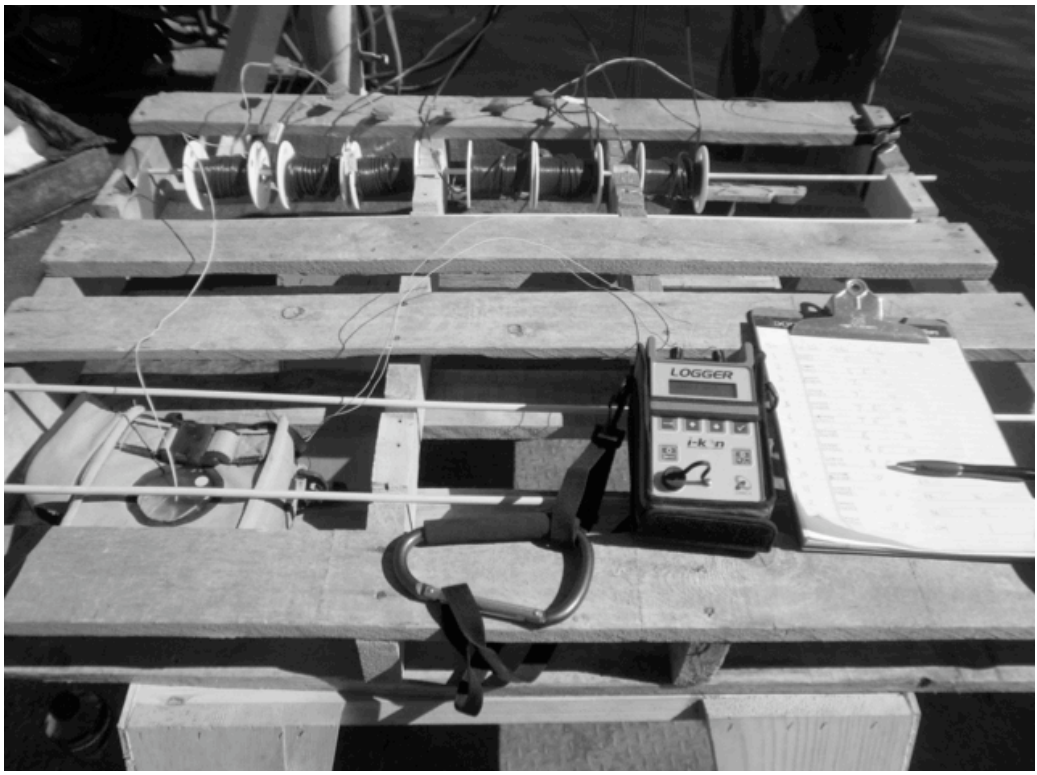

Figure 7. Spool rack tester and paper log during loading.

preparing the charges in such a way that would minimize diver workload and eliminate potential problems. A good drilling log was kept. A blast plan was drawn up for each blast with the specific charge length and weight designed for each individual hole.

On each blast day, the blasting crew of 4 assisted by any available deckhands put together a reusable prep bench on board the work barge. Charges were constructed by the blasting crew by taping the charges to light wood dowels for the first few blasts, then a change was made to use light, flexible plastic piping, cut to the proper length, to which the charges were taped, Figure 6.

The charges were lowered one at a time by the deckhands along a lowering line affixed to the barge and to an anchor at the blast site in the sequence requested by the diver. Two members of the blasting crew managed the detonator leadwire spools during the lowering. The diver inserted the charge into the proper drill hole, then informed the blasting crew. A blasting crew member on the surface then clipped the detonator onto the trunk line and tested the detonator to ensure that a signal could be read. Upon a positive response, a surface blasting crew member programmed the appropriate delay timing into the electronic detonator. Once the detonator was successfully timed and tested, the diver installed a hole plug and underwater grout for stemming then moved on to the next hole.

The blasting log contained all pertinent blasthole loading information including detonator serial number as well as delay timing and into which hole the charge had been loaded. Any changes from the plan were duly noted.

After the entire blast was loaded, a complete test of all detonators was again run prior to having the diver return to the surface. One of the advantages of the detonator system used was that the testing instrument could not inadvertently charge and fire the detonators. That took a distinctly different machine which was kept in a secure location until the diver was on the surface, Figure 7.

Figure 8. Retrieved old valve with a small part of the overall team.

After the diver surfaced, the blast area was secured, seismic instruments turned on and water overpressure gauges lowered from the barge at measured distances. Following the blast warning signal the fish-scare detonator was lowered and fired at a safe distance from the blast detonator leadwires. In the 2 minutes between the fish-scare charge firing and the main blast firing, all the detonators were tested again, then wired into the blasting machine for completion of the blasting cycle.

A total of 9 blasts were fired with charge weights varying from 0.45 kg per cubic meter to 1.35 kg per cubic meter in the mass excavation. Trim blast charge weights varied from 0.13-40 kg per linear meter of hole. The higher charge weights were used at the greater depths. Breakage was acceptable throughout.

Pre-compression failure of a detonator in blast #2 lead to changes. Two detonators were installed in each string charge, and staggered within the column so that adjacent holes did not have primers at the same locations in the string. Timing was reduced to 3ms as well. No further pre-compression failures were found.

14. CONCLUSION

Training the divers to drill and load blast holes was clearly necessary, and was begun at project start up. The divers were highly experienced and accustomed to learning new skills and following job-specific procedures. As a result, drilling and loading proceeded with few problems despite the difficult working conditions at these depths. There is no room for error when working under the conditions faced in this project. The great water depth coupled with the close proximity of fragile, failing structures nearby presented unique challenges.

Teamwork, training, flexibility and attention to detail by skilled workers attuned to safety was key to the successful conclusion of the project, Figure 8.

15. ACKNOWLEDGEMENTS

Susan McAdams, editing; and Tobias Wallace, technical assistance.

REFERENCES

Hempen, G.L. & Ruben, H.J. 2005. Underwater Blast Pressures from Confined Rock Removal Shots. The Kill Van Kull Deepening Project. *Proceedings, ISEE*, 2005, Volume 1.

Hempen, G.L., Keevin, T.M. & Jordan T.L. 2007. Underwater Blast Pressures from a Confined Rock Removal During the Miami Harbor Deepening Project. *Proceedings, ISEE*, 2007, Volume 1.

Wright, D.G. & Hopky, G.E. 1998. Guidelines for the use of Explosives in or near Canadian Fisheries Waters.

Lisbon Conference Proceedings 2011, R. Holmberg et al

Vibration velocities resulting from the use of explosives in different rock masses.

F. Tavares de Melo
MaxamPor, S.A., Lisboa Portugal
C. Galiza & A. Vieira Instituto Superior Engenharia, Porto

ABSTRACT: The work presents a study of the vibration particle velocity resulting from the use of explosives in different rock masses. This study was performed on three kinds of rock masses, such as granite, limestone and quartzite. There has been a monitoring phase and data collection phase in each situation. Three different laws of propagation of vibration velocity, Johnson (1971), Langefors & Kihlström (1978) and Chapot (1981) were used to calculate their site specific constants by statistical method of multiple linear regressions. After obtaining the constants, studies were made to predict the particle velocities when applying the same explosive charges in the rounds. The vibration values obtained in each round for each kind of rock mass were measured and the two equations compared to register which one had the smaller deviation. This study shows that the Johnson equation appears to be better at predicting the vibration velocities because it had the smallest deviation acting favourably at a no-damage safety perspective. Using the Langefors equation as a predictor gave good results when applying the safety coefficient of 90 % of the highest particle velocity value obtained in the tests. In conclusion this last predictor can easily be used with good results for preventing vibration damage. The constants were used as a base for the daily work and could be used in future works for the same kind of mass and location. In future projects it would be useful to compare with different laws like Chapot (1971), and create a vibration descriptor map for each location.

1. INTRODUCTION

The movement of rock masses became central to the implementation of major projects such as tunnels, roads and dams. The importance of quality, safety and environment, becomes essential from the beginning to the end of each project to ensure the least impact on the surrounding environment, people and goods. It is already common practice in geotechnical studies to use explosives in areas with several constraints, causing potential environmental impacts in particular vibrations in structures. The operation of rock blasting moves rock masses. This often causes various side effects affecting directly the surrounding environment and sometimes restricting and hindering the implementation of projects.

Based on this it becomes essential to find a method of recording and quantifying the side effects caused by the use of explosives. This approach will register the velocity of vibration caused on the ground after the detonation, which will serve to evaluate and anticipate side effects and possible damages occurring while performing the work.

Standard scaling laws of charge weight are used commonly in the prediction at ground level.

2. OBJECTIVE

This work aims to characterise the attenuation law of propagation speeds of vibration of some rock masses. This characterisation is performed by a linear regression on the formula of Johnson, Langefors and Chapot characterised later in this work.

Through the formulation of the law, the value of vibration is achieved by setting the maximum amount of explosives to be used at any given time, ensuring minimal environmental impact associated with the standard Portuguese Norm.

The aim of this study was to identify which of the formulas is the best for each type of mass studied, using real data from several blasts done in different types of geological mass (quarries and construction sites).

3. PREVENTION

Before the execution of each project it is necessary to choose the excavation method, in accordance with technical and environmental factors. Therefore, knowledge of geotechnical and mechanical properties of the soil where the project will be executed will provide valuable information for selecting the excavation method.

According to Olofsson (1997) environmental impacts associated with this activity can easily be controlled if the following additional information of the site is provided:

- Features of the rock mass;
- Geology of the foundation, land and surrounding structures;
- Knowledge of the exact distance between the detonation and monitoring points;
- Quantity of explosives applied per delay;
- Degree of the explosive charge confinement.

Knowing these properties will permit damage control so as to avoid all the negative impacts related to the use of explosives in surrounding populated areas.

4. SEISMIC PROPAGATION EQUATION

The amplitude of vibration expressed in particle speed, depends fundamentally on the magnitude of the explosives charge weight and distance between the monitoring and detonation points, which can be mathematically written as:

$$V = a\, Q^b R^c \tag{1}$$

Where V is the maximum amplitude of particle velocity, Q the weight of explosives detonated per delay and the distance R between the point of detonation and registration. The parameters a, b and c are constants dependent on the locale and diagram of wave propagation.

Several authors acknowledge that this formula, named Johnson, is the most commonly used equation to define the propagation law of velocity. It is important to note that this kind of equation defining the vibration velocity is dependent on the maximum instantaneous delay and not on the total amount of charge used in the blast (Blair 1990).

Knowing the values of the distance and the maximum allowable vibration it is possible to calculate the maximum charge that should be applied per delay. Initially it is necessary to have clear values of the constants or define them by linear regressions after execution of blasting tests. The techniques of statistical regression applied in the management of data of the field which provide, after applying the minimum squares method, the characteristic constant values for the real situation in analysis. Knowing the values of the vibration obtained in each blast, correlated with the distances between the detonation and monitoring points and the charges detonated by delay.

The definition of the constants is established with the best correlation coefficient of all and then the propagation law of vibrations is defined, as well as the characteristic of each place and the lithology in question (Bernardo 2004). This mathematical correlation between the variables is valid for each rock type and for each direction of space. Once the boundary to comply with this methodology is identified, the prevention of damage is determined by the law of propagation of vibrations specific to each site and can extrapolate the maximum charge per delay according to the distance between the point of detonation and the structure to be protected.

Another methodology for determining the mass transfer coefficient is based on the use of Langefors formula to determine the vibration velocity directly from the explosive charge and the maximum distance from the detonation to the monitoring point.

$$V = K \sqrt{\frac{Q}{R^{\frac{3}{2}}}} \tag{2}$$

Q corresponds to the maximum load detonated per time, R the distance between measurement and detonation points and K to the constant of transmission coefficient of the soil, which depends on the homogeneity of the rock and the presence of fissures and faults.

The relationship between load and distance can be used to build simple tables that can be very useful in planning blasts. These tables that describe the value of vibration velocity and the relation between load and distance are used to determine the coefficient of transmission of the ground (K). This will be determined with experimental sections and continuous and rigorous seismographic monitoring. This coefficient will depend directly on the characteristics of the soil. Loose materials have low transmission coefficient as the homogeneous rock has higher values (Olofsson 1997). This coefficient also depends on the existing cracks in the massive and will be reduced as the number of fissures increase. Once again, similarly to Johnson's equation, the vibration velocity depends on the maximum instantaneous charge.

Another example of the definition of one of the parameters related to the properties of vibration transmission can be calculated using linear regression of Chapot formula.

$$V = K \left(\frac{R}{Q^{0.5}} \right)^{c} \quad (3)$$

Q corresponds to the maximum load detonated per time, R the distance between measurement and detonation points, K to the coefficient of transmission of the soil and c the coefficient of attenuation of the soil. These two values depend on the homogeneity of the rock and the presence of fissures and faults.

These kinds of formulas produce a large amount of scatter data due to many influences like the type of detector, delay and initiation times and waveform attenuation (Blair 1990).

5. MONITORING

The continuous monitoring of vibrations is required since the dynamic characterisation of the soil where the project will grow is unknown. There is no descriptive law for the propagation of vibrations for one particular mass and without this it is difficult to preview the effects caused by excavation (Jimeno *et al*. 2003).

The geophones should be located in structures or sensitive areas in the area surrounding the excavation from where complaints of nuisance could be expected. The parameters that must be monitored are:

- Vibration wave propagation resulting from the three main components of the space;
- Distance between the detonation and monitoring points;
- Quantity of explosives per delay.

6. FIELD TESTS

The first blasts carried out should be experimental measurements of vibrations and should be used as a guide for planning the optimisation of the extraction process. These results should be constantly used as a way to reach the economic level between the stages of drilling and blasting. It should, however, leave some margin of safety in relation to the value obtained and the attenuation coefficient calculated to avoid the appearance of some factors that change the previous vibration level (Jimeno *et al*. 2003). The determination of dynamic properties due to the recurrence of the massive records of vibrations, serve to characterise the type of rock present and to predict the mechanisms of propagation and attenuation of vibrations on the ground.

The statistical tests applied to this data are not used to detect trends of each property but only to lump all the variation of properties in one single velocity law (Blair 1990)

The following plan for testing must be followed:

- Definition of monitoring structures;

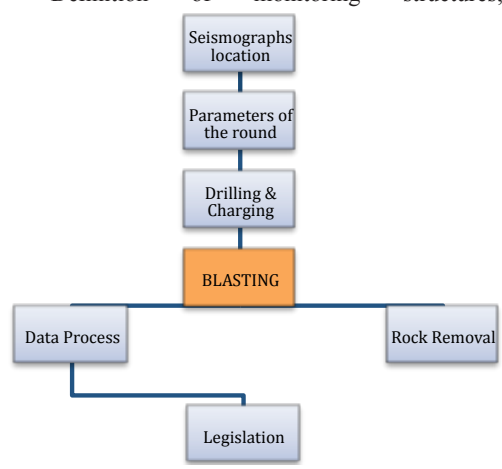

Figure 1. Flowchart of the test plan.

Table 1. Specifications of the explosives used in the tests:

Explosive type	ANFO	Emulsion	Bulk Emulsion	Watergel
Density (g/cm3)	0,85	1,2	1,15	1,25
VOD (m/s)	3000	5600	4200	5000
Total Energy (kJ/Kg)	1078	3600	3600	4400
Calibre used (mm)	Bulk	60; 70	bulk	60; 70
Cartridge Length (m)	-	0,5	-	

- Distribution of equipment by the places of monitoring;
- Definition of geometrical parameters of the blast;
- Drilling, loading and detonation;
- Data processing and checking with the Portuguese Norm;
- Changes in the geometrical parameters of the blast if necessary.

6.1 Test A

The massive studied is in the complex morphology of schist with quartzite. The blast tests were executed only on the quartzites. These sites are essentially hard rock with some embedded shales. In this rock mass all the rounds were loaded with cartridge emulsion and ANFO.

Table 2. Vibration values for rock mass A.

Date	Q (kg / delay)	R (m)	v (mm/s)
10-Ago	48,4	335	2,45
28-Ago	43,2	326	1,75
08-Sep	58,8	392	1,17
10- Sep	61,2	326	2,35
15- Sep	43,2	375	1,6
17- Sep	38	380	1,5
22- Sep	38	355	2,23
28- Sep	45,8	225	2,34
01- Oct	61,3	241	1,92
08- Oct	38	229	3,89
12- Oct	14,28	47	6,99
14- Oct	48,4	102	5,78
15- Oct	37,5	62	9,8
16- Oct	7,14	52	4,6
19- Oct	7,14	37	6,02

The values obtained with the use of the seismograph No. 1 are in Table 2::

Once we have these values for the parameters v, Q and R, the determination of the constants a, b and c will be done using the linear regression method. The application of a numerical method of linear regression to the propagation law requires the use of logarithms in all the terms of the equation in order to transform all exponents in coefficients constants.

Table 3.Values of constants in the equation of Johnson rock mass A.

$\mathbf{a = 10^{b0}}$	88,61352
$\mathbf{b = b_1}$	0,397998
$\mathbf{c = b_2}$	-0,929721

$$v = 88{,}6135\ Q^{0{,}398}R^{-0{,}9297} \quad (4)$$

After this, a calculation was used to the different values of the constant transmission of vibrations on the ground (K) which is also determined by linear regression method. Therefore, for the purpose of calculating the predictor of vibration velocity using the Langefors equation, the previously calculated K was considered.

Table 4. Langefors transmission of vibration constant calculated for rock mass A.

K
29,6388

$$V = 29{,}6388\sqrt{\frac{Q}{R^{\frac{3}{2}}}} \quad (5)$$

Using linear regression methods, the different values of the constant transmission and attenuation of vibrations on the ground (K and c) were defined. Therefore, for the purpose of calculating the predictor of vibration velocity using the Chapot equation, the previously calculated K and c were considered.

Table 5. Chapot transmission and attenuation of vibration constants calculated for rock mass A

K	C
76.2656	-0.9489

$$V = 76{,}2656 \left(\frac{R}{Q^{0{,}5}}\right)^{-0{,}9489} \quad (6)$$

Table 6. Differences and comparisons of values from the equations.

		Johnson	Langefors	Chapot	V REAL (mm/s)	Dev Johnson	Dev Langefors	Dev Chapot
R (m)	Q (kg)	V (mm/s)	V (mm/s)	V (mm/s)				
335	48,4	1,8647	2,6333	1,9297	2,45	0,5853	0,1833	0,5203
326	43,2	1,8281	2,5392	1,8763	1,75	0,0781	0,7892	0,1263
392	58,8	1,7409	2,5798	1,8232	1,17	0,5709	1,4098	0,6532
326	61,2	2,0992	3,0222	2,2134	2,35	0,2508	0,6722	0,1366
375	43,2	1,6051	2,2860	1,6428	1,6	0,0051	0,6860	0,0428
380	38	1,5067	2,1228	1,5265	1,5	0,0067	0,6228	0,0265
355	38	1,6051	2,2340	1,6283	2,23	0,6249	0,0040	0,6017
225	45,8	2,6404	3,4527	2,7426	2,34	0,3004	1,1127	0,4026
241	61,3	2,7811	3,7938	2,9506	1,92	0,8611	1,8738	1,0306
229	38	2,4120	3,1037	2,4684	3,89	1,4780	0,7863	1,4216
47	14,28	7,1208	6,2395	6,9725	6,99	0,1308	0,7505	0,0175
102	48,4	5,6283	6,4244	5,9647	5,78	0,1517	0,6444	0,1847
62	37,5	8,0768	8,2145	8,4759	9,8	1,7232	1,5855	1,3241
52	7,14	4,9230	4,0898	4,5592	4,6	0,3230	0,5102	0,0408
37	7,14	6,7537	5,2791	6,2972	6,02	0,7337	0,7409	0,2772
					Deviation average	0,5216	0,8248	0,4538

Comparing in a graph the values obtained with the values expected in all the formulas concludes that, Chapot causes a smaller difference between the real values.

6.2. Test B

The geological nature of this soil is fundamentally solid granite with small massive rocks. It is a grey

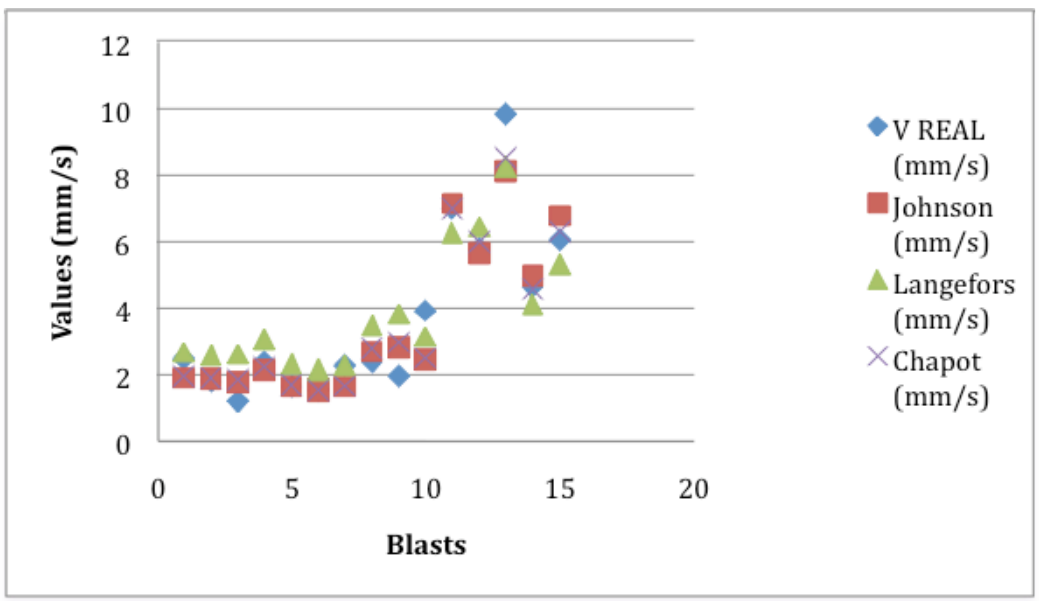

Figure 2. Chart comparing the values of the real and expected vibration in rock mass A.

type of granite with medium to fine grade with the presence of mica and slightly porphyritic. This is a type of rock from the group of the calc alkaline granites tardi post tectonic in relation to the third phase of the orogen Hercynian.

In this rock mass all the blasts were done with Bulk emulsion.

Table 7. Vibration values in rock mass B.

Date	Q (kg / delay)	R (m)	v (mm/s)
10-Nov	55,65	288	4,87
25-Jun	53	323	2,27
04-Jun	53	150	8,82
01-Feb	53	360	1,95
07-May	63,5	365	1,96
24-May	63,6	304	3,15
10-Oct	63,6	298	3,51
09-Feb	63,6	311	3,93

Table 8. Values of constants in the equation of Johnson rock mass B.

$a = 10^{b0}$	1282,2369
$b = b_1$	1,003
$c = b_2$	-1,7668

$$v = 1282{,}2369\ Q^{1{,}003} R^{-1{,}7668} \quad (7)$$

Table 9. Langefors transmission of vibration constant calculated for rock mass B.

K
36,7159

$$V = 36{,}7159 \sqrt{\frac{Q}{R^{\frac{3}{2}}}} \quad (8)$$

Table 10. Chapot transmission and attenuation of vibration constants calculated for rock mass B.

K	C
2024.5633	-1,7586

$$V = 2024{,}5633 \left(\frac{R}{Q^{0{,}5}}\right)^{-1{,}7586} \quad (9)$$

Table 11. Differences and comparisons of values from both equations

		Johnson (mm/s)	Langefors (mm/s)	Chapot (mm/s)	V REAL (mm/s)	Dev Johnson	Dev Langefors	Dev Chapot
R (m)	Q (kg)	V (mm/s)	V (mm/s)	V (mm/s)				
288	55,65	3,2615	3,9178	3,2815	4,87	1,6085	0,9522	1,5885
323	53	2,5361	3,5082	2,5695	2,27	0,2661	1,2382	0,2995
150	53	9,8333	6,2363	9,9004	8,82	1,0133	2,5837	1,0804
360	53	2,0938	3,2342	2,1234	1,95	0,1438	1,2842	0,1734
365	63,5	2,4496	3,5037	2,4295	1,96	0,4896	1,5437	0,4695
304	63,6	3,3892	4,0219	3,3557	3,15	0,2392	0,8719	0,2057
298	63,6	3,5107	4,0824	3,4754	3,51	0,0007	0,5724	0,0346
311	63,6	3,2556	3,9538	3,2240	3,93	0,6744	0,0238	0,7060
					Deviation average	0,5544	1,1338	0,5697

Comparing in a graph the values obtained with the values expected in all formulas concludes that, Johnson causes a smaller difference between the real values.

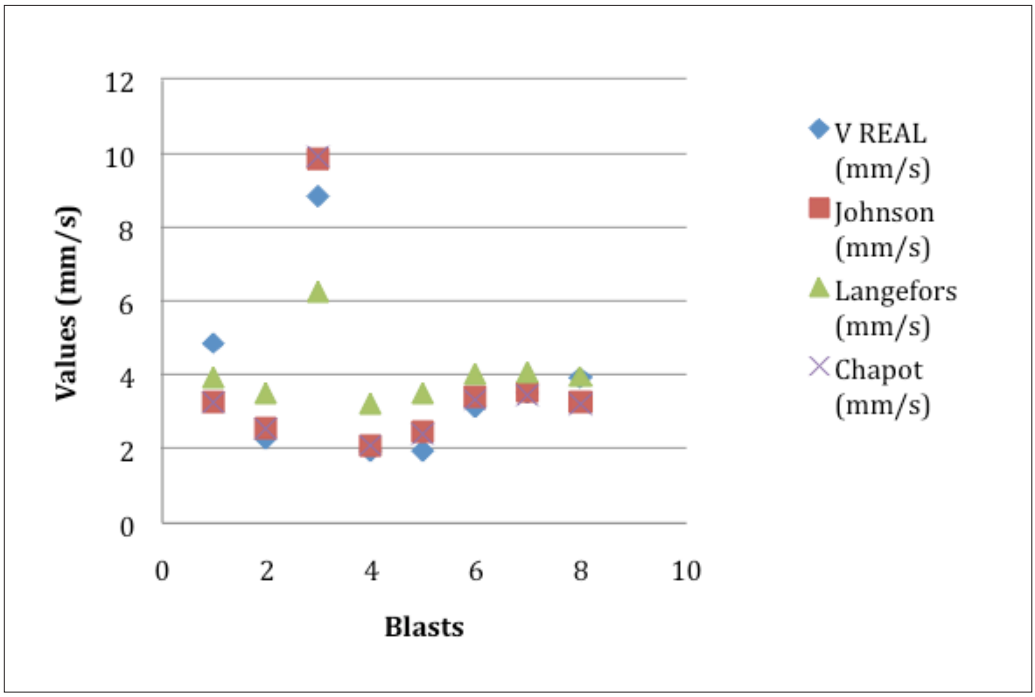

Figure 3. Chart comparing the values of the speed of vibration and the expected in rock mass B.

6.3. Test C

This formation consists of calcareous detrital clay, marl and sandstone.

The explosives used in this blast were a combination of cartridge Watergel at the bottom and ANFO in the column.

Table 12. Vibration values in rock mass C.

Date	Q (kg / delay)	R (m)	v (mm/s)
04-Mar	54,1	275	4,94
11-Mar	55	700	2,08
05-Feb	48,33	220	6,52
05-Feb	100	180	8,89
04-Mar	37,5	200	7,05
08-Jun	47	285	3,98
16-Jul	48,33	520	2,13
16-Jul	48,33	520	2,05
30-Oct	42,5	300	3,06

Table 13. Values of constants in the equation of Johnson rock mass C.

$a = 10^{b0}$	622,8508
$b = b_1$	0,3251
$c = b_2$	-1,1002

$$v = 622{,}8508 Q^{0{,}3251} R^{-1{,}1002} \quad (10)$$

Table 14. Langefors transmission of vibration constant calculated for rock mass C.

K
45,3252

$$V = 45{,}3252 \sqrt{\frac{Q}{R^{\frac{3}{2}}}} \quad (11)$$

Table 15. Chapot transmission and attenuation of vibration constants calculated for rock mass C.

K	C
2024.5633	-1,7586

$$V = 208{,}9915 \left(\frac{R}{Q^{0{,}5}}\right)^{-1{,}0459} \quad (12)$$

Table 16. Differences and comparisons of values from both equations.

R (m)	Q (kg)	Johnson (mm/s) V (mm/s)	Langefors (mm/s) V (mm/s)	Chapot (mm/s) V (mm/s)	V REAL (mm/s)	Dev Johnson	Dev Langefors	Dev Chapot
275	54,1	4,7204	4,9367	4,7341	4,94	0,2196	0,0033	0,2059
700	55	1,6977	2,4700	1,7972	2,08	0,3823	0,3900	0,2828
220	48,33	5,8168	5,5161	5,6361	6,52	0,7032	1,0039	0,8839
180	100	9,1883	9,2233	10,1687	8,89	0,2983	0,3333	1,2787
200	37,5	5,9485	5,2190	5,4532	7,05	1,1015	1,8310	1,5968
285	47	4,3356	4,4798	4,2370	3,98	0,3556	0,4998	0,2570
520	48,33	2,2576	2,8937	2,2922	2,13	0,1276	0,7637	0,1622
520	48,33	2,2340	2,8730	2,2694	2,05	0,1840	0,8230	0,2194
300	42,5	3,9658	4,0992	3,8098	3,06	0,9058	1,0392	0,7498
					Average deviation	0,4753	0,7430	0,6263

Comparing in a graph the values obtained with the values expected in all formulas concludes that, Johnson causes a smaller difference with the real values.

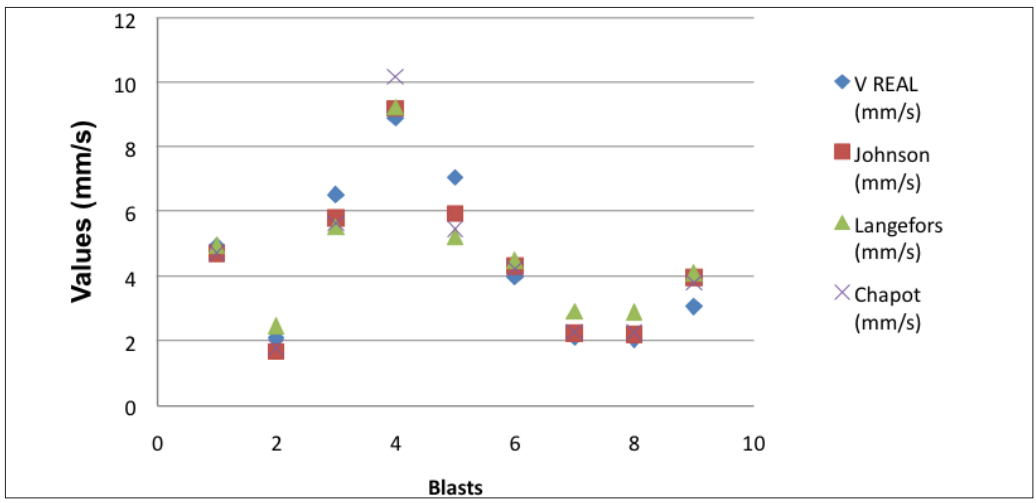

Figure 4. Chart comparing the values of the speed of vibration and the expected in rock mass C.

6.4. Summary of constants

The values calculated in the three different rock masses were:

Table 17. Values for the constants Langefors and Johnson for different rock masses.

		Rock Mass A	Rock Mass B	Rock Mass C
Johnson	a	88,6135	1282,2369	622,8508
	b	0,398	1,003	0,3251
	c	-0,9297	-1,7668	-1,1002
Langefors	K	29,6388	35,6735	45,3253
Chapot	K	76,2656	2024,5633	208,9915
	c	-0,9489	-1,7586	-1,0459

7. SUMMARY AND CONCLUSIONS

Environmental impacts from the use of explosives are explainable, measurable and controllable.

The calculation of the environmental impact related to the vibrations can be done.

Testing prior blasts with controlled charges can be a safe method for detecting the particular characteristics of the mass and the propagation law. With these tests and statistical work the constants can be obtained and make up the propagation law, even if this statistical method only defines the variation of all the properties in one law.

As shown in this study, the rates of vibration

testing did not show a large deviation from those that had been calculated as planned. The correlation obtained using the equation with three variables instead of the equation that has only one variable, was more similar to reality.

However after applying any equation using the linear regression method to calculate the coefficients it was estimated to be a good option for the security as it showed almost always higher values than the actuals.

In conclusion the propagation law of velocities corresponding to Johnson is the closest choice to the implementation of projects using explosives. The use of this law in obtaining the constant variables and formulating the propagation speed should be applied for each different area or mass.

The propagation law corresponding to Johnson is the safest choice. However the use of Langefors, can lead to the actual design of the explosive charge in the case of safety and prevention of risk. This formula is easy to use without resorting to the use of statistical management of Johnson or Chapot and it is an immediate easy tool to use and characteristic in risk prevention. The use of this law directly sets the amount of charge to be used, with a margin of safety to achieve the required results. This should always be the case when the transmission coefficient of the terrain is unknown.

The laws achieved by this simple method have two large gaps: one related with the ignorance of the contribution of each variable for the law, and in some cases can be contrary to what is expected. It would be necessary in future works to isolate and study the dominant influences of the velocity law, and to consider not only the individual delay with the maximum instantaneous charge but a delayed sequence of blast holes. In this way it should also study the influence of the multiple blast hole and their influence in the vibration velocity with the travel of all the different waves and in this way the value will depend on the total amount charge and not only from the charge delay. A realistic model of attenuation should be done in order to describe the influence of the total charge quantity in the vibration level taking into account the multiple delay holes. So the predictor of velocity can be obtained with the parameters: distance between monitoring point and blast, delay interval, number of holes and total charge quantity.

REFERENCES

Bernardo, P. A. M., 2004. Impactes Ambientais do Uso de Explosivos na Escavação de Rochas, com Ênfase nas Vibrações. *Dissertação para obtenção do grau de Doutor em Engenharia de Minas. I.S.T. - U.T.L.*

Blair, D.P. 1990. Some problems associated with standard charge weight vibration scaling laws. *Third Int. Symp. Rock Fragmentation by Blasting,* Brisbane, Queensland, Australia, 149-158.

Chapot, P. 1981. Etude des vibrations provoquées par les explosifs dans les massifs rocheux. Paris: *Laboratoire Centraldes ponts et chausses*.

Jimeno, E. L., Jimeno, C. L. & Bermudez, P. G. 2003. Manual de Perforación y Voladura de Rocas. *ITGE. 2ª Edição. Espanha.*

Langefors, U. & Kihlström, B. 1963. The Modern Technique of Rock Blasting. *Wiley*, New York

Nicholls, H. R., Johnson, C. F., Duvall, W.I. 1971. Blasting Vibrations and Their Effects on Structures: *(Bulletin 656), U.S. Department of the Interior.*

Olofsson, S.O. 1997. Applied Explosives Technology For Construction and Mining. *Applex AB publisher*, Arla Sweden. 342 pp.

Lisbon Conference Proceedings 2011, R. Holmberg et al
©2011 European Federation of Explosives Engineers, ISBN 978-0-9550290-3-5

Estimation of powder factor and fragmentation from blasting based on rock mass properties in some zones of Sungun Copper Mine

M.A. Framooshi
M.S, Student in Mining Engineering, Faculty of Engineering, Mining Engineering Department, Urmia University, Iran.

A. Nasirinejad
M.S, Mining Affairs Department, Sungun Copper Mine, Iran.

N.Nouri
M.A, Engineering Affairs Department, Sungun Copper Mine, Iran.

ABSTRACT: Rock mass has various discontinuities that affect the rock fragmentation results by blasting. The revised Kuz-Rom model is the most comprehensive model predicting rock fragmentation size by blasting, based on considerable numbers of in-situ rock mass properties and blasthole patterns. After monitoring in-situ rock mass properties and blasthole patterns in zone 1 of the Sungun Copper Mine, the size of fragments was estimated by the revised Kuz-Rom model. Image Analysis Technique and efficient GoldSize software was used after each blasting to determine the blast fragmentation and average size of fragmented pieces ($\overline{X}$). The results were compared with the revised Kuz-Rom model. The estimated average size of fragments using Kuz-Rom model was higher in fragment size with Image Analysis Technique and Goldsize Software. The rock mass properties such as the discontinuity plane aperture that affects the powder factor and blasthole pattern has not been considered in the revised Kuz-Rom model. This can be a reason why the predicted results are not accurately equal to the measured blast fragments of rock mass obtained from photos via the GoldSize Software.

1. INTRODUCTION

For the drilling and blasting design, a blasting engineer is required to know the particular environment we are concerned with. Rock mass is not a solid continuous, homogeneous and isotropic material and may be accompanied with discontinuities (Moomivand, 2007). Rock mass properties also have important effects on drilling and blasting performances. In previous decades, different methods for the design of blasthole patterns have been presented. Some methods, like Konya (1983) and Ash (1963) and others have only pointed to one property and are not indicative of various rock mass characteristics in blasting performance. Nowadays research and education authorities pay less attention to such methods. The number of categories that account

for the purposes of blasting and drilling is not numerous. The most important and most common method based on characteristics of rock mass due to consideration of more classification parameters is Lily (1986) entitled "Blastibility Index" (BI).

Fragmentation of blasting produces one of the most significant blast results with remarkable influence in drilling, blasting, loading, carrying and crushing costs. Increased fragmentation of blasted rock mass results in an increase in blasting and drilling costs, since this method facilitates the loading and carrying operations and reduces energy consumption in primary crushing. It also obviates the need for secondary crushing. The mentioned increase will be compensated though and certain increases in fragmentation will decrease costs. Therefore, the main factor in the success of a blasting in a breast is adequate fragmentation, which plays a key role in minimizing mining costs. Rock mass fragmentation depends on various factors such as rock mass properties, Blasthole geometric specification and type of explosive material (Moomivand, 2007; Bhandari, 1996; Sunu, 1989; Rustan, 1983). Present study evaluates the degree of rock mass fragmentation on the basis of the measurement of in situ rock mass characteristics using the Blastibility Index of the modified Kuz-Ram model for the main powder of Anfo. Image Analysis Technique and GoldSize Software have been utilized to draw grinding diagrams.

2. ROCK FRAGMENTATION ANALYSIS USING BLASTABILITY INDEX, REVISED KUZ-RAM MODEL AND IMAGE ANALYSIS TECHNIQUE

Lily (1986) indicated Blastibility Index based on rock mass properties as the flowing relationship:

(RMD + JPS + JPO + SGI + H) 5/0 = BI (1)

Lily (1986) used empirical data of Anfo powder factor (kg/tons) and Blastibility Index.

q=0.004 (BI) (2)

Blastibility Index techniques indicate rock mass properties due to considering more parameters in comparison with other methods. Due to numerous and complex rock mass properties the Blastibility Index technique for an explosive type (Anfo) is more logical and valid than earlier empirical formulas. That is why this method has been used more than other ones. But unfortunately, this reasonable and common technique, which has been developed in 1986 has not been utilised by blasting engineers for many years and mines have been optimised according to mono-parametric methods like Anderson (1952), Ash (1963) and Konya (1983) and others.

Using the Blastibility Index, Cunningham modified his earlier model (Cunningham, 1983) entitled modified model. As the following:

$$\overline{\mathbf{X}} = 0.06BI\left(\frac{V}{Q}\right)^{0.8} Q^{0.167}\left(\frac{115}{S_{ANFO}}\right)^{0.633} \quad (3)$$

$\overline{\mathbf{X}}$: Average dimensions of fragmental after main blasting in centimeter

- BI: Blastibility
- S_{ANFO}: Weight strength of explosive to Anfo (100 for Anfo and 115 for T.N.T)
- V: Volume of every Blasthole in kilogram
- G: Weight of each blast hole in kilogram

The revised Kuz-Ram model (Cunningham, 1987), predicts average fragmented dimensions as a function of G and V (powder factor) for rock mass properties (BI). The revised Kuz-Ram model has been welcomed by blasting engineers because it uses the Blastibility Index which itself is based on various properties. This means that for certain rock mass characteristics (BI), if the powder factor increases, the average size of pieces decreases. An important point in Revised Kuz–Ram model is that the cost of fragmentation from drilling to crushing processes has been eliminated. This model does not show the average size of pieces ($\overline{\mathbf{X}}$) of the main blasting to minimize the cost of the grinding process from drilling to the beginning of crushing (main blast and secondary, etc.). Since the final cost includes the cost of drilling, the cost of explosives, blasting wage costs, labour costs and sometimes additional loader and bulldozer costs (due to large pieces of blasted rocks which are required to be crushed) and the cost of secondary crushing which is the percentage of mineral with larger size pieces from stones in a crusher after blasting.

The cost of primary fragmentation and the cost of secondary fragmentation (blasting) of a ton of mineral is approximately two times more than drilling and blasting of in-situ rock mass (Moomivand, 2008). Several mathematical models like Dinis da Gama´s model (Dinis da Gama, 1996), Larson (Hustrulid, 1999), SveDeFo (Ouchterlony, 1990), Kuz-Ram (Cunningham, 1983) and revised

Table 1. Rock mass blastibility parameters and their scores.

Blastibility Index Parameters (BI)	***Score***	***Blastibility Index Parameters (BI)***	***Score***
Rock Mass Description (RMD)		Specific Gravity (SGI) SGI= 25G-50	50-10
1-Powder (Fragmented)	10		
2- Block	20		
3- Mass	50		
Discontinuity Plane Aperture ((JPS		Hardness Factor (HF)	
1-m Near <0,1	10	< 50 : E Gpa	E/3
2- Average m 1 0.1 –	20	E: > 50 Gpa	UCS/5
3- Wide 1 m	50	UCS	
Discontinuity Orientation ((JPO			
1- Horizontals	10		
2- slope toward out of breast	20		
3- Perpendicular to breast	30	BI= (RMD+JPS+JPO+SGI+ HF)/2	
4- slope toward the inner part of breast	40		

Kuz-Ram model (Cunningham, 1987) have been presented to determine the size of fragmented pieces after the main blasting, to predict rock mass fragmentation. Recent research results (Osanloo and Bakhshandeh, 1999) show that among mathematical models presented, the revised Kuz–Ram model, because of using more parameters, especially the geo-mechanical properties of rock mass, is more efficient than other models.

In recent years, extensive studies have been conducted to predict and determine the rock mass fragmentation. Researchers have tried to present an acceptable method for estimating rock mass fragmentation that is easy to use and also the cost is economical (Dey et al., 1996). Generally, methods presented to assess the rock mass fragmentation are divided into three categories: mathematical methods, photography and screening.

In this article, methods to predict fragmentation are reviewed and then more reasonable methods are selected and used and from these the extent of the fragmentation of Sungun Copper Mine Ore is determined. One common method in determining the classification of blast fragmentation is photography. In this method, in the first instance a number of images of blasted breast are captured at different time intervals and then using image analysis techniques, the distribution of rock mass fragmentation is determined (Franklin & Katsabanis, 1996).

Regarding the fact that performing such action manually is very time consuming, the use of existing softwares in this field such as: Wip Frag, Frag Scan, Spiltonling and GoldSize" was indispensible. The only calibrated software in Iran is GoldSize" so it has been used in this study.

3. CONDUCTING RESEARCH

Considering the great changes of geo-mechanical properties of rock mass in the Sungun Copper Mine and the direct connection of the revised Kuz-Ram model results with it, the first step was to divide the Sungun Copper Mine into five zones. After the classification of mine zones and in order to predict the fragmentation of the rock mass, we discussed and exchanged opinions with colleagues and selected several breasts. Then in each of them using Scanline Blastibility, parameters of rock mass were specified and the amount of rock mass Blastibility (BI) was calculated. Calculated results of the Blastibility Index of rock mass for the breasts of zone 1 are shown in Table 2. Afterwards, the average size of blasting fragmentation was estimated using the revised Kuz-Rom model, its results along with powder factors are shown in Table 3.

After the blasting of breasts under study and in several steps photographs have been taken. The photos took place in consecutive time intervals to ensure that captured images represent a total mass of fragmented rock, Figure (1). After the images were produced, we used GoldSize" software to show a grinding classification diagram of blasting for the breasts under investigation, see figure (2). The results of the average size of fragmented pieces from the revised Kuz-Ram model and Image Analysis Technique have been shown in Table (4). The revised Kuz-Ram model predicts the average size of fragmented pieces ($\overline{\mathbf{X}}$) more than the average measured size of pieces ($\overline{\mathbf{X}}$).

Although 5 properties of rock mass have been used in the Blastibility Index (BI) of rock mass, the rock mass characteristics which are effective in rock mass fragmentation mechanisms have not been taken into account. Moomivand (2006) showed that the size of the discontinuity plane aperture is also effective in powder factors and patterns of blast holes. This could be one reason for the inconsistency of the average size of fragmented pieces of rock mass with images obtained using the GoldSize software and other errors of determining the size of fragmented rock mass images taken using GoldSize Software.

Table 2. Scores of rock mass characteristics and Blastibility Index (BI) in Zone 1of Sungun Copper Mine.

Breast 3	Breast 2	Breast 1	Parameter
		10	1.(RMD) Rock Mass Description Powdered (pulverized)
		20	.2 Joint Aperture (JPS) average m- 2 - 2 0/1 - 1
		40	3. Aperture Orientation (JPO) Slope into the Breast - 2 - 3
		*(25/8) 10	4. Special Gravity Influence 50 G - 25SGI =
		7	5. Hardness Factor (HF) or Resilience Coefficient
		5/43	6.Blastibility Index

* Regarding fundamentals of this method score 10 is allocated for SGI<10.

Table 3. Results pertained to Blastibility Index, powder factor and average size of fragmented rock mass in breasts under study.

Number of breast	*Rock type*	*Blastibility Index*	*Powder factor (kg\ton)*	*Average Dimension (cm)*
1	Sungun porphyry	43.5	0.174	12.3
2	Sungun porphyry	33.5	0.134	9.35
3	Sungun porphyry	33.5	0.134	7.25

Figure 1. Photo of rock fragmentation after blasting in breast 1.

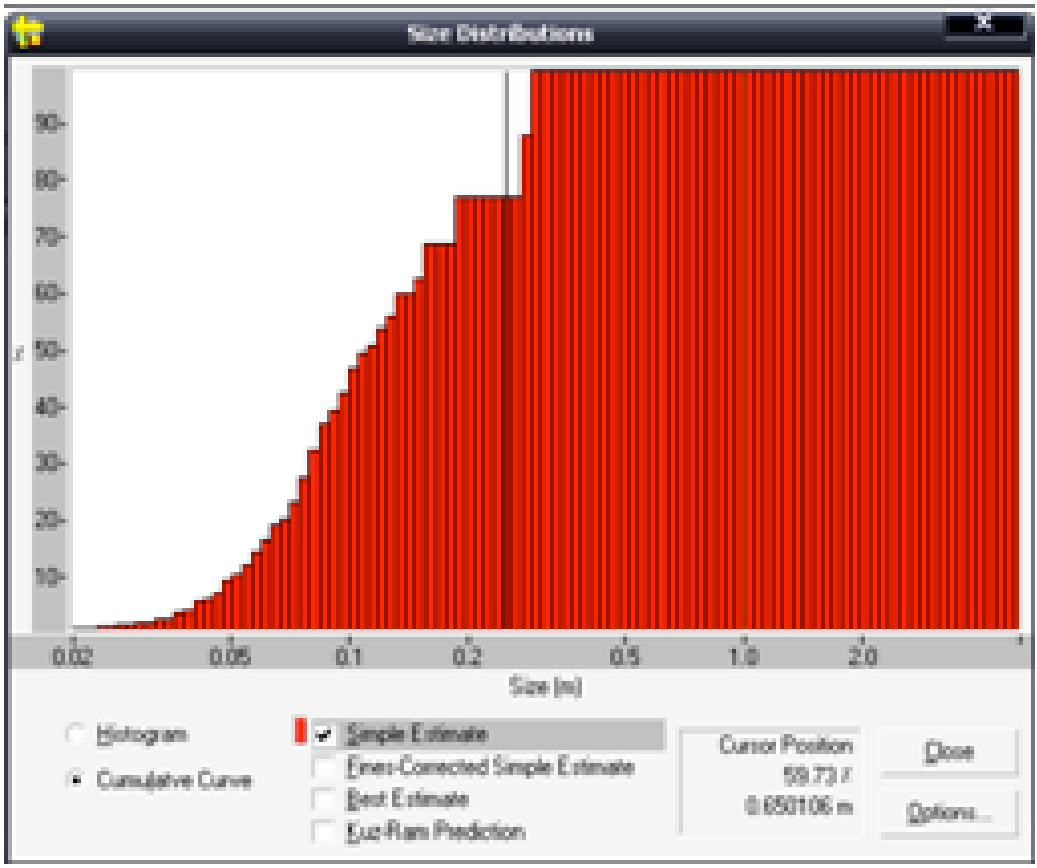

Figure 2. Cumulative frequency graph of grain size of fragmented rock after blasting for breast.

Table 4. Comparison of average size of fragmented pieces of modified Kuz-Ram Model with Image Analysis Technique.

Model	Breast 1	Breast 2	Breast 3
Kuz-Ram (cm)	12.3	9.3	7.25
Image analyses (cm)	9	7	6

4. CONCLUSION

Research results show that the revised Kuz-Rom model estimates the size of fragments bigger than using the image analyses technique. However in the Blastibility Index, 5 properties of rock mass fragmenting mechanisms which are effective were not considered. Discontinuities of the plane aperture also influences the powder factor and blasthole pattern, this could be a reason why the predicted results by GoldSize software are not accurately equal to the measured blast fragments of rock mass.

5. SUGGESTIONS

For further use of the findings from the existing study, the following practical approaches have been presented for researchers:

1. Discontinuities planes are one of the important factors in creating errors in the Kuz-Rom model. For reducing errors in this model it has been suggested that this parameter should be considered in calculating the average size of fragmentation.

2. In order to improve the results of blasts, it is suggested that during the drilling and blasting for running the exact drilling pattern, for locating the correct location of holes and for clearing the breast, etc, responsible persons should be chosen to observe and control the operation.
3. The blasting system used in the study sites is Cortex. For improving the results using the Nonel system, blasting is recommended.
4. For the best usage of crusher screening before crushing, it is suggested smaller ores do not enter the crusher, since it leads to an increase in production and decrease in energy consumption.

6. ACKNOWLEDGEMENT

We express our sincere gratitude to all Sungun Copper Mine staff that helped us in this investigation.

REFERENCES

Ash, R.L. (1963). "The mechanics of rock breakage (Part 2) – Standards for blasting design", *Pit and Quarry Vol. 56 No. 3,* pp. 126-131.

Bhandari, S. (1996), Changes in fragmentation processes with blasting conditions, *Rock fragmentation by blasting- Fragblast 5*, ed. B. Mohanty, Montreal, Cananda, pp, 301-312.

Cunningham, C.V.B (1983), The Kuz-Rom model for prediction of fragmentation from blasting, *The lst International Symposium on Rock Fragmentation by Blasting*, vol.2, Lulea, Sweden, Pp.439-453.

Cunningham, C V B, (1987), Fragmentation estimations and the Kuz-Rum Model, four years on, in proceedings *2nd International Symposium on Rock Fragmentation by Blasting*, Keystone Colorado, Pp.475-487.

Dey, A., R. N. Ghose, A. K.) 1996) , Fragmentation predication and assessment in open cast blasting a case study, *Journal of Mines, Metals, Fuels*,. No. 9. pp.1144-1160.

Dinis da Gama, C. (1996), A model for rock mass fragmentation by blasting, Proceedings *8th International Congress on Rock Mechanics*, Tokyo, Setembro de 1995, Vol. 1. Pp.73-76 Tambem publico na Revista Geoticnia No76, Marco de, pp.41-51.

Franklin, J. & Katsabanis, T. (1996), Measurement of blast fragmentation, Taylor & Francis.

Hustrulid, W. (1999). "Blasting principles for open pit mining, *Volume 1- General design concepts*" A. A. Balkema, 382 p.

Konya, C. J. (1983). "Blasting design, surface mining environmental monitoring and reclamation handbook".

Anderson, O. (1952). "Blast hole burden design - introducing a new formula", *Australian Institute of Mining and Metallurgy*, No. 166 – 167, pp. 115 – 1130.

Lily. P.A. (1986). "An empirical method of assessing rock mass blastability.", Proceeding Large Open Pit Mining Conference, ed. by Davidson, J. R., *The Australian Institute of Mining and Metallurgy*, Parkvaille, Victoria, October, pp. 89-92.

Moomivand, H. (2007) Eraee-ye Ravesh-i Jadid baray-e Tarrahi-ye Olgoo-ye Chal-ha-ye Enfejar dar Maaden-e Roo-baz (Persian) Presenting a new method for the design of the blasthole pattern in open pit mines. *Journal of Tehran University Faculty of Engineering,* No. 3, Volume 41, September 2007, PP. 355-361.

Moomivand, H., (2008) Baravard-e Gheimat-e Tamam Shod-e-ye Enfejar-e Asli and Enfejar-e Sanavi-ye va Moghaye-se-ye Hazine-ha (Persian). Estimation of final cost of the main blasting and secondary blasting and comparison of costs. Second Conference of Mining Engineering, Faculty of Engineering, Tehran University, 2008, Page 1-8.

Rustan, A. & Yang, Z.G. (1983), The influence from primary structure on fragmentation. *1st. Int. Symposium on rock fragmentation by blasting*, Vol. 2, Lulea, Sweden, pp. 581-604.

Sunu, M.Z. & Singh, R.N. (1989), Application of modified rockmass classification system to blasting assessment in surface mining operations, *Mining Science and Technology*, No.8, , pp. 285-296.

Lisbon Conference Proceedings 2011, R. Holmberg et al

Asymmetric propagation of airblast from bench blasting

P. Segarra, L.M. López & J.A. Sanchidrián
Universidad Politécnica de Madrid -ETSI Minas, Ríos Rosas, 21, 28003 Madrid, Spain

J.F. Domingo
MAXAM Europe, Av. del Partenón, 16, 28042 Madrid, Spain

ABSTRACT: This paper investigates the propagation of airblast from quarry blasting. Peak overpressure is calculated as a function of blasting parameters (explosive mass per delay and velocity at which the detonation sequence proceeds along the bench) and polar coordinates of the point of interest (distance to the blast and azimuth with respect to the free face of the blast). The model is in the form of the product of a classical scaled distance attenuation law times a directional correction factor. The latter considers the influence of the bench face, and attenuates overpressure at the top level and amplifies it at the bottom. Such factor also accounts for the effect of the delay by amplifying the pressure in the direction of the initiation sequence if the velocity of initiation exceeds half the speed of sound and up to an initiation velocity in the range of the speed of sound. The model has been fitted to an empirical data set composed by 134 airblast records monitored in 47 blasts at two quarries. The measurements were made at distances to the blast less than 450 m. The model is statistically significant and has a determination coefficient of 0.869.

1. INTRODUCTION

Bench blasting produces environmental concerns in the form of vibrations and airblast in the surroundings of the blasting site. In addition to dynamic stresses produced in the ground by seismic waves, airblast waves will impact the walls, roof and windows of nearby structures and may induce damage on them and annoyance to their occupants (Siskind *et al*. 1980, Persson *et al*. 1994, Mohanty 1998, ISSE 1998). An accepted starting point to assess the risk of damage consists of comparing the measured peak overpressure (i.e. highest sound pressure above the atmospheric pressure) with the maximum pressure that structural elements can resist (Mohanty 1998). US Bureau of Mines recommendations (Siskind *et al*. 1980), worldwide used, follow that approach and set a threshold overpressure as function of the frequency response band of the transducers. Although peak overpressures from rock blasting are usually well below compliance values, the major drawback of airblast is that the induced noise may lead to buildings occupants to believe that permanent damage may have occurred (ISEE 1998).

The maximum amplitude of pressure waves in air from blasting is predicted at small pressure levels with the following formula (Persson *et al*. 1994):

$$P = a_0 Z^{a_1} \tag{1}$$

Table 1. Coefficients (a0 and a1) of peak overpressure attenuation function of mass-scaled distances.

Source	Description of the tests	a_0	a_1
		$Pa\cdot[m\cdot kg^{-1/3}]^{-a1}$	
Siskind et al. (1980)	Quarry blasts. Behind face	622	-0.515
	Quarry blasts. Direction of initiation	19010	-1.12
	Quarry blasts. Front of face	22182	-0.966
ISEE (1998)	Confined blasts for airblast suppression	1906	-1.1
	Blasts with average burial of the charge	19062	-1.1
Kuzu et al. (2008)	Quarry blasts in competent rocks	261.54	-0.706
	Quarry blasts in weak rocks	1833.8	-0.981
	Overburden removal	21014	-1.404
Hustrulid (1999)	Detonations in air. Unconfined	185000	-1.2

where a_0 and a_1 are coefficients of the model, and Z is the scaled distance defined as (Marchand 1999):

$$Z = R/M^{1/3} \quad (2)$$

or

$$Z = R/E^{1/3} \quad (3)$$

where R is the distance from the centre of the explosive source, M is the explosive mass, and E is the energy of the explosive.

Equation 1 presupposes that the detonation of different sized charges with similar geometry and of the same explosive in an isotropic medium (i.e. flat ground surface and identical atmosphere conditions) produces self- similar blast waves at identical scaled distances Z. The coefficients a_0 and a_1 are calibrated for each site by fitting Equation (1) to empirical data. They can be considered as fitting constants that lump the influence of other variables not included explicitly in Equation 1 (Hustrulid 1999). Table 1 summarises fitting results from different work in which the scaled distances were calculated with Equation 2.

Table 1 shows that the coefficient a_0 has a large variability, nearly three orders of magnitude, which confirms that there are a number of variables that influence this coefficient. The scatter in the a_0 coefficients reported by Siskind *et al*. (1980) is an example of the directionality of the propagation of blast waves. In fact, the contour curves of equal overpressures from bench blasting have a shape similar to an 'egg' curve, longer at the floor level and shorter at the top (Griffiths *et al*. 1978, Moore *et al*. 1993, Richards & Moore 2002, Rudenko 2002, Domingo 2007). These azimuthal variations may be reinforced in specific directions depending on the characteristics of the sequence of the blast (Siskind *et al*. 1980, Egorov 1996, Richards & Moore 2002). The influence of the rock type on the peak overpressure is apparent from the differences in a_0 values given by Kuzu *et al*. (2008). The effect of charge confinement is shown by the dispersion of a_0 from ISEE data (1998), and most significantly by the high value reported by Hustrulid (1999) from shots of unconfined charges. This is consistent with other works (Siskind *et al*. 1980, Persson *et al*. 1994).

The variability of a_1 is moderate, which indicates that the influence of distance and charge is in general relatively well described by this coefficient. Atmospheric conditions also play an important role in the attenuation of airblast; they are more relevant in the far field than in the near field (Siskind *et al*. 1980, Persson *et al*. 1994, Richards and Moore 2002).

Some of the above mentioned variables are considered together with the scaled distance to predict peak overpressures by a number of

references in the literature (Moore *et al*. 1993, Egorov 1996, Richards & Moore 2002, Domingo 2007). This work provides a new prediction formula of the peak overpressure that accounts for asymmetrical propagation of airblast around the block to be blasted due to effect of the bench face and blast initiation.

2. DESCRIPTION OF DATA

Data arise from one single shot and 46 production blasts monitored in two quarries located in the South-East of the province of Madrid (Spain): El Alto and Monte Espartinas. A 67 % of airblast records were monitored in El Alto, and 33 % in Monte Espartinas.

El Alto belongs to Cementos Portland Valderrivas and produces 2.25 Mt/year of limestone and marl (production data from the period of study) for the cement industry. The deposit of Miocene and lacustrine origin has in the upper four to six meters an overburden of clayish-marl. The limestone pack of 12 to 19 m thick is located below the overburden. In the floor of the limestone there is a clay body, which is not mined. The ore composed by limestone and clayish marl is mined in one bench by drilling and blasting.

Monte Espartinas is some 11 km to the West of El Alto. It is owned by Saint Gobain Placo Ibérica S.A and produces 0.6 Mt/year of gypsum. The genesis of the deposit is the same than El Alto. The geology consists of a gypsum pack with a thickness of 20-30 m that underlies a vegetal soil of 0.5-1 m thick. The overburden is removed mechanically and the gypsum is mined with bench blasting techniques.

To describe the conditions in which the tests were carried out, Table 2 show the main blasting parameters. All the blasts had one free face. The number of rows was usually one. The blastholes were charged with gelatine cartridges in the bottom of the blasthole and bulk explosives above them. These were ANFO, aluminized ANFO, high density aluminized ANFO, low density ANFO and 80/20 emulsion blend. The holes were stemmed with drilling cuts. The stemming retained well detonation gasses except in 13 % of the blasts in which there was a limited stemming ejection that produced a particularly strong wave in air (i.e. stemming release pulse). The explosives were down-hole initiated with non-electric or electronic detonators. The blastsholes were delayed from the hole in one end of the block towards the other end, so the firing sequence progressed parallel to the free face of the blast. This also applies to the six blasts with multiple rows since the delay between rows was very long compared to the in-row delay. The results of the blasts in terms of toe breakage, face control, fragmentation, and muckpile characteristics are qualitatively ranked as good in all the blasts.

Dynamic overpressure in air was monitored with linear L type microphones connected to the airblast channels of recording units manufactured by Vibra-Tech and Instantel. The other channels of the units were occupied by geophones. Air overpressures were measured in a range from 0.5 to 500 Pa with a resolution of 0.25 Pa. The microphones had an operating frequency response from 2 to 250 Hz, which is adequate to measure accurately overpressures in the frequency range critical for structures and in the range of frequencies critical for human hearing (Siskind *et al*. 1980, Dowding 2000). The accuracy of airblast devices is ±10 % or ±1 dB between 4 and 125 Hz, whichever is larger (ISEE 2000). The recording units were triggered when the particle velocity in the ground exceeds 0.5 mm/s. Other setups used were: sample rate of 1024 samples per second, continuous record mode of the full waveform, and automatic stop mode (the unit stops recording 2 s after the particle velocity falls below the trigger level).

The microphones were fitted with a foam windshield and mounted at a height of 1 m above the floor and oriented visually towards the blast. This is enough to get accurate recordings (ISEE 2009). The sensors were placed in the top level, in the bottom level or in both. When multiple microphones were used in the same blast, they were placed in different positions in El Alto and very close to each other in Monte Espartinas. The reference system used to locate the measuring stations is based on that given by Griffiths *et al*. (1978) and shown in Figure 1; the pole is the gravity centre of the blast and the polar axis is drawn perpendicularly to the line that joins the first and last blastholes, towards the bench floor. The coordinates for each microphone position are (R, θ), where R is the distance from the pole to the microphone and θ is the angle from the polar axis towards the first hole nominally fired (in the single shot, θ is counted clockwise). The position of all sensors is shown in Figure 1, and the statistics of the polar coordinates are given

Table 2. Summary of blasting and airblast data.

	Mean±std.*	Range
Blasting		
Hole diameter, mm	127±24.7	89–155
Bench height, m	14.5±4.8	4.8–20.5
Blasthole length, m	15.7±4.8	5.6–23.5
Burden, m	4.4±0.7	2.9–5.5
Spacing between blastholes (S), m**	5.7±2.8	3–6.6
Mass of expl. detonated in a delay (M), kg	148±86.6	21.3–296
Energy (heat of explosion) in a delay (E), MJ	646±389	83.3–1391
Stemming length, m	3.84±1.5	1.5–6.4
Powder factor, kg/m^3**	0.40±0.07	0.17–0.51
Delay within rows, ms**	48±22	17–84
Delay between rows, ms**	161±29	100–192
Firing velocity down the face (V_f), m/s***	134±103	67–383
Airblast		
Distance to blast (R), m	136±97.5	45.1–444
Azimuth of sensor position (θ), °	162±108	2–358
Peak overpressure (P), Pa	98.2±113	6.0–482
Relative uncertainty of peak overpressure, %	3.6±4.8	0.3–19.8

* std: Standard deviation
**Data from single blasthole shot is not considered.
*** Ratio of spacing between blastholes to the delay within rows

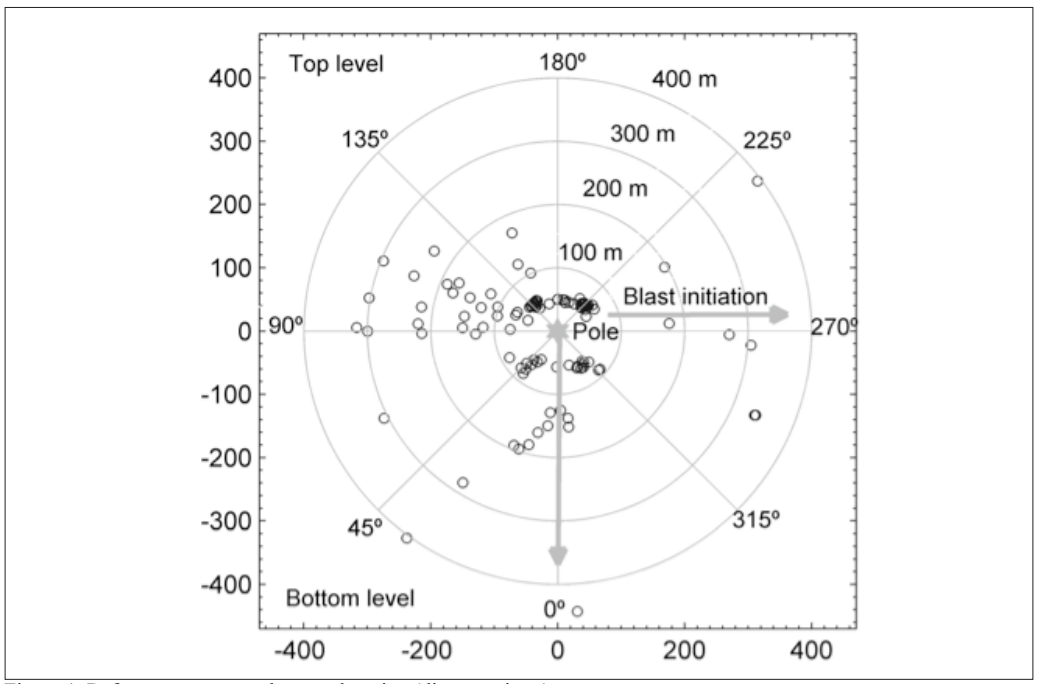

Figure 1. Reference system and sensor location (distances in m).

in Table 2. Meteorological conditions are expected to have little influence in peak overpressures at the distances at which the sensors were placed (ISEE 1998, Richards & Moore 2002).

Peak overpressures vary between 6 to 482 Pa (see Table 2). Their uncertainties are assessed from the ratio of the standard deviation of the mean (i.e. standard deviation divided by the square root of the measurements) to the mean of the overpressures measured in the same blast with microphones positioned right next to one another. Dispersion values of experimental errors in peak overpressure are shown in Table 2. The mean of the experimental errors is 3.6%.

3. ANALYSIS AND RESULTS

Peak overpressures versus mass-scaled distance calculated with Equation 2 are plotted in Figure 2. A similar relation with the overpressure is obtained if the distance is normalized by the energy of the explosive as in Equation 3 or if the explosive mass is converted to an equivalent mass of a standard explosive. Straight mass has been used since it can be readily obtained in the field. Data in Figure 2 is split in two series as function of the level of the block to be blasted in which the sensors were placed (top and floor levels). The scatter in the data is high, and if natural logarithms are taken in Equation 1, and the resulting Equation fitted to data, the model only explains a 20.0 % of the variability of the logarithms of peak overpressure. In order to improve the prediction ability of the model, Equation 1 has been modified to account for the directional propagation by including a variable factor A:

$$P = AZ^{a_1} \tag{4}$$

A is defined as follows:

$$A = a_0 A_f A_s \tag{5}$$

where a_0 is a coefficient of the model, similar to the lead factor in Equation 1, A_f is the bench face factor that considers the influence of the azimuth of the measurement point with respect to the bench face, and A_s is the initiation sequence factor, that accounts for the effect of the blast initiation (i.e. initiation direction, delay between blastholes and relative position between blastholes along the face).

Replacing Equation 5 into 4 leads to:

$$P = a_0 A_f A_s Z^{a_1} \tag{6}$$

The rock displacement at the bench face is the main source of airblast in properly designed blasts in which the explosive is well confined (Siskind *et al*. 1980). This leads, for a given scaled distance, to higher overpressures in front of the face and smaller behind it (see Figure 2). In order to account for this directional effect, the factor A_f amplifies the overpressure $a_0 Z^{a1}$ in the bench floor level and attenuates it in the top one. Functions like: $1+a_2\cos\theta$, $1/(1-a_2\cos\theta)$ or $\exp(a_2\cos\theta)$, with a_2 a positive coefficient, could be used with similar results; the first function type was used by Griffiths *et al*. (1978). They are positive for all θ and are maximum at θ=0 (i.e. in front of the face) and minimum at θ=180º (i.e. behind the face). In this study, for convenience in the model fitting, the exponential form has been chosen:

$$A_f = \exp(a_2 \cos\theta) \tag{7}$$

The detonation of the explosive in each blasthole produces a pulse of air waves that may interact with the waves from nearby blastholes depending on the blast sequence and propagation path (Siskind *et al*. 1980, Richards and Moore 2002, Egorov 1996). If the initiation of the blast proceeds at a velocity (i.e. ratio of the spacing between blastholes to the delay within rows) close to the speed of sound, the wave generated from the detonation in a hole will reach the next hole in the sequence at about the same time that it detonates, resulting in a reinforcement of the airblast in the direction of initiation. This overlapping can also take place at subsonic velocities of initiation, with diminishing effect as initiation is slower. Siskind *et al*. (1980) suggest that the initiation velocity be less than half the speed of sound in order to prevent airblast reinforcement in the direction of initiation. For propagation paths in an opposite direction to the blast initiation (i.e. θ=90°, see Figure 1), the blast wave from a newly detonated hole never reaches the waves from previous ones, independently of the initiation velocity. Snell and Oltmans (1971) examined the supersonic range of initiation velocities in the direction parallel to the row of blastholes. They concluded that in such direction,

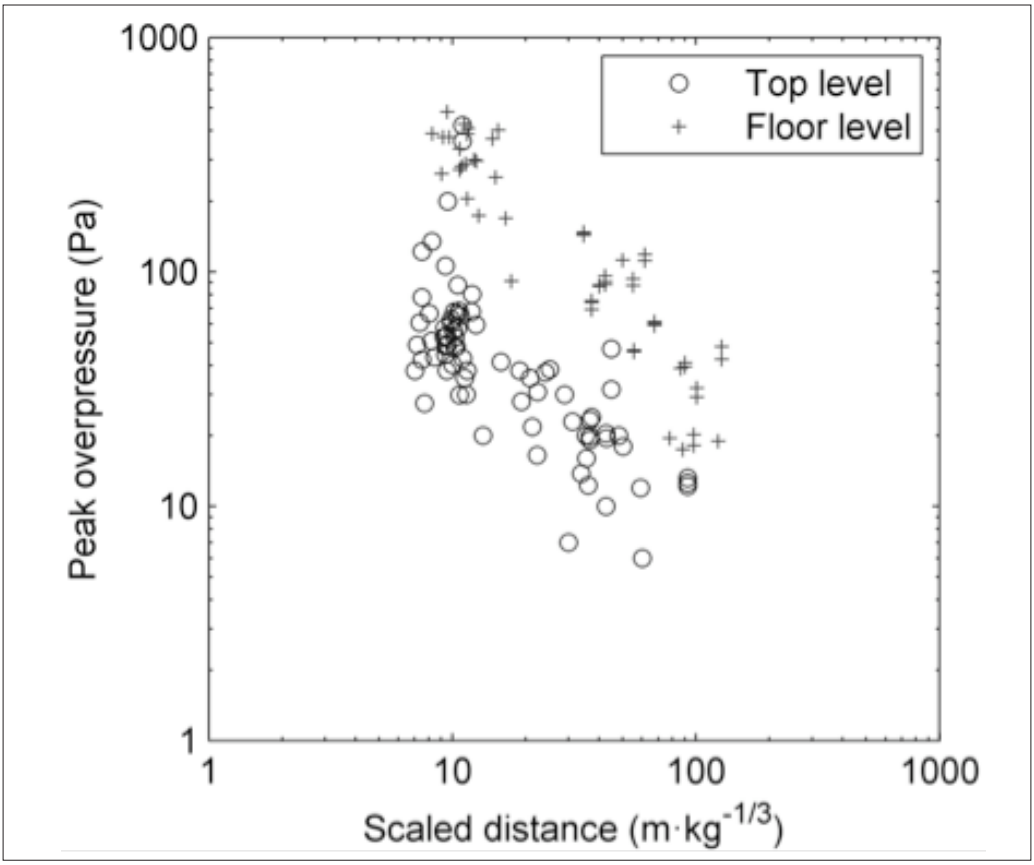

Figure 2. Peak overpressure versus mass-scaled distance.

reinforcement would not occur for initiation velocities higher than 1.89 times the speed of sound. Air wave reinforcement can take place at initiation velocities in excess of that figure in directions other than the direction of blastholes initiation (i.e. directions on which the projection of the initiation velocity is approximately sonic). It should be noted, however, that highly supersonic initiation along the face is unusual in quarry blasting since it encompasses short delay times which are disfavoured for rock fragmentation performance and ground vibration, see for instance (Konya 1995). In our data the initiation velocity varies from 67 to 383 m/s (see Table 2); the latter is a fairly high value in quarry blasting.

The initiation sequence factor A_s, that accounts for the wave superposition in the direction of initiation has been defined as follows:

$$A_s = \exp(a_3 W_0) \tag{8}$$

and W_0 is defined as function of the polar angle of the position of interest and of the initiation velocity relative to the speed of sound $v_I = V_I/c$ (c is calculated from the average conditions of the tests and it is equal to 338 m/s):

$$W_0 = (1 - \sin\theta)\, L(v_I) \tag{9}$$

where $L(v_I)$ is a logistic function of v_I in two parameters λ_1 and λ_2:

$$L(v_I) = \frac{1}{1 + \lambda_1 \exp(\lambda_2 v_I)} \tag{10}$$

The parameters λ_1 and λ_2 are selected so that $L(v_I=0.5) = 0.01$ and $L(v_I=1) = 0.99$: $\lambda_1 = 9.703 \times 105$ and $\lambda_2 = 18.380$. Therefore W_0, and hence A_s, are maximum in the direction of initiation and for velocities of initiation around the speed of sound, and minimum in directions opposite the initiation

Table 3. Coefficients of the linear least squares regression.

Coefficient	Mean	SE*	p-value**	Conf. Interval 95 %	
				Min.	Max.
$\log a_0$	6.934	0.135	<0.0001	6.668	7.200
a_0	1027			786.8	1339
a_1	-0.953	0.042	<0.0001	-1.03	-0.870
a_2	1.24	0.050	<0.0001	1.14	1.34
a_3	1.08	0.115	<0.0001	0.855	1.31

*SE: standard error of the regression coefficients estimates.
**p-value for the t-statistic applied to the regression coefficients estimate

one and at initiation velocities below half the speed of sound.

Note that if initiation velocities are much higher than the speed of sound, a bell-like or band-pass filter-type function should be required instead, with an upper cut-off value at relative initiation velocities of about 1.89, at which wave reinforcement no longer happens in the direction of initiation. In this case, other directions of reinforcement (on which the projected initiation velocity is approximately sonic) appear. Since in our data the maximum relative initiation velocity is $v_I = 1.13$, such upper cut-off is not required and only the direction of initiation (θ =270º) bears the maximum pressure reinforcement, as shown by the term (1-sin θ) in Equation 9.

Replacing A_f from Equation 7 and As from Equation 8 in Equation 6 leads to an overpressure function of three variables (Z, cos θ and W_0) with four coefficients (a_0, a_1, a_2 and a_3):

$$P = a_0 \exp(a_2 \cos\theta + a_3 W_0) Z^{a_1} \quad (11)$$

Taking natural logarithms in Equation 11 gives the linear function:

$$P = \log a_0 + a_2 \cos\theta + a_3 W_0 + a_1 \log Z \quad (12)$$

Equation 12 is fitted to the data set using ordinary least squares. The overpressure is given in Pascal. The scaled distance is calculated with Equation 2 as function of the explosive mass detonated in a delay. The coefficients of the regression and their main statistics are given in Table 3; the units employed are Pa for pressure and $m/kg^{1/3}$ for scaled distance. The low p-values of the coefficient estimates are strong evidence that the model is statistically valid. The determination coefficient of the model is 0.869 and the adjusted determination coefficient R_a^2 (best indicator of the fit quality in multiple regression) is 0.866; the goodness of the fit does not change whether Equation 2 or 3 is used to calculate scaled distances. If the addend a_3W_0 is discarded in Equation12 and the resulting Equation fitted to the data, R_a^2 decreases to 0.776.

A plot of the measured peak overpressures versus the predicted ones is given in Figure 3; the data are differentiated as function of the blast type (single shot and production blast) and existence of stemming ejection. The regression line has a slope of one with a zero constant term. The fact that overpressures from the single blasthole shot are below the regression line is consistent with the effect of the volume of displaced rock on airblast (ISEE 1998), since a single blasthole moves less volume of rock compared with a delayed production blast. Figure 3 also shows that the upper prediction band at a 95 % confidence level is a safe rank for blasts with stemming ejections. The residuals of the fit are also plotted in Figure 3.

Contour maps of equal overpressure *P* show by inspection the main propagation features in one area (More *et al*. 1993, Richards and Moore 2002). Figure 4 shows, as a matter of example, the effect of the firing velocity in the propagation of blast waves. The contours of peak overpressure equal to 89.3 Pa are plotted for blasts with constant explosive mass per delay of 148 kg (mean value from the blasts monitored) and different firing velocities along the face; 89.3 Pa is the limit established by US Bureau of Mines (Siskind *et al*. 1980) for linear type microphones.

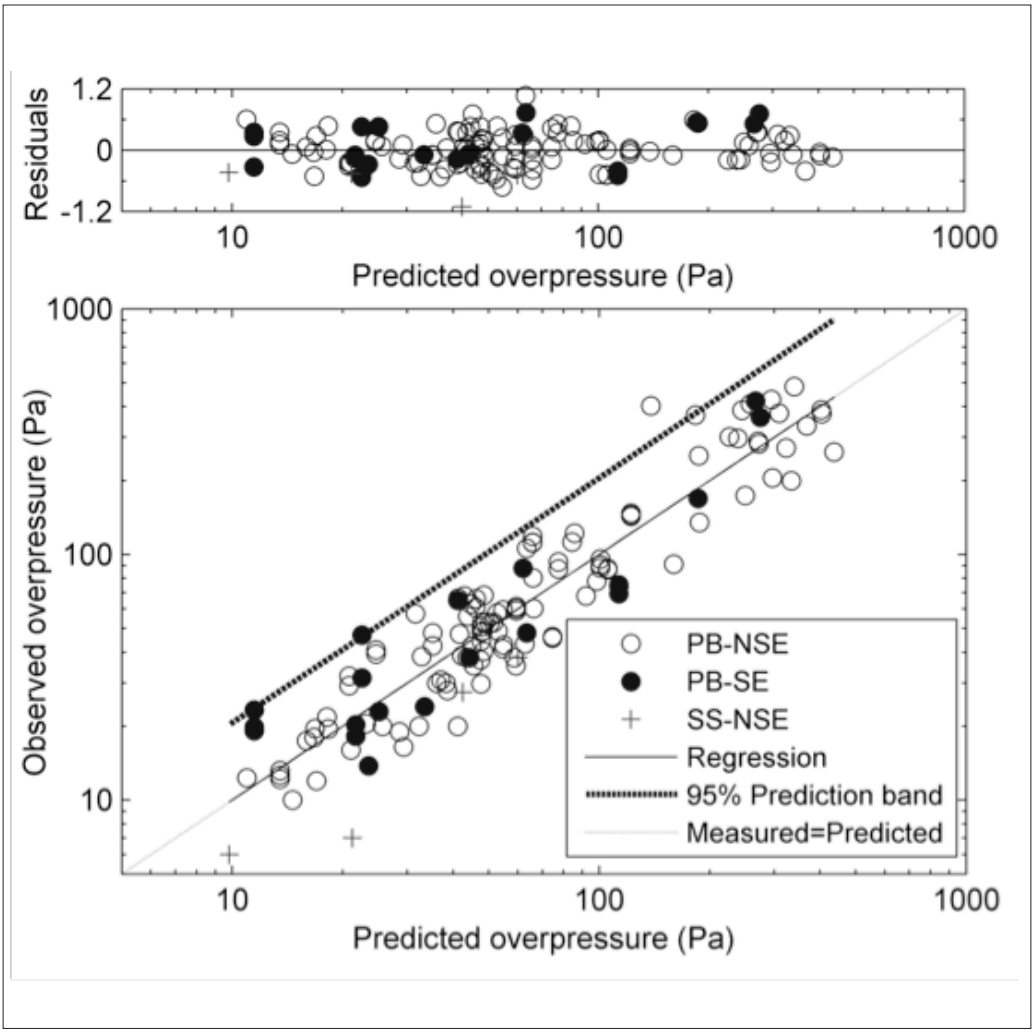

Figure 3. Measured versus predicted peak overpressures (PB: production blast, SS: single shot, NSE: no stemming ejection, and SE: stemming ejection) and residuals of the fit.

Figure 5 shows a plot of the factor $A=a_0 \exp[a_2\cos\theta + a_3 Wo(\theta,v_I)]$ as function of its two variables, θ and v_I. It varies from 300.4 to 15381; the lower bound is obtained behind the face (i.e. θ=180º) for relative velocities equal to 0.5, and the largest for measurements in front of the face (i.e. θ=319º) from blasts with sonic initiation velocities. This range agrees quite well with the highest and smallest values of the coefficient a_0 for quarry blasts with confined charges given in Table 1.

The knowledge of the maximum likely peak overpressure (P_{max}) from a given blast at a certain position is useful to avoid damage and also for control purposes. Such value is estimated as the upper prediction bound of the peak overpressure at a 95 % confidence level from our model. It is given in Figure 6 as a function of the scaled distance; for each initiation velocity, lines of maximum and minimum overpressure P_{max} (corresponding to polar angles θ_{max} and θ_{min}, respectively, given in the legend of Figure 6) are plotted. As a matter of comparison, propagation laws from blasting handbooks (ISEE 1998 and Hustrulid 1999) are also represented in Figure 6.

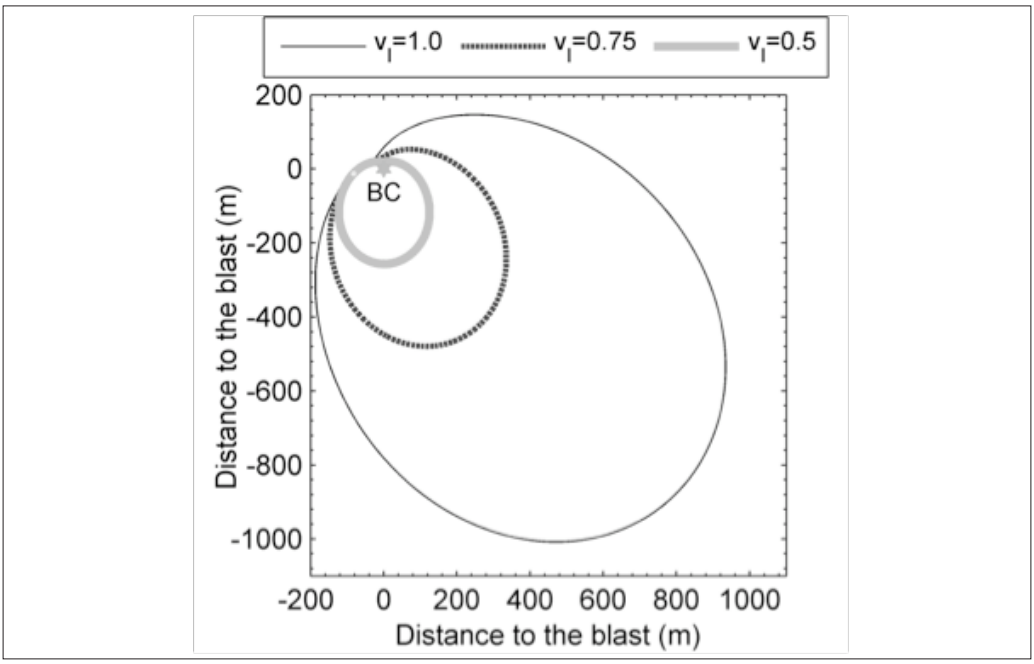

Figure 4. Contours of 89.3 Pa peak overpressure as function of the relative initiation velocity (v_I); BC is the blast centre.

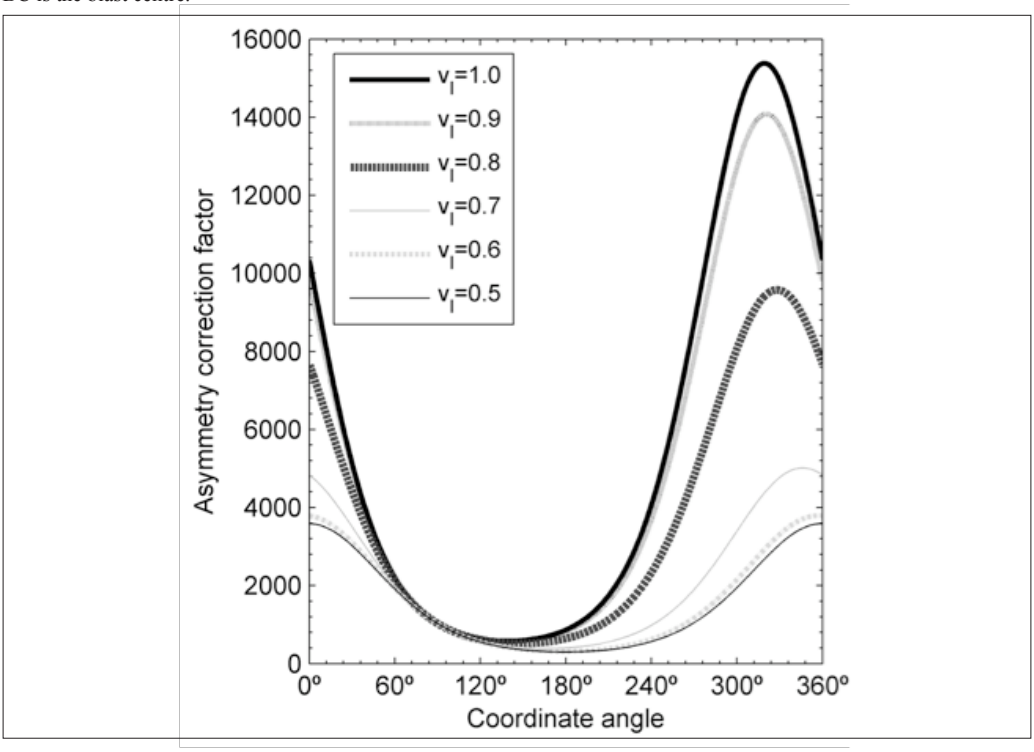

Figure 5. Asymmetry correction factor as function of the coordinate angle and relative initiation velocity (v_I).

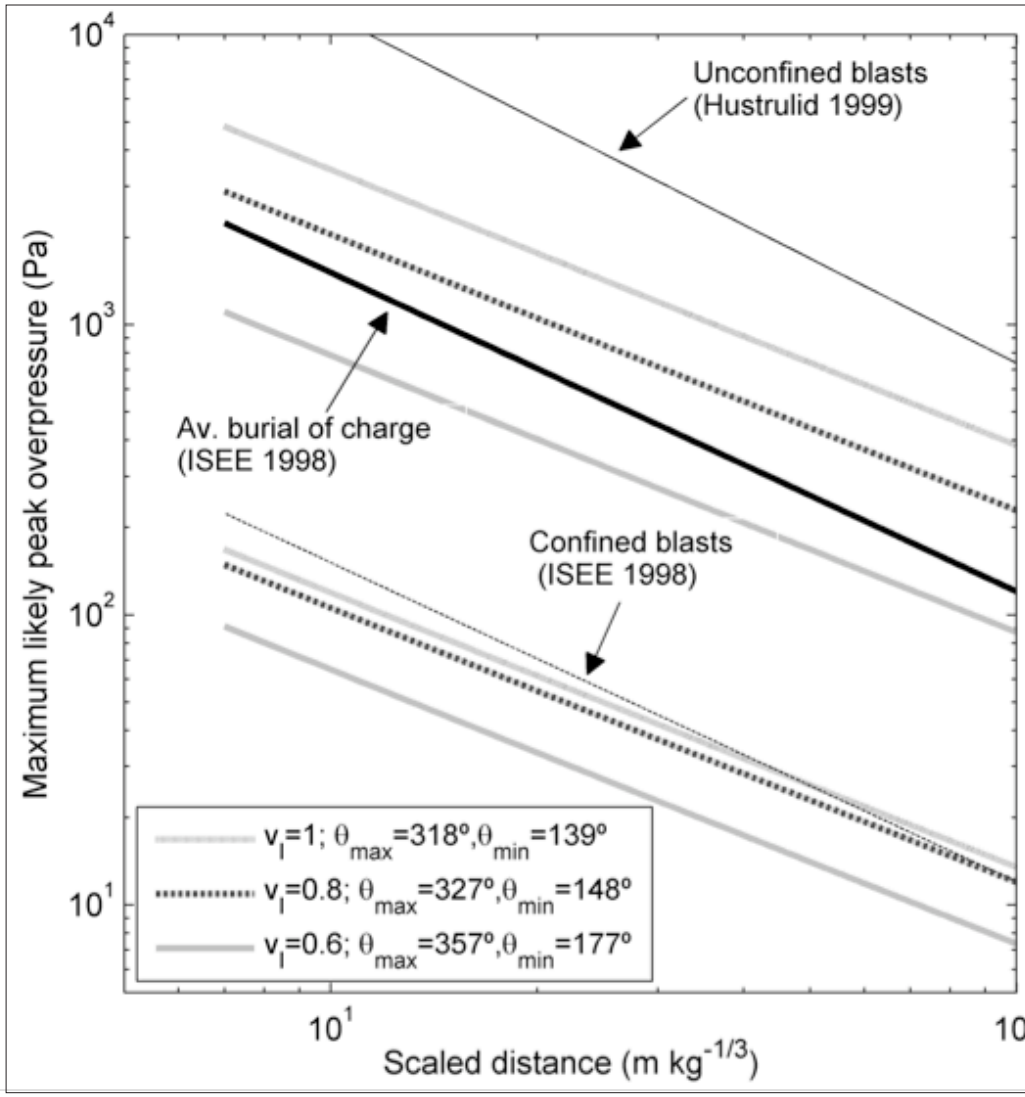

Figure 6. Maximum likely overpressures as function of the scaled distance and relative initiation velocity of the blast (v_I). Lines drawn correspond to the propagation paths at which pressure is maximum and minimum. The polar angles of these paths, θ_{max} and θ_{min} are given in the legend.

4. CONCLUSIONS

Peak overpressure is a useful indicator of the damage and disturbance that airblast may produce nearby a blasting site. This work provides a model for such pressure from blasts with one free face in which the blastholes are delayed in a typical quarry blasting practice, from the hole in one end of the block towards the other end. The peak overpressure is obtained as the product of a classical scaled distance function times a directional correction factor. The scaled distance law is based on the mass of explosive per delay. The directional correction factor considers the influence of:

- Bench face: it amplifies overpressure at the bottom level (i.e. in front of the rock movement) and attenuates it at the top (i.e. behind the rock movement) through a cosine function of the polar angle or azimuth of the position of interest.

- Blast delay: It amplifies blast waves in the direction of the initiation sequence if the velocity of initiation exceeds half the sound speed, increasing the amplitude up to an initiation velocity in the range of the speed of sound.

Blasting data and airblast measurements from 134 records in 46 blasts and one single shot made in rocks with low to very low strength are used to build the model. The explosive mass in a delay varied from 21.3 to 296 kg, and the initiation velocity of the blast ranged between 67 m/s and 383 m/s. Airblast was measured with linear type microphones around the blasted blocks at distances from the blast of 45 to 444 m. The measured peak overpressures ranged from 6 to 482 Pa with a relative mean uncertainty of 3.6 %. The model explains 86.9 % of the variance in the logarithm of overpressure and is statistically meaningful. No difference in the goodness of the fit is observed when explosive energy is used instead of explosive mass.

The model is used to derive upper prediction bounds at a 95 % confidence level of peak overpressure as function of the scaled distance, initiation velocity and propagation paths. The corresponding plots can be used to assess the range of maximum blast overpressure levels expected in a particular blast design. These values are useful to evaluate whether the model can be applied in different sites.

5. ACKNOWLEDGEMENTS

Cementos Portland Valderrivas and Saint Gobain Placo Ibérica are acknowledged for their permission and support to carry out the field work. The experimental work in El Alto was partially funded by the European Union under contract no. G1RD-CT-2000-00438, 'Less Fines Production in Aggregate and Industrial Minerals Industry'. The collection of data in Monte Espartinas quarry was partially funded by MAXAM, which support is gratefully acknowledged. Special recognition is due to Alberto Gómez, Javier Gutiérrez and Javier Quemada for their help and enthusiastic cooperation in the data gathering.

REFERENCES

Domingo, J.F., 2007. Análisis de la onda aérea producida por voladuras en banco en el campo cercano, *PhD Thesis*, Madrid: Universidad Politécnica de Madrid. In Spanish.

Dowding, C.H., 2000. *Construction Vibrations*, United States: C.H. Dowding, pp.204-207.

Egorov, M.G., 1996. Blast design optimization to minimize effect of airblast, *Proc. of the 22nd Annual Conference on Explosives and Blasting Technique*, Vol. 1, Orlando, pp.286-293.

Griffiths, M.J., Oates, J.A.H & Lord, P., 1978. The propagation of sound from quarry blasting. *Journal of Sound and Vibration*, 291:358-370.

Hustrulid, W., 1999. *Blasting Principles for Open Pit Mining, Vol I– General Design Concepts*, Boca Raton: CRC Press, pp. 281-285.

ISEE, 1998. *Blasters' Handbook*, 17th Edition, Cleveland: International Society of Explosives Engineers, pp. 626-644.

ISEE, 2009. *ISEE field practice guidelines for blasting seismographs 2009 edition*. Cleveland: International Society of Explosives Engineers.

ISEE, 2000. *Performance specifications for blasting seismographs*, International Society of Explosives Engineers,www.isee.org/media/pdf/2SeisPerf Specs00.pdf.

Konya, C.K., 1995. *Blast design*, Montville: Intercontinental Development Corporation.

Kuzu, C., Fisne, A. & Ercelebi, S.G., 2008. Operational and geological parameters in the assessing blast induced airblast-overpressure in quarries. *Applied Acoustics* 70(3): 404-411.

Marchand, K.A., 1999. Load definition, in E.J. Conrath (Ed.), *Structural Design for Physical Security: State of the Practic*e, Reston: Structural Engineering Institute, American Society of Civil Engineers, pp.2.7-2.18.

Mohanty, B., 1998. Physics of explosions hazards, in: A. Beveridge (Ed.), *Forensic Investigation of Explosions*, London: Taylor&Francis, pp. 22-32.

Moore, A.J., Evans, R. & Richards, A.B., 1993. An elliptical airblast attenuation model. *Proc. of the 4th International Symposium on Rock Fragmentation by Blasting- Fragblast 4*, Vienna, pp.247-252.

Persson, P.A., Holmberg R. & Lee, J., 1994. *Rock*

Blasting and Explosives Engineering, Boca Raton: CRC Press, pp. 375-386.

Richards, A.B. & Moore, A.J., 2002. Airblast design concepts in open pit mines, *Proc. of the 7th International Symposium on Rock Fragmentation by Blasting- Fragblast 7*, Beijing, China, pp. 553-561.

Rudenko D., 2002. Airblast an often overlooked cause of structural response, *Proc. of the 28th Annual Conference on Explosives and Blasting Technique*, Vol. 2, Las Vegas, pp.153-166.

Siskind, D.E., Stachura, V.J., Stagg, M.S. & Koop, J.W., 1980. *Structure response and damage produced by airblast from surface mining*, USBM Report of Investigation 8485. Twin Cities: United States Bureau of Mines.

Snell, C.H. & Oltmans D.L., 1971. *A revised empirical approach to airblast prediction*, Report No. 39, Livermore: US Army Engineer Explosive Excavation Research Office, pp. 44-51.

Lisbon Conference Proceedings 2011, R. Holmberg et al
©2011 European Federation of Explosives Engineers, ISBN 978-0-9550290-3-5

Test blasts and vibration prediction, AVM project Klinthagen Quarry, Gotland, Sweden

M. Jern
Nitro Consult AB, Göteborg, Sweden

ABSTRACT: An AVM project has been performed at the Nordkalk's limestone quarry at Klinthagen, Gotland, Sweden. The aim of the project was to make recommendations concerning the excavation of a new area in the quarry mainly in order to keep vibration levels within limits. The article demonstrates the method of study, results from test blasts and the modelling of blasting in the area. In the end a comparison is made between the Monte Carlo simulation model used in the project and more conventional prediction of vibrations, i.e. by regression analysis and the charge weight scaling law equation.

1. INTRODUCTION

AVM (Advanced Vibration Modelling) is a concept to optimize vibrations from blasting. The general idea is to use a modern technique and knowledge in order to go another step forward and to model blasts in order to recommend drilling, charging, initiation etc., to keep vibration levels within specified limits.

Central in the concept is the Monte Carlo model which originally was developed at Orica Technical Centre, Kurri Kurri Australia. The Model, which is described in a number of articles (Blair 1999, 2004, 2007), is included as a module in Orica Mining Services software: SHOTPlus-i Pro.

Klinthagen limestone quarry is owned and operated by Nordkalk AB, the quarry is situated on northern Gotland and produces annually approximately 2 Mt limestone, mainly for the steel industry. As a part of a project to enlarge the production area an AVM project has been performed. The aim was to suggest a way to excavate the area

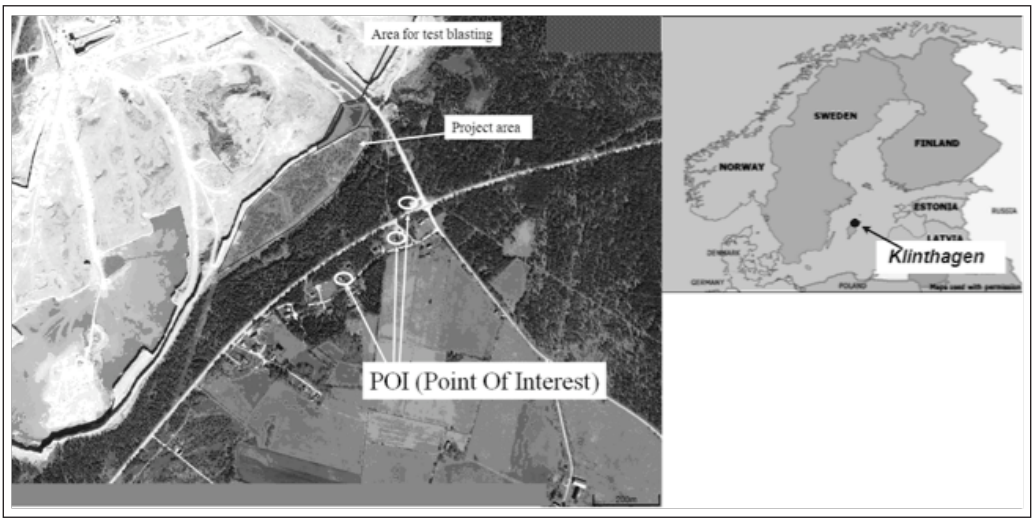

Figure 1. Aerial photograph showing the area for test blast, the project area and closest buildings (POI).

without exceeding the permitted vibration level (4 mm/s) at multiple points of interest (POI).

The area is situated on the eastern border of the quarry and holds approximately 2 Mt or approximately one year production in the quarry. This volume is extremely important for the quarry since it's needed in the time before the operation can be moved to a new location (the Bunge quarry).

The area for the project is situated quite near dwellings. The closest houses will be at distances of around 200 m from production. Before the project started it was decided that all blasting in the new area would be performed with 76 mm bore holes and blasts would be limited to one row at the time. Since the bench height is around 12 m the charge weight in a fully charged hole is limited to around 50 kg. Test blasts were fired close to, but not within, the actual project area, this since authorities are yet to give permission for blasting within the project area. Vibration monitoring was performed in the surrounding area with focus on three nearby houses (the points of interest seen in Figure 1).

According to Swedish Standard SS 460 48 66 vibrations are only monitored in the vertical direction, hence all vibration data presented in this paper relates only to the vertical direction.

2. MONTE CARLO SIMULATION

The difference between the Monte Carlo Model and the way vibrations traditionally have been calculated (charge weight scaling law equation) is mainly that the concept of time is introduced in the calculations, and in this way it's possible to optimize the blast also regarding different initiation plans.

The model uses Monte Carlo simulation i.e. you include variability in governing parameters which cannot be exactly determined (due to geological uncertainties, delay scatter in the initiators etc.) and then you run the model many times in order to quantify a statistical distribution. The model is a waveform superposition model; so that the result is calculated by superposition of several charges which have similar vibration shapes but are different in time and space.

In the calculations you use a seed wave which gives information about how the vibration changes depending on the medium it travels through between the place of the detonation and the monitoring point. The properties of the seed wave are a "finger print" that consists of information regarding the geological properties that governs the vibration. The principle of the model is shown in figure 2.

2.1 The seed model

By monitoring the signature waveform (the seed wave) from a single detonation it is possible to determine properties of the vibration that is valid at a given monitoring point. The effect of many detonations can then be calculated through waveform super-position. This approach can today be seen as established in vibration analysis in blasting, see Spathis (2009) and Anderson (2008).

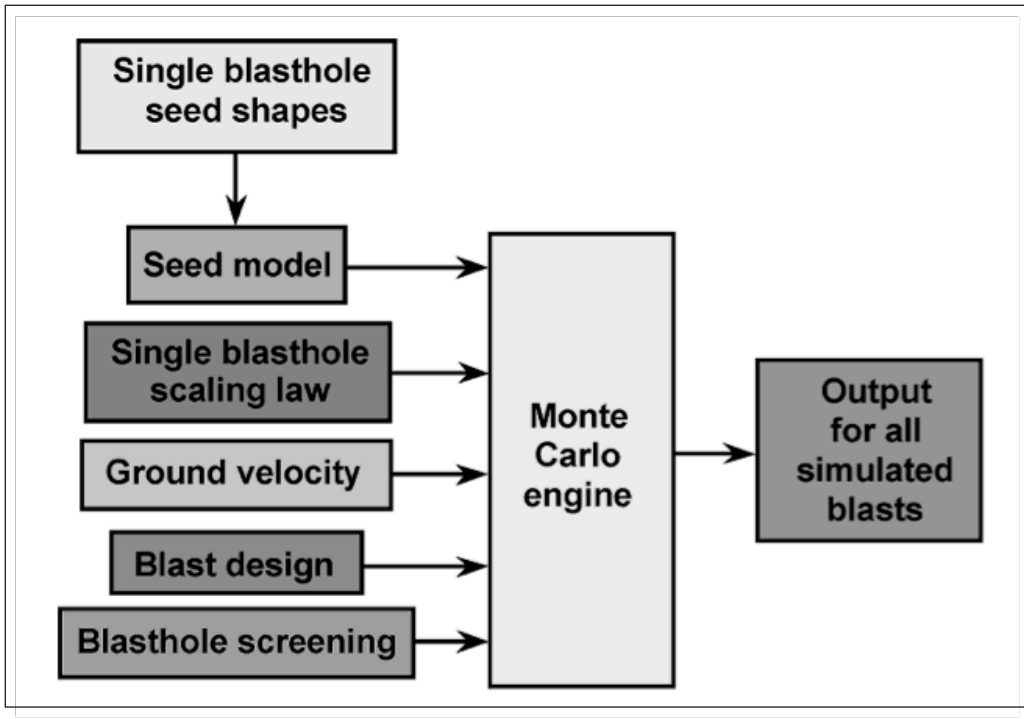

Figure 2. A block diagram of the Monte Carlo model.

2.2 Scaling law

The charge weight scaling law equation is the most common method to calculate vibrations from blasting regarding size and distance. In the Monte Carlo simulation however, it is just a part of the model, the equation is in this case:

$$v_{max} = A \cdot \left(\frac{r}{\sqrt{q}}\right)^{-B}$$ the parameter: $$\left(\frac{r}{\sqrt{q}}\right)$$ is often called SD (scaled distance

where v_{max} = maximum peak particle velocity (mm/s)
r= distance (m)
q= charge weight (kg)
A= site specific constant
B= site specific constant

The charge weight scaling law equation is normally determined through regression analysis where you curve fit measured data to determine the equation and how good the fit is.

2.3 Ground velocity

In order to calculate the effect from different detonations on a certain point the aspect of time has to be correctly included. Besides the delay between detonations the travel time in the ground is of importance. In order to calculate it, you must measure the travel times of the vibrations to surveyed locations and fit a linear curve to the data, the slope of which is the required ground (P-wave) velocity.

2.4 Blast design

Information like position, number of holes, charge in each bore hole, charge geometry and initiation plan is defined together in a blast plan (in the software) and is used in the simulation.

2.5 Blasthole screening

Detonations close to each other effect each other by creating a 'vibration shadow' in the direction of former detonations, due to damage and fragmentation around the blasthole. This effect is called screening (Blair 2007) and is included in the calculations by a specific screening algorithm.

2.6 The process of calibration

In order to optimize the precision of the model it has to be calibrated. The calibration process means that you shoot full scale blasts and compare the results with simulated blasts from the same location. The main parameter in the calibration process is the A-parameter (the level of the charge weight scaling law equation); the reason why this calibration has to be performed is mainly that we perform the test blasts in pristine ground. This gives higher vibrations than what you get in the normal situation during a production blast.

3. TEST SETUP

3.1 Vibration monitoring

Two different vibration monitors were used. At five points the monitor Kelunji ECO Pro from ES&S was used: mp 1, 5, 7, 9 and 11. At the other 7 points: mp 2, 3, 4, 6a, 6b, 8 and 10 the Infra monitor from Sigicom was used (see Figure 4). The advantage of the Kelunji instrument was mainly the gps-synchronised clock that allows determination of P-wave velocity. The Infra instrument on the other hand, has a better sampling frequency (4000 Hz instead of 2000 Hz). The Infra system is also used for 'every day' monitoring at the site which means that the test was performed with the same instruments that in the future will control upcoming blasts.

The area consists of a horizontally layered limestone that is covered with a thin layer of till, 1-2 m thick. Where it was possible the transducers were placed on solid rock, where it was not possible the transducers were placed in soil.

All mounts made in rock and at the houses (POI) where done by drilling a bore hole (φ 8 mm) and bolting the transducers to the surface. Regarding the mounts in soil, specially made cylinders were used as mounts, the cylinders were buried level with the top of soil, and the soil was tamped around the base to ensure firm contact between the soil and the transducer's base.

3.2 Test blasts

In total 17 single hole shots were fired during three different occasions, upon that five calibration blasts were shot. The purpose of the calibration blasts was to tune the model and to confirm that the simulations made gave a good approximation to reality.

At the 'main test' 10 single holes were fired, vibrations from these shots were monitored at 11 different locations, this was in order to construct a careful investigation aimed at finding how the vibration waveforms change depending on distance travelled and amount of charge, (at the other 7 single hole shots and the five calibration blasts the vibrations were only monitored at the buildings mentioned previously - POI). Monitors were placed at ranges between 18 and 800 meters from the detonations.

The charge in each hole varied from fully charged, down to 75%, 50% and 25% of maximal charge. Two different kinds of explosives were used: Centra Gold (SME-emulsion) and Fordyn (dynamite type). The charge for each test hole is listed in Table 1. The position of the holes can be seen in Figures 3 and 4. The position of the monitors can be seen in Figure 4. Two of the single hole shots were shot with 'normal' burden (2.7 m) and 8 in pristine ground (infinite burden).

Table 1. The charge and explosive for each test hole.

Shot		**Charge(kg)**		**Explosive**	
1		52		1.	SME+2 kg boost
2.	2	3.	52	4.	SME+2 kg boost
5.	3	6.	45	7.	Fordyn
8.	4	9.	39,5	10.	SME+2 kg boost
11.	5	12.	52	13.	SME+2 kg boost
14.	6	15.	12,5	16.	Fordyn
17.	7	18.	39,5	19.	SME+2 kg boost
20.	8	21.	27	22.	SME+2 kg boost
23.	9	24.	52	25.	SME+2 kg boost
26.	10	27.	27	28.	SME+2 kg boost

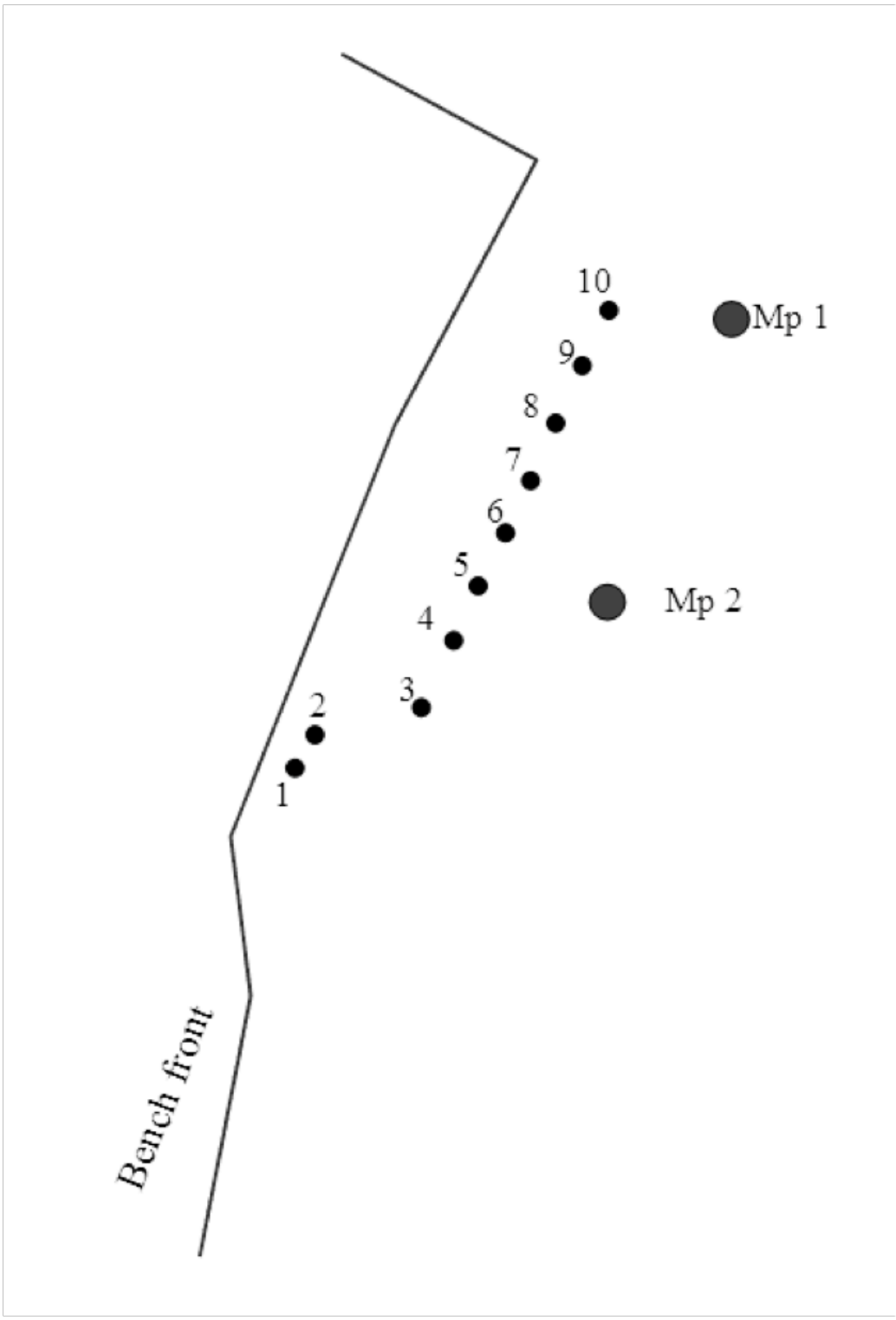

Figure 3. Position of single hole shots. The figure is a close-up of the ‘single hole shot’ area shown in Figure 4.

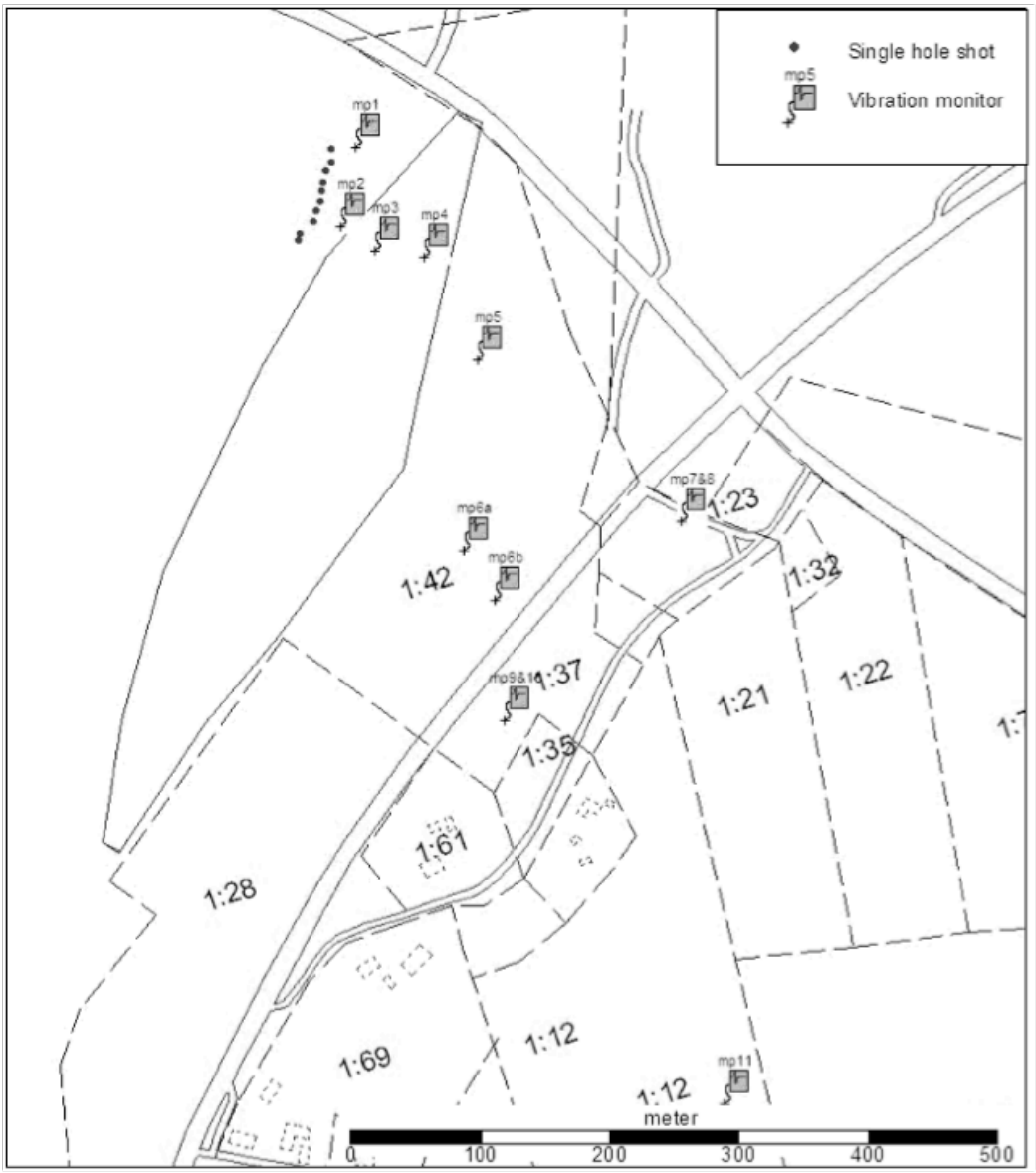

Figure 4. The setup of test blast: Ten single hole shots were monitored at 11 different locations.

Table 2. Data from the five blasts.

Blast	Holes	Max. Inst. charge (kg)	Total charge (kg)	Delay (ms)	Init syst.	Note.
1	20	56	1100	42	Nonel	
2	7	56	390	42	Nonel	
3	26	55	1325	35	i-kon	
4	27	31	1350	35* & 17**	i-kon	2 deck
5	23	30	1150	70* & 35**	i-kon	2 deck

*delay between holes. ** delay between decks (upper deck first).

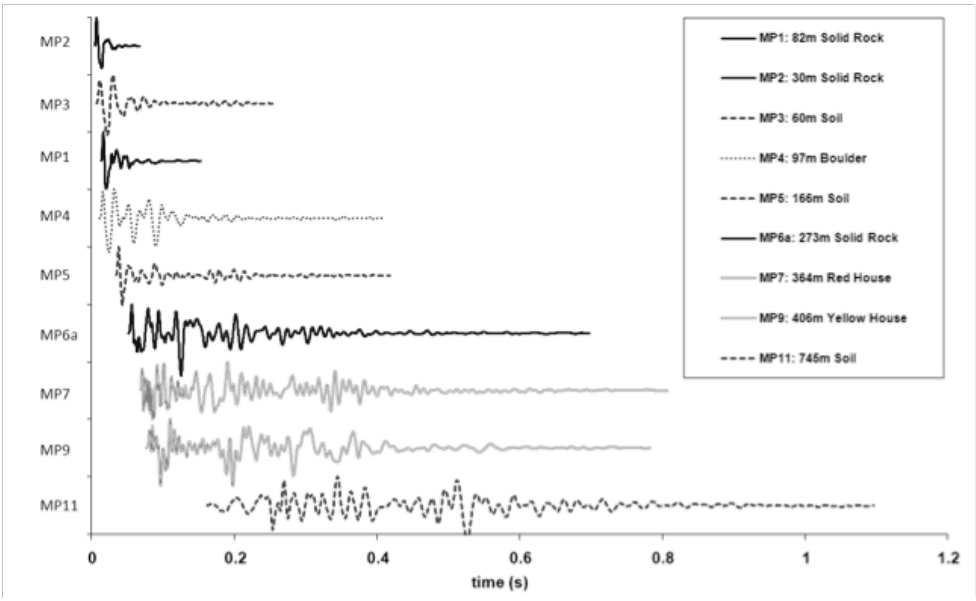

Figure 5. Signature waveform for 8 of the monitoring points.

3.3 Calibration blasts

In addition to the 17 single hole shots that were performed in order to build the model, 5 calibration blasts were shot in order to calibrate the model. These blasts were performed to fine tune, to test and validate the model. A summary of the properties of the five blasts are seen in Table 2.

4 RESULTS OF THE TEST BLASTS

4.1 Single hole shots

It is of vital importance that the signature wave form is monitored on the same spot as the modelling will be performed at, this due to the fact that the wave form is highly affected by how far the wave travels between place of monitor and place for detonation and also due to the response in the constructions monitored. Examples of how the waveform varies due to place and distance can be seen in Figure 5 (data from single hole shot 1).

Position of monitor (distance to detonation) is seen together with mount coupling in the figure. The waves are 'normalized' regarding vibration velocity amplitude and consequently only the shape, time and duration can be seen.

A condition in order to be able to use the signature wave form is that each blast hole in the modelled blast is similar to the seed hole. In Figure 6 an example of 4 different signature waveforms monitored at the same spot (mp 7) are shown.

What we can see is that the four curves are similar both regarding duration and dominating frequencies. However, you can see that they are not identical, in the model a certain amount of randomization is introduced to the seed wave form in order to compensate for this variation.

4.2 Regression analysis – all data

In Figure 7 a curve fit between v_{max} and SD (scaled distance) for all monitored data can be seen.

The inclination and position of the line determines the A and B parameters of the charge weight scaling law equation, the correlation coefficient (R=0.95) shows that the curve fit is good.

The fact that different points in the graph are from different places, which are positioned on different type of ground, as well as the fact that some of shots have been fired with different explosives implies that there is a reason to look at the data more carefully. In Figure 8 the same data

as in Figure 7 is plotted, however in Figure 8 the different monitoring points are shown and it's also highlighted if the monitor sits on soil or on rock. It is obvious that the place where the transducer is mounted is important for the result.

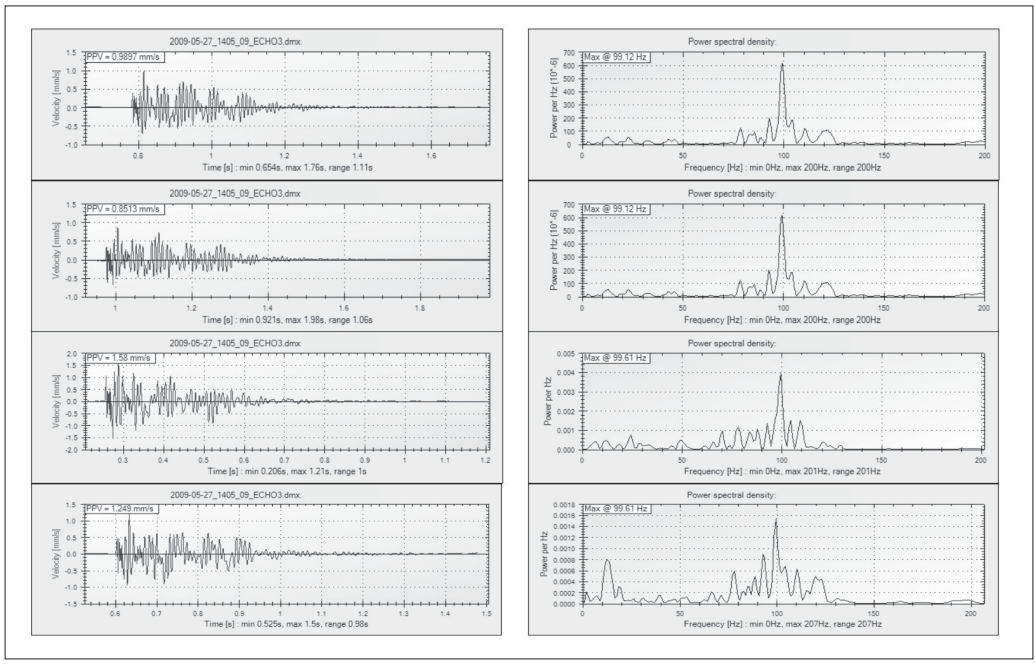

Figure 6. Example of four different single hole shots recorded at monitoring location mp 7.

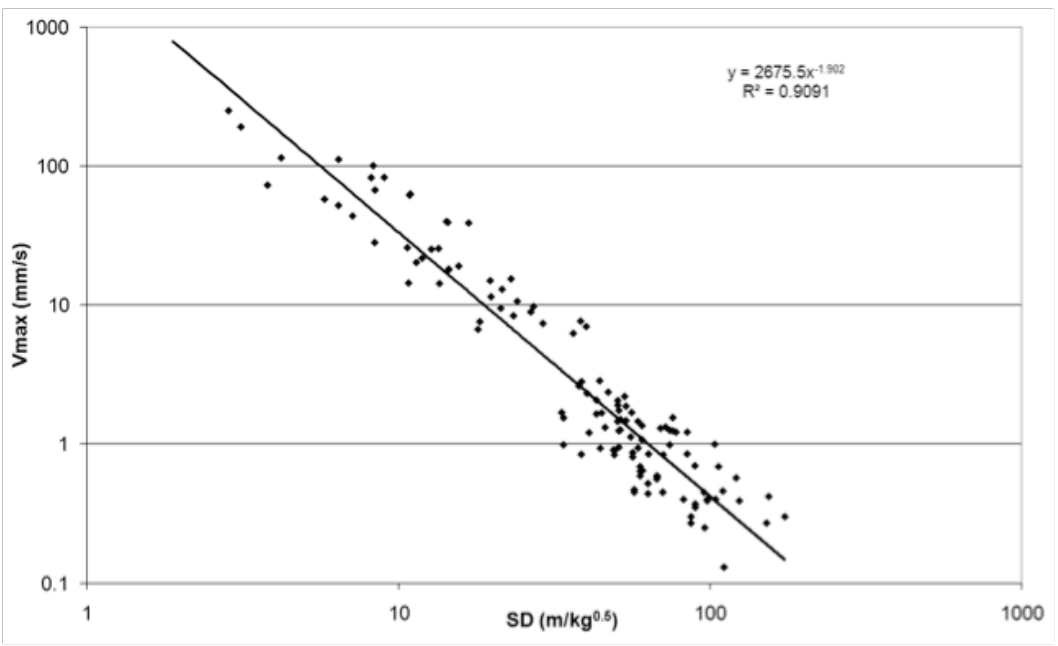

Figure 7. All scaled distance data from the single hole test blasts.

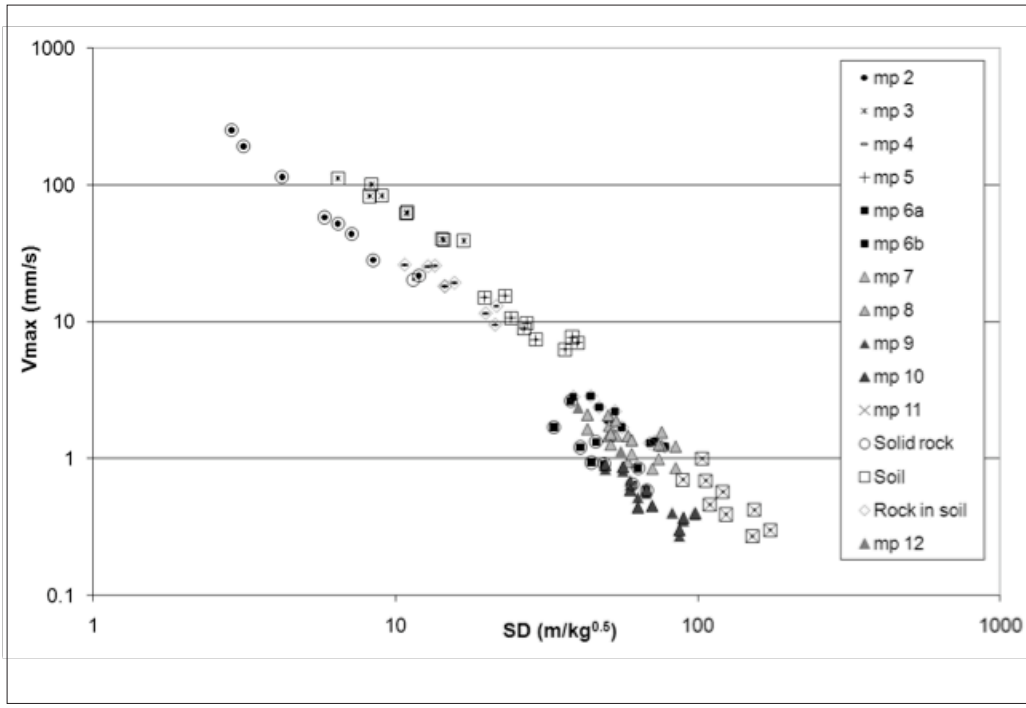

Figure 8. All results, monitoring point and type of surface layers is shown. mp 7-10, the triangles represents the two houses (POI).

4.3 Regression analysis – soil or rock

If one looks at Figure 8 it's obvious that data for the soil mounts plots higher than data for solid rock mounts (vibration in soil is higher than vibration in rock, it should be noted that the soil is only a thin top layer). This leads us to the conclusion that these two may be separated. In Figures 9 and 10 the data for only solid rock and soil respectively is plotted. What we can see is that the correlation coefficient increases considerably in relation to Figure 7, this shows that the result is highly dependent on the position of the transducer.

The correlation coefficient (R) for solid rock becomes 0.996 which of course is extremely good. We can also see that the two lines plot almost parallel; from this we can draw the conclusion that other types of layers, at this quarry, should have the same slope on the regression line.

4.4 Regression analysis – different explosives

The normal explosive used at Klinthagen is Centra Gold (SME); this kind of explosive is mixed at site and loaded directly into the bore holes through a hose. When the test blasts in Klinthagen were performed SME could not be used on all occasions. The reason for that was that the SME – truck was not able to accurately load charges smaller than 25 kg. For the smaller charges a dynamite type explosive was used (Fordyn).

To control that the two explosives gave similar result one hole was also fully charged with Fordyn to allow comparisons with SME. The results when separating the type of explosives can be seen in Figure 11.

What we can see is that the vibrations from Fordyn are considerably higher than from Centra Gold. In order to compensate for this the amount of Fordyn was recalculated to 'SME-equivalents' through their relation in weight strength (Persson et al. 1993). Consequently each kg of Fordyn was multiplied by 1.59 (SME was 84% of ANFO and ANFO is 75% of Dynamite, 1/0.84×0.75= 1.59), the result after that is plotted in Figure 12, as can be seen the two curves plots almost on each other.

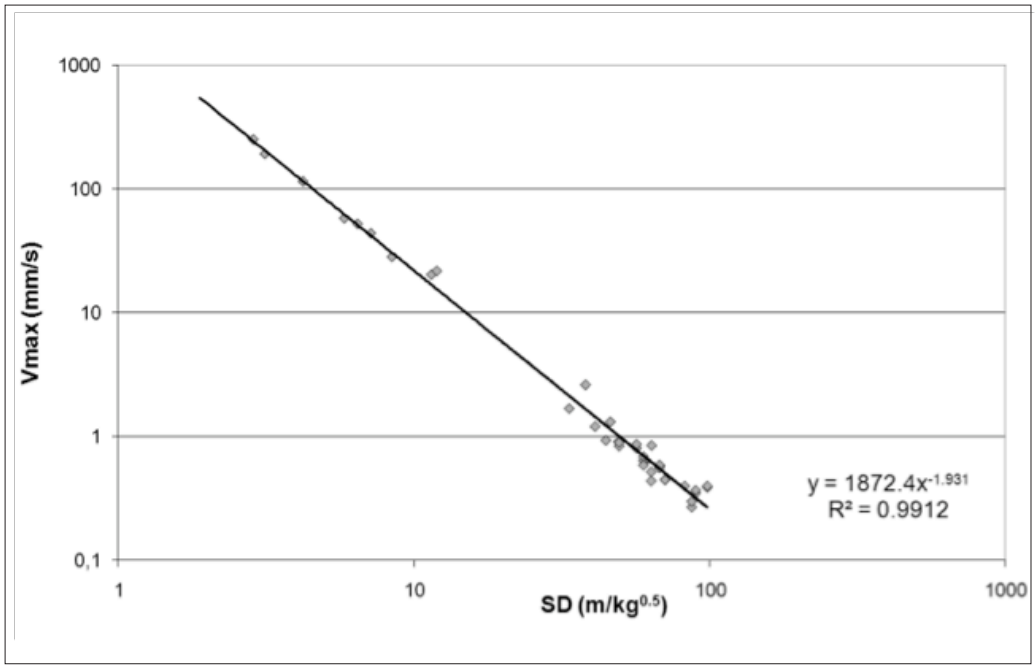

Figure 9. Measurements on solid rock.

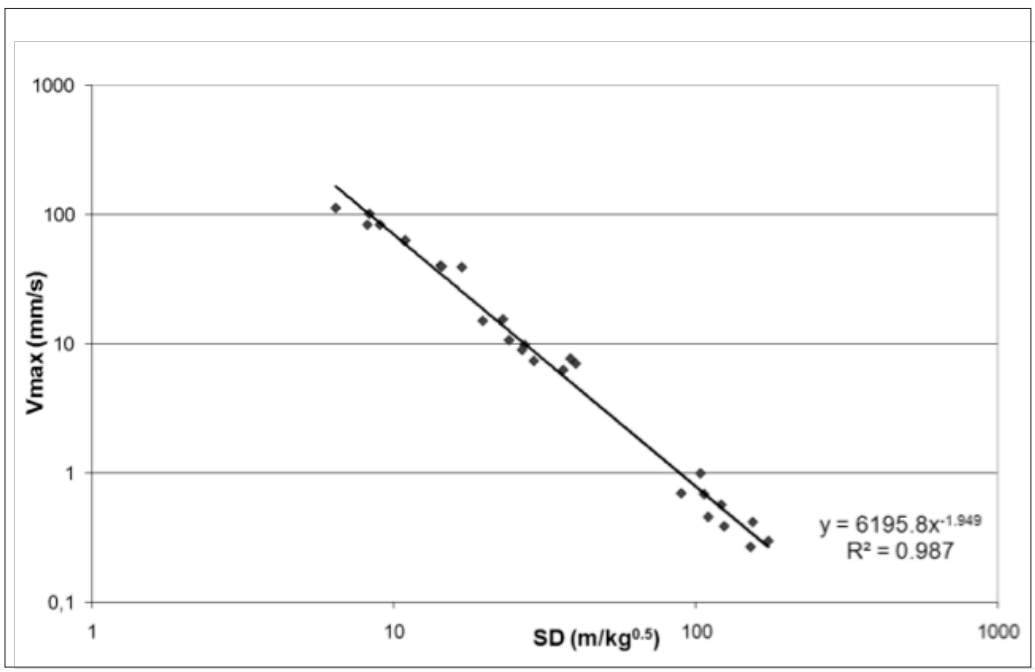

Figure 10. Measurements in soil.

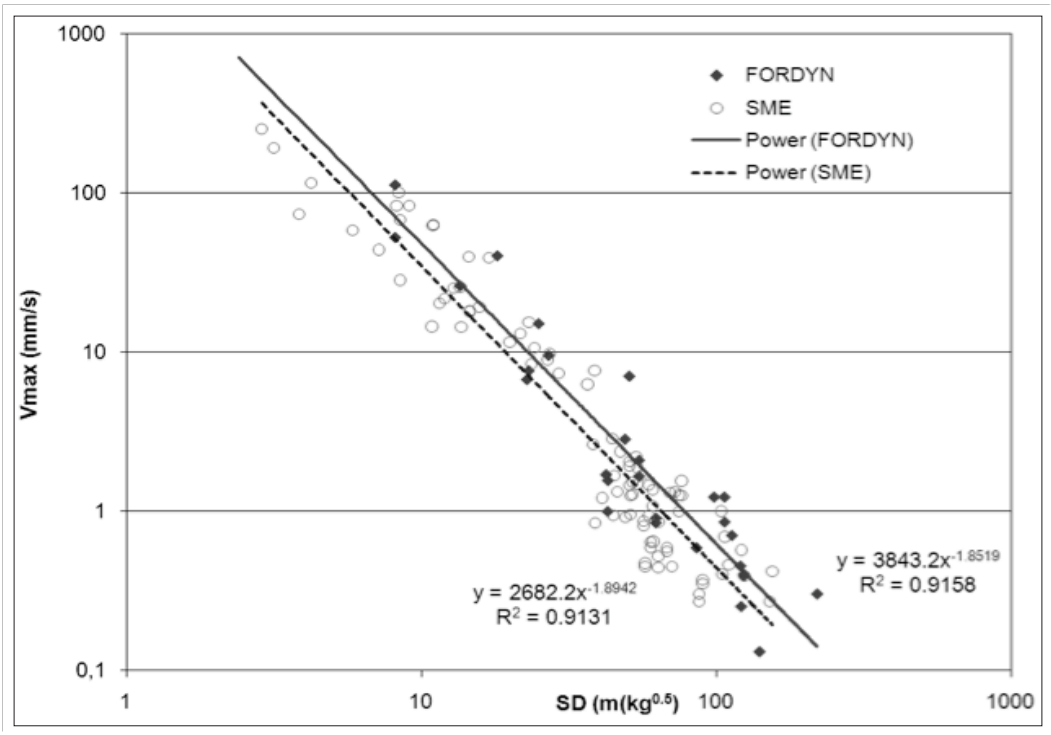

Figure 11. Comparison between SME and Fordyn 'kg to kg'.

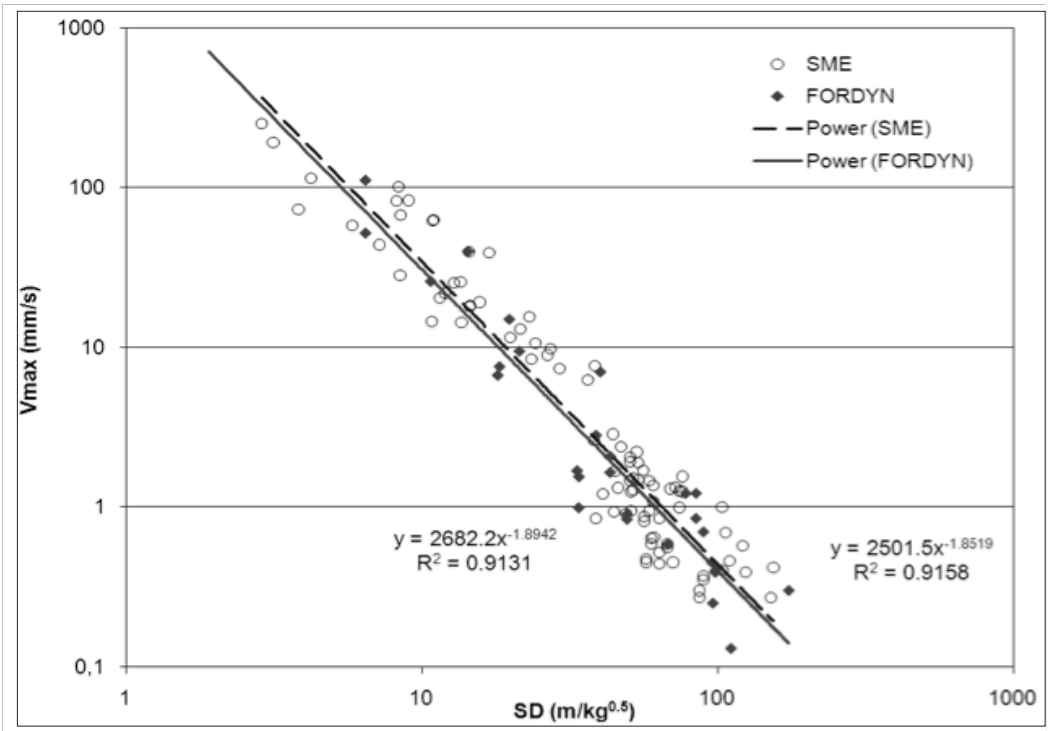

Figure 12. Comparison between SME and Fordyn regarding weight strength.

4.5 Regression analysis – burden

Two of the test blasts were shot with normal burden (see Figure 3); the reason for this was to compare typical site blast conditions with blasting in pristine ground which is normally performed in a project like this.

The vibrations from these two shots are compared to the others shot in pristine ground, as seen in Figure 13. What can be seen is that shot 1 show the same response as the other shots while the second shot gives much lower vibrations. The reason is probably the different conditions that these two detonations had (see Figure 14). Shot number one has been shot towards a free surface with a constant burden forward. When shot two detonates the surroundings have changed, the free surface looks completely different and we can also assume that fracturing around shot 1 affects the area around shot 2. Previous investigations have shown that the burden does not affect the size of the vibrations (Blair & Armstrong 2001), however it is probable that there is an influence from the surrounding ground due to damage and fracturing. This is also the explanation why the model has to be calibrated with respect to the A - parameter.

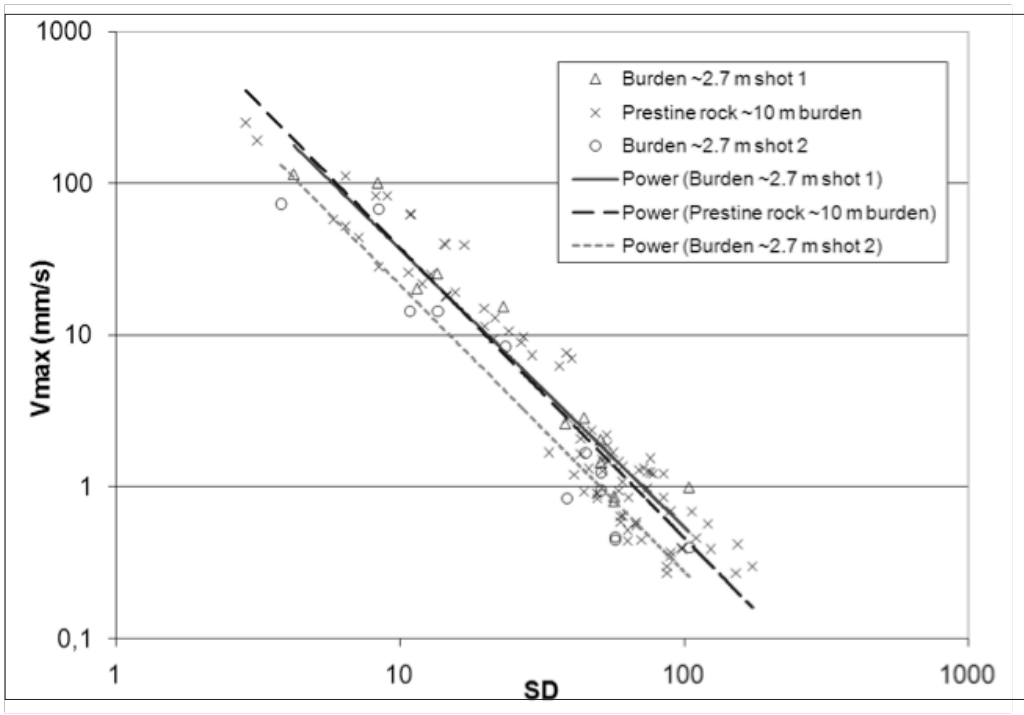

Figure 13. Variation in peak vibration due to test burden.

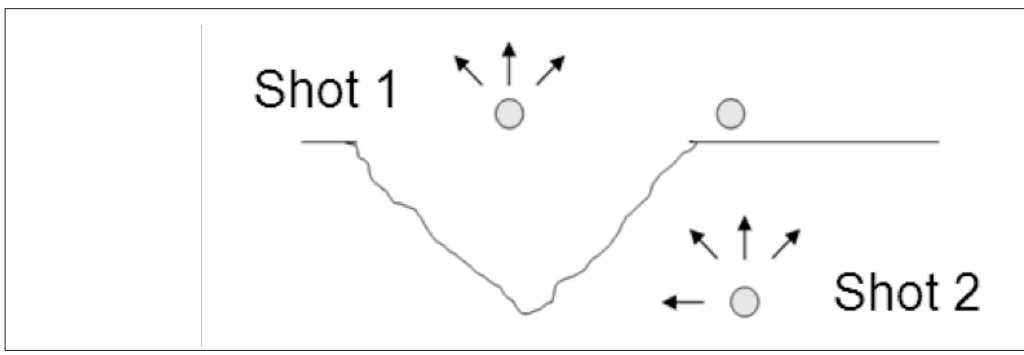

Figure 14. Sketch (plan view) conditions around blast holes during shots 1 and 2.

4.6 Regression analysis –buildings (POI)

The focus for the investigation was three houses located close to the project area. These houses have in the investigation been named from their monitoring point number. Mp 7&8 were mounted on the property Lilla Takstens 1:20, mp 9 was on the property Stora Källstäde 1:35 and mp 12 was mounted on the property Stora Källstäde 1:36 (see Figure 19).

All three houses had quite different responses to the incoming vibrations and consequently each house had to be treated separately. The most straight forward approach could be made to mp 9 & 10. That building had a response almost identical to what was monitored in solid rock. Consequently the charge weight scaling law equation for solid rock could be used in simulations made for that building, see Figure 15.

Regarding mp 7, mp 8 and mp 12 the situation was a bit more complicated. As can be seen in Figure 8 data from these monitors plots in between the line for solid sock and the line for soil. To find a charge weight scaling law equation that could be used for these two buildings the inclination was borrowed from the solid rock line (since the inclination was the same for the soil line it's a fair assumption that points that plot between these two lines should follow the same trend) and then the line was moved parallel upwards to fit the data for the two buildings, see Figure 16.

4.7 Ground (P-wave) velocity

During the test blasts an instrument with GPS-synchronized clock (Kelunji ECO Pro from ES&S) was used. The instrument updates itself via satellite and provides time synchronisation accurate to 0.1 microseconds.

In Figures 17 and 18 the time when the vibration from shot 1 reaches mp 1 and mp 9 can be seen. The time difference was 61 ms and since the difference in distance was 324 meters the velocity of the wave can be deduced as approximately 5300 m/s.

5. CALIBRATION BLASTS

5.1 Running the model

Calibration of the model is an iterative process, data from the single shots is used but to some extent parameters have to be adjusted to account for parameters that are related to the actual blast. The A-parameter is adjusted by calibration, by doing single hole blasts in pristine ground a maximum value is determined that in the calibration process

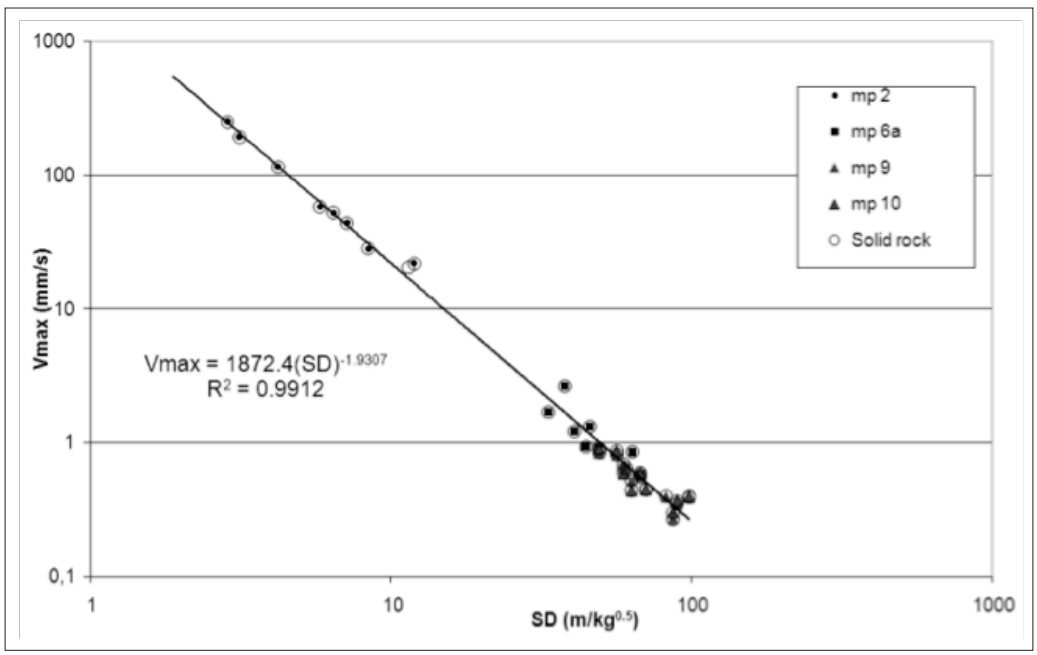

Figure 15. The graph is identical to the similar for solid rock (Figure 9), mp 9 & 10 plots perfectly in this graph.

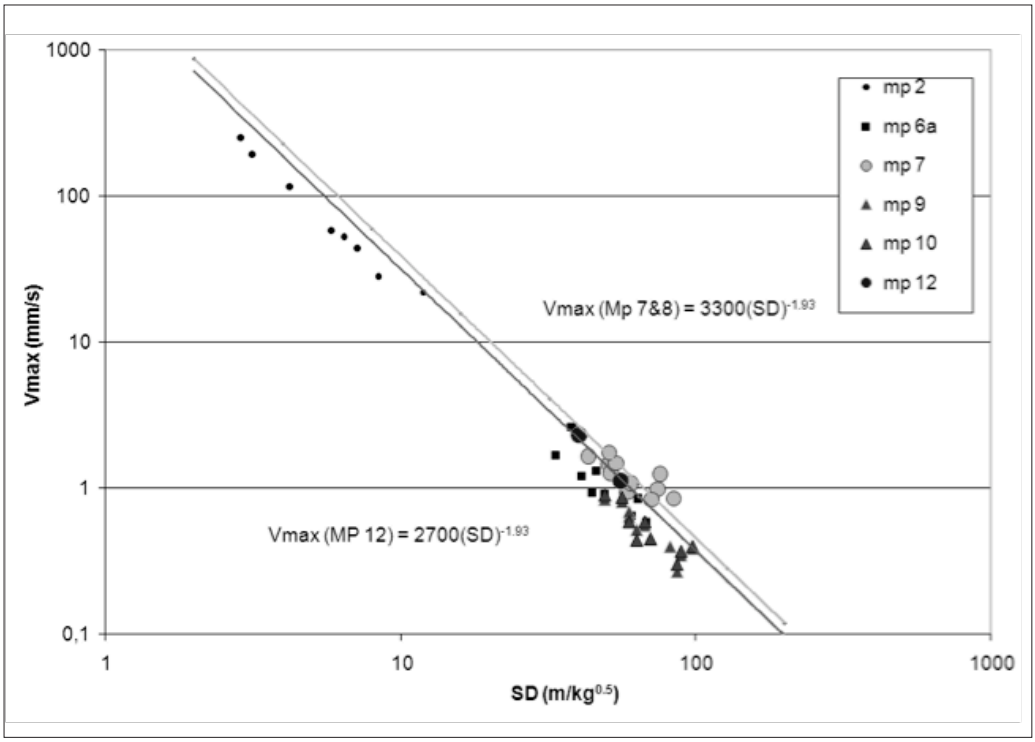

Figure 16. The graph shows the regression lines for mp 7&8 and mp 12.

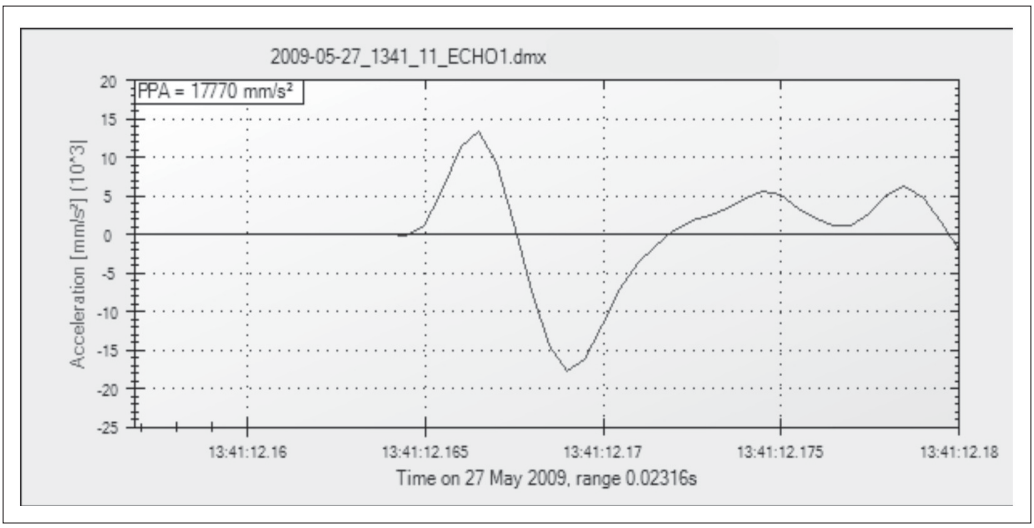

Figure 17 shows the first wave form at mp 1 and shot 1, time is: 13:41:12,164.

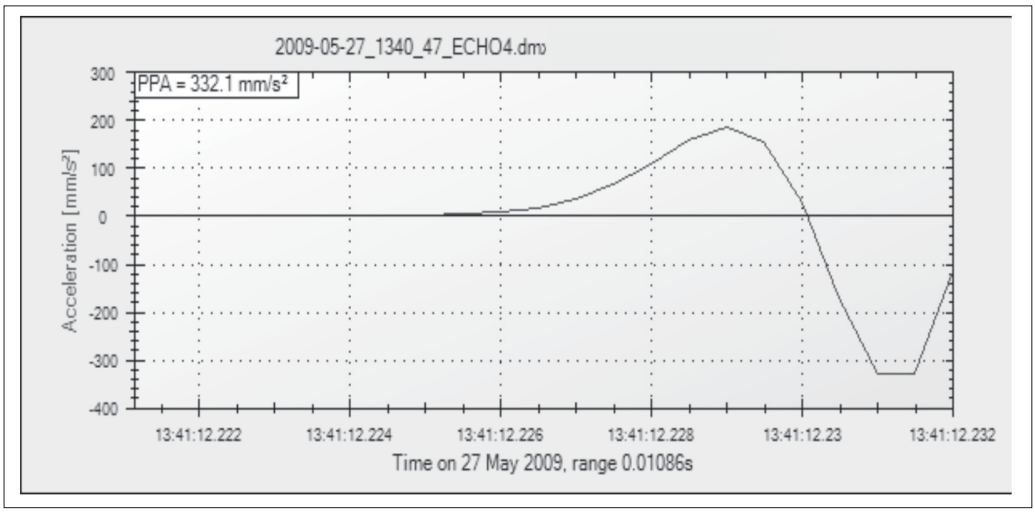

Figure 18 shows the first wave form at mp 9 and shot 1, time is: 13:41:12,225.

Table 3. The parameters used in the model, all parameters are calculated/ monitored except A (used) which is calculated through calibration.

	mp 7-8	mp 9-10	mp 12
A (calculated)	3300	1875	2700
A (used)			
(75% of A(calculated))	2475	1410	2025
B	1,93	1,93	1,93
v_p	5300	5300	5300
COV*	0.25	0.15	0.25

* COV (coefficient of variation) is used to describe the spread of data around the regression line.

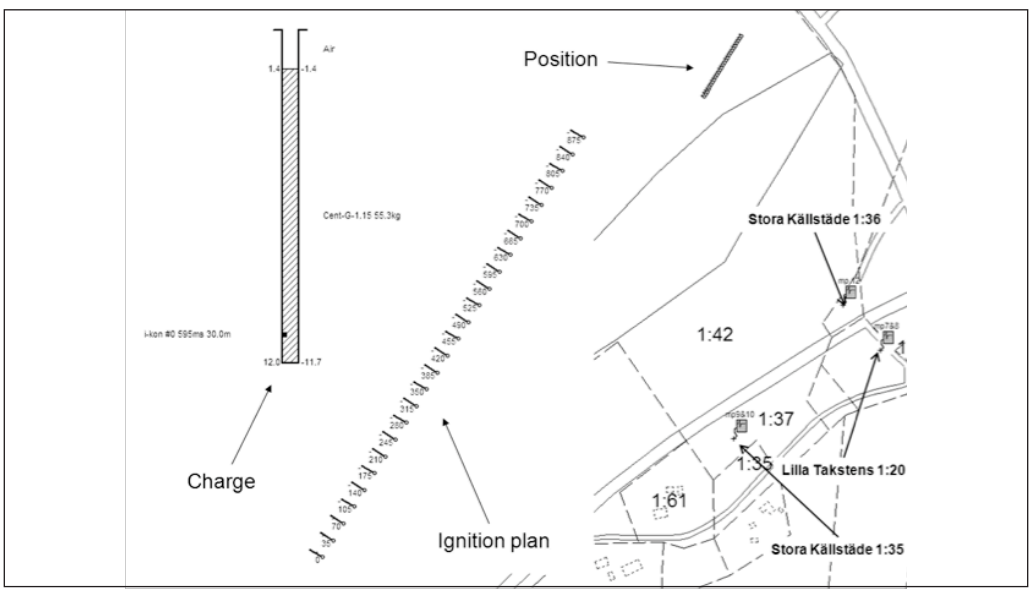

Figure 19. Calibration blast 3.

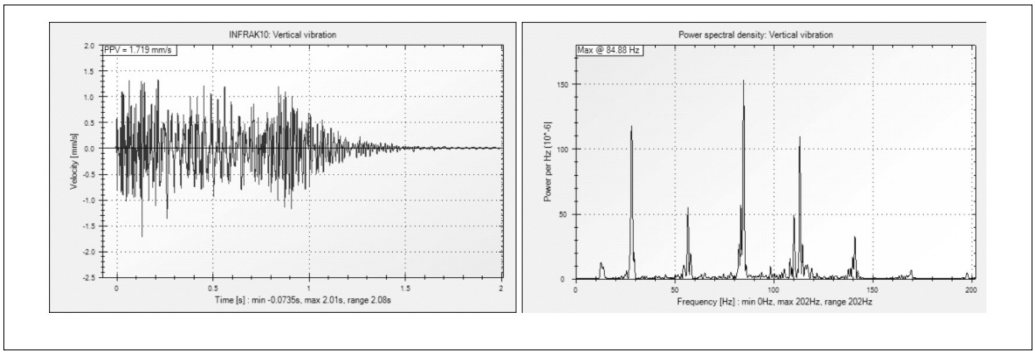

Figure 20. Time curve and frequency analysis, mp 8 calibration found 3. v_{max} = 1.72 mm/s.

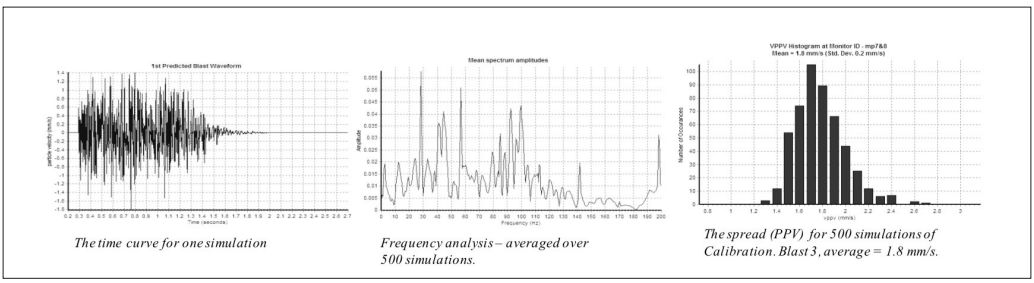

Figure 21. Result from the Monte Carlo model. This data can be compared to actual data in Figure 20.

is adjusted to more 'realistic' conditions.

In the calibrated model all parameters below are used (Table 3) together with the signature wave form (seed wave).

An example is shown below in Figure 19; the example comes from calibration blast 3. All the data necessary to construct the model is supplied by the blast plan (Figure 19), seed wave (Figure 6) and the parameters (Table 3).

The result from the actual blast can be seen in Figure 20; this result can then be compared with a simulated result. Since the model is based upon probabilities the blast is modelled many times and the result is presented as a statistical distribution

The simulation gives a v_{max} distribution but it's also possible to look at the time-curve, the frequency distribution etc., see Figure 21.

5.2 Result - calibration

How well the model fits reality can be evaluated by comparing the monitored vibrations on each point, for each calibration blast, with the simulated results for the same point and blast. Altogether 5 calibration blasts were shot, these blasts were monitored at three buildings, this gave in all 14 data points (one point is missing).

In Figure 22 the calculated value (including one standard deviation) is plotted on the y-axis against the monitored value on the x-axis. Consequently: if the diagonal line in the graph crosses the 'error-bars' for the calculated value, then the outcome of the prediction is within one standard deviation of the simulated value.

Figure 22 compares monitored values (x-axis) with calculated (y-axis). '●' symbols are Nonel blasts and '■' are from i-kon. The error bars indicates the calculated +/- one standard deviation.

Since (purely statistically) 68 % of the events should be within one standard deviation the model seems to work fine. In the figure we can see that 4 out of 14 calculations are more then one standard deviation away (29%), consequently 71 % of the observations are within one standard deviation.

Now a functioning model of the area has been established and consequently the same model can be used to test the effect of different actions in order to decide the optimal way to excavate the area.

6. USING THE MODEL

What we need to evaluate is how large the effect different actions will have for the outcome. In the

following text we will for this purpose focus on the most critical point which is mp 7&8.

6.1 Delay times

The impact of different delay times can be seen in Figure 23. In a test calibration blast 3 was simulated with delay times between 1 and 50 ms (the charges in the simulation were smaller than in the actual blast). The graph shows that 35 ms is the shortest time where an average below 1.5 mm/s can be expected, we can also see that more than 11 ms delay is required to stay below 2 mm/s in average $v_{max.}$

6.2 Direction of excavation

The direction of blasting has an impact on the result, how large this impact is was tested below. In the first example the blast was made along the border of the project area (Figure 24) while in the other simulation, the blast was turned into 90° from the same border (Figure 25), this manoeuvre lets us examine the effect of screening.

In the first blast there is no screening effect while in the second simulation the closest hole detonates first and hence creates a zone of damaged rock in front of the other holes, which transmits vibrations to a lesser extent. In the simulation we detonate the holes fully charged and then we can compare the results, 35 ms delay time was used.

The result shows that the vibrations become considerably less if we blast in a direction away from that monitoring point. Regarding the goal to stay below 4 mm/s we can see that there is a problem; the probability of exceeding 4 mm/s is 100% for blast direction 1 (Figure 26) and by changing it to direction 2 we reduce the same probability to 70% (Figure 27), nowhere near what has to be achieved.

Since the delay time and direction of excavation must be seen as optimized at this stage there are two other parameters that can be changed in order to decrease the vibration level. Either we decrease the charge or we increase the distance.

In order to decide the minimum distance we need in order to use fully charged holes we have to move the blast towards the west until we can fire it and be more than 90 % confident of being below 4 mm/s.

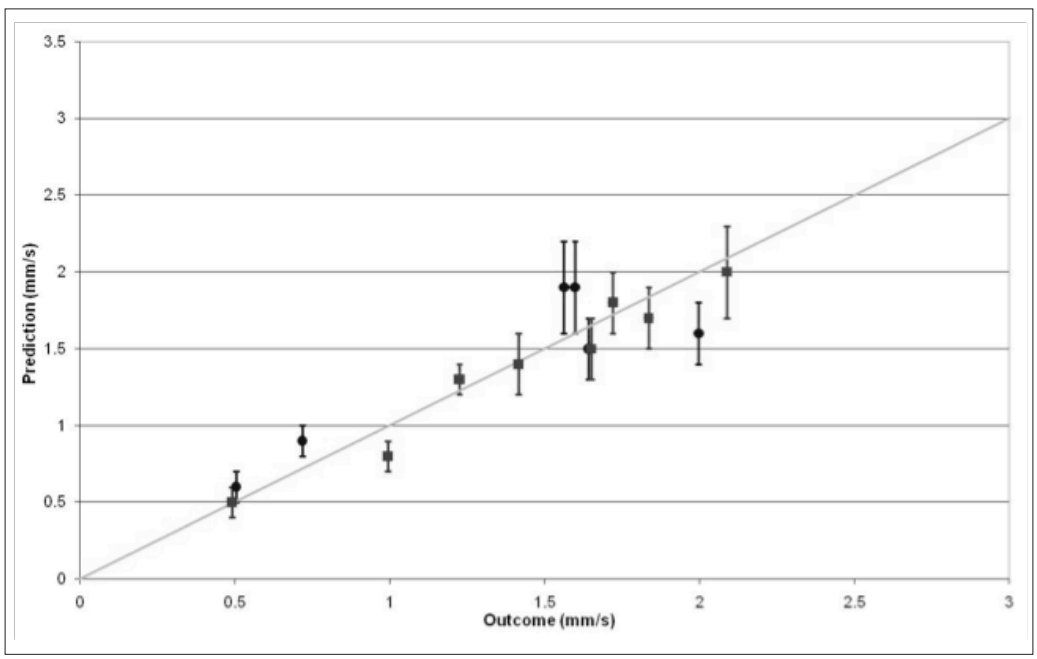

Figure 22. Results from the calibration blasts

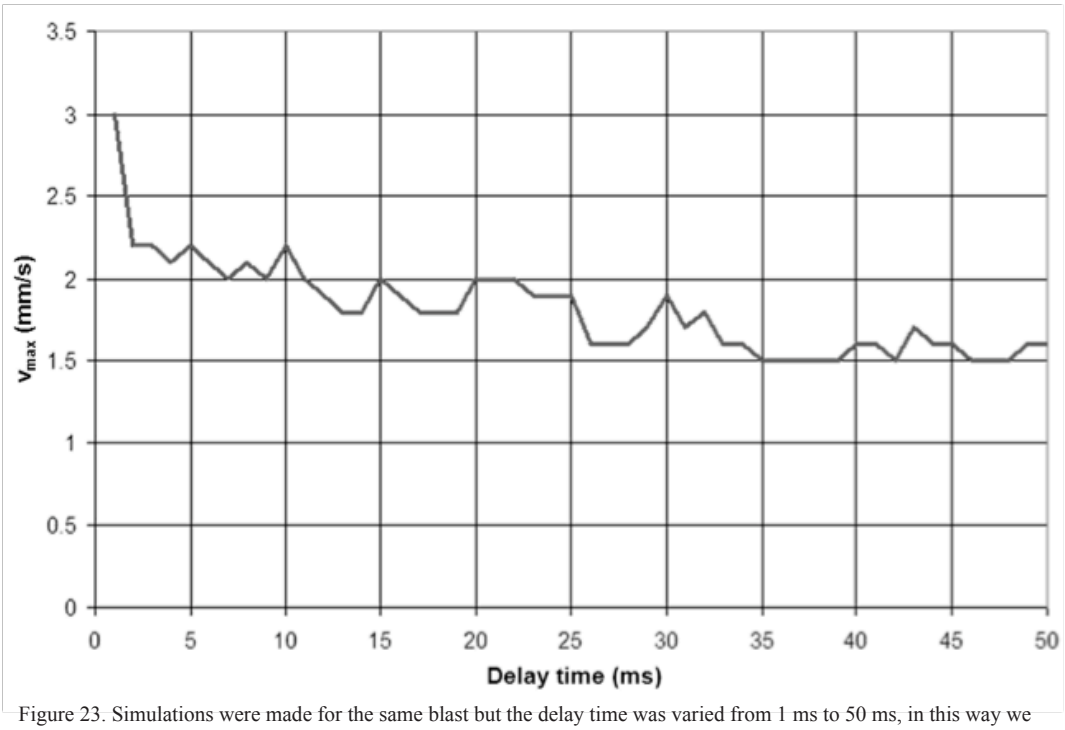

Figure 23. Simulations were made for the same blast but the delay time was varied from 1 ms to 50 ms, in this way we can search for optimal delay times.

Figure 24. Simulation excavation direction 1, distance from blast to mp 7 & 8 ca 215 m.

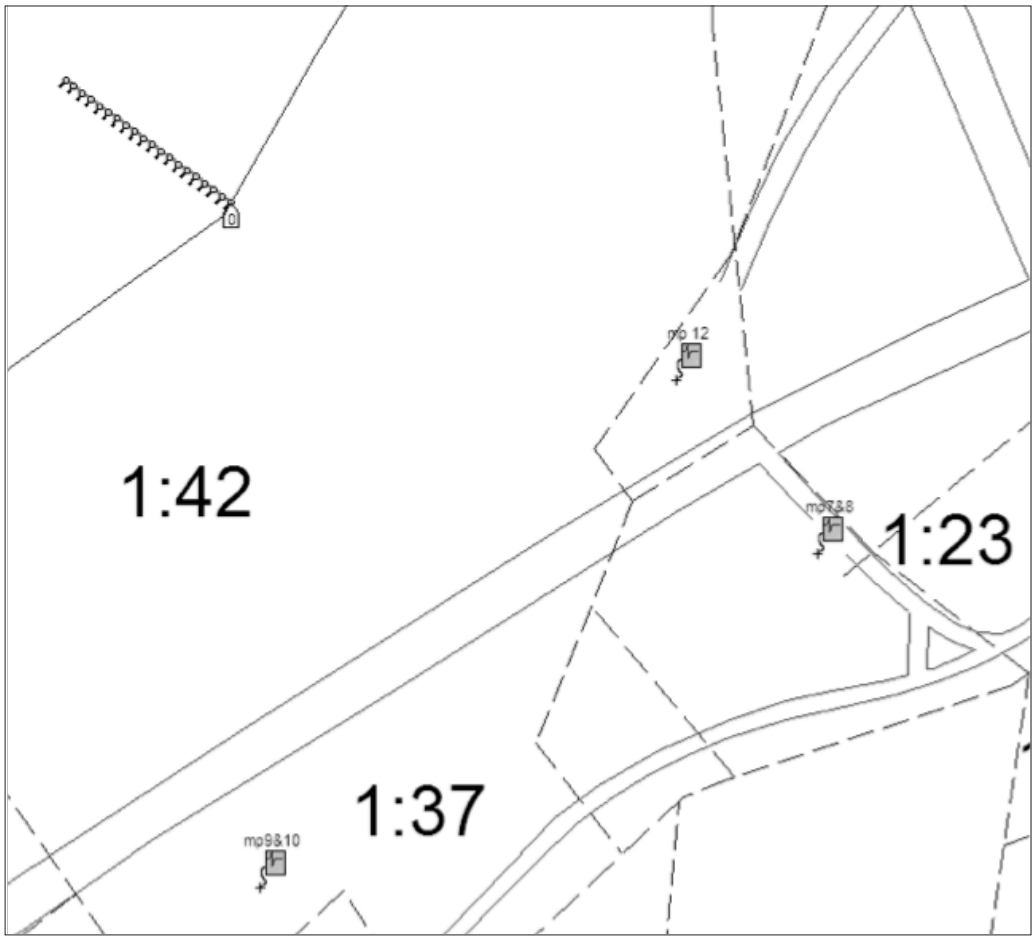

Figure 25. Simulation excavation direction 2, distance from blast to mp 7 & 8 ca 215 m.

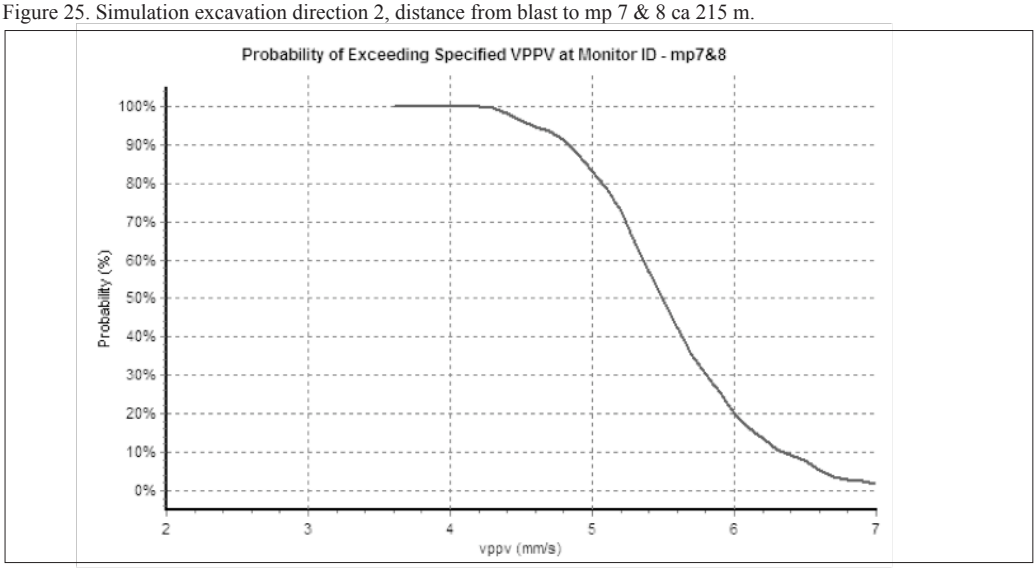

Figure 26. Blasting direction 1, probability of exceeding 4 mm/s is 100%, average value 5.5 mm/s.

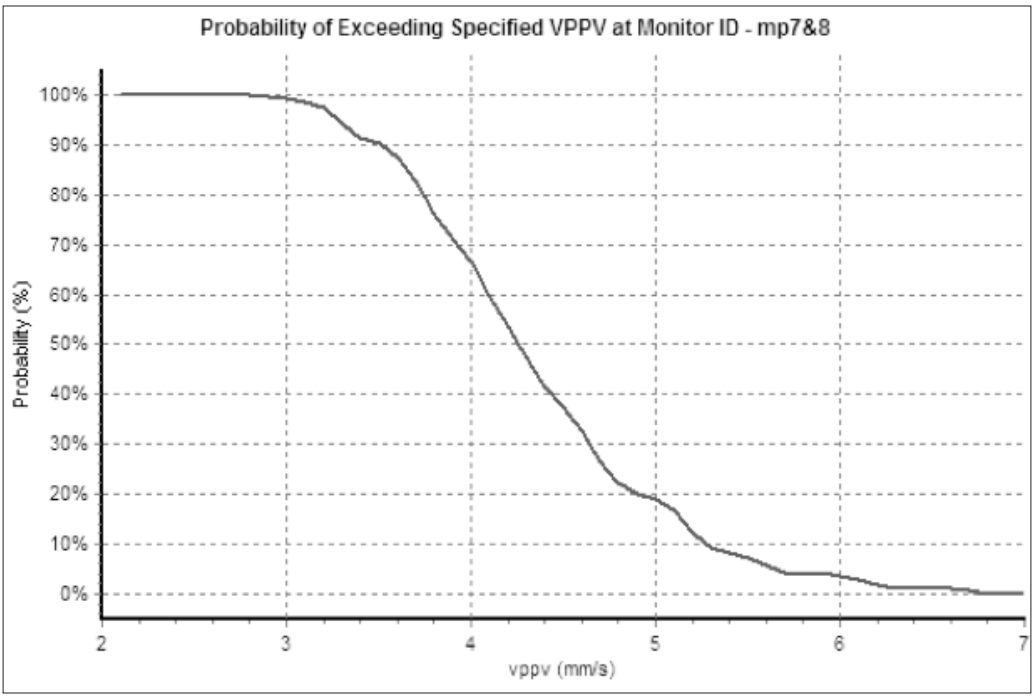

Figure 27. Blasting direction 2, probability of exceeding 4 mm/s is 70%, average value 4.3 mm/s

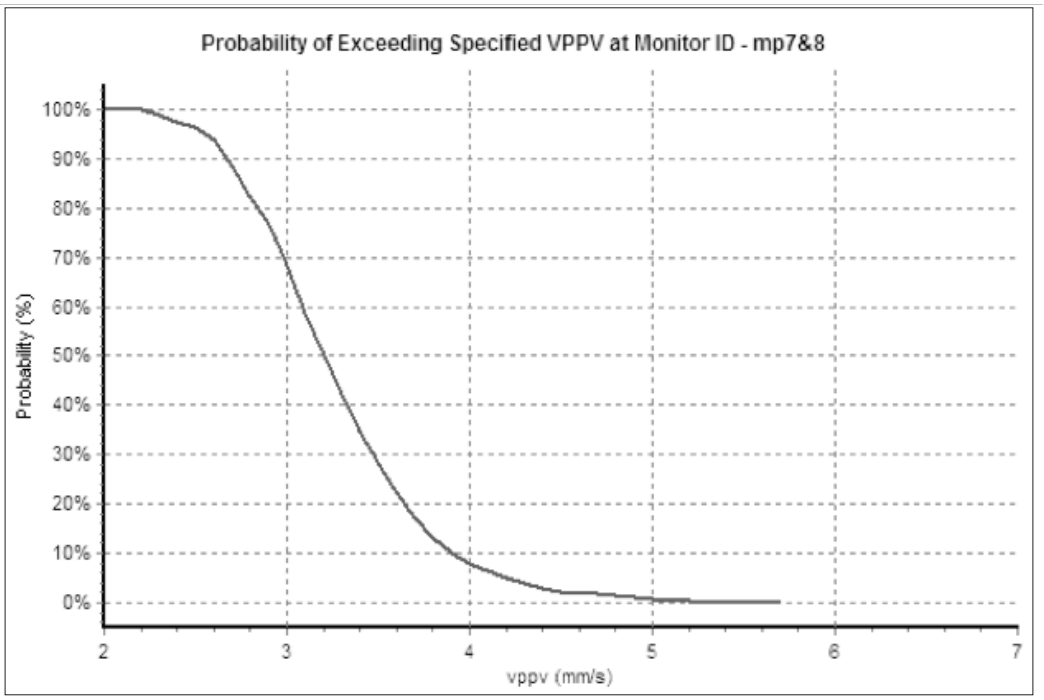

Figure 28. Mp 7&8, 255m distance. Probability to be above 4 mm/s is 8 %, average value is 3.2 mm/s.

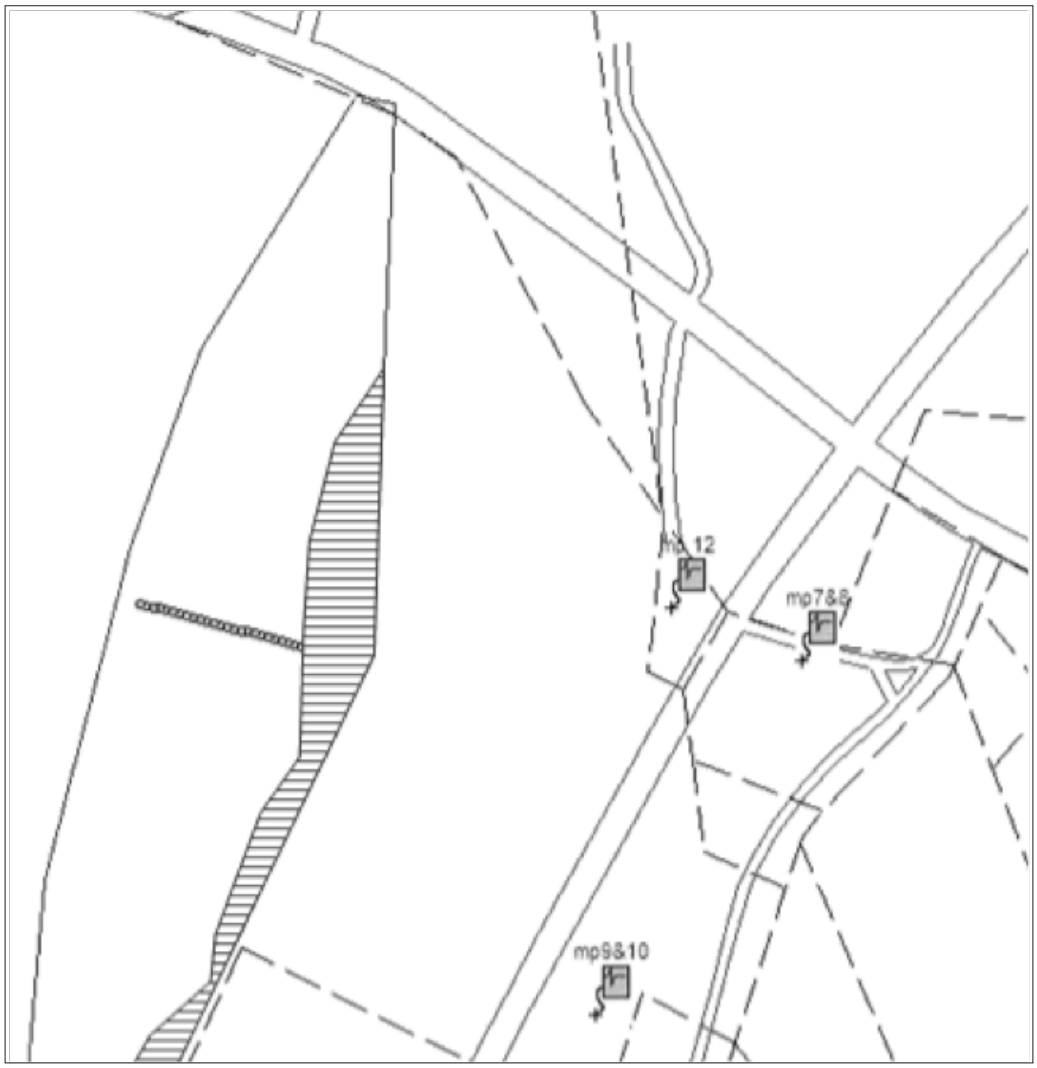

Figure 29. The patterned area shows the part of the project area where it will be problematic to stay below 4 mm/s.

6.3 Smallest distance

The result from a test to evaluate the smallest distance where it's possible to fire blasts with fully charged holes and still stay below 4 mm/s can be seen in Figure 28. If the distance is increased to 255 m the risk of going above 4 mm/s is reduced to 8% (figure 28), this with the condition that the delay times are the same as previously.

The position of this blast can be seen in Figure 29. In the figure is also shown a patterned area. That area is the area that is predicted to be problematic to blast and still keep vibrations below 4 mm/s at surrounding dwellings.

6.4 Initiation system

All the simulations that have been presented previously in this report are simulated for electronic detonators (I-kon). The most common initiation system is however pyrotechnic (Nonel/Excel). An important issue is how big the difference is between the two systems when it comes to vibrations. In Figure 30 the results from a simulation with the Nonel system are shown. The blast is identical with the blast described in Figures 28 and 29. The difference is that instead of I-kon 35 ms we use Nonel 42 ms (and U 475).

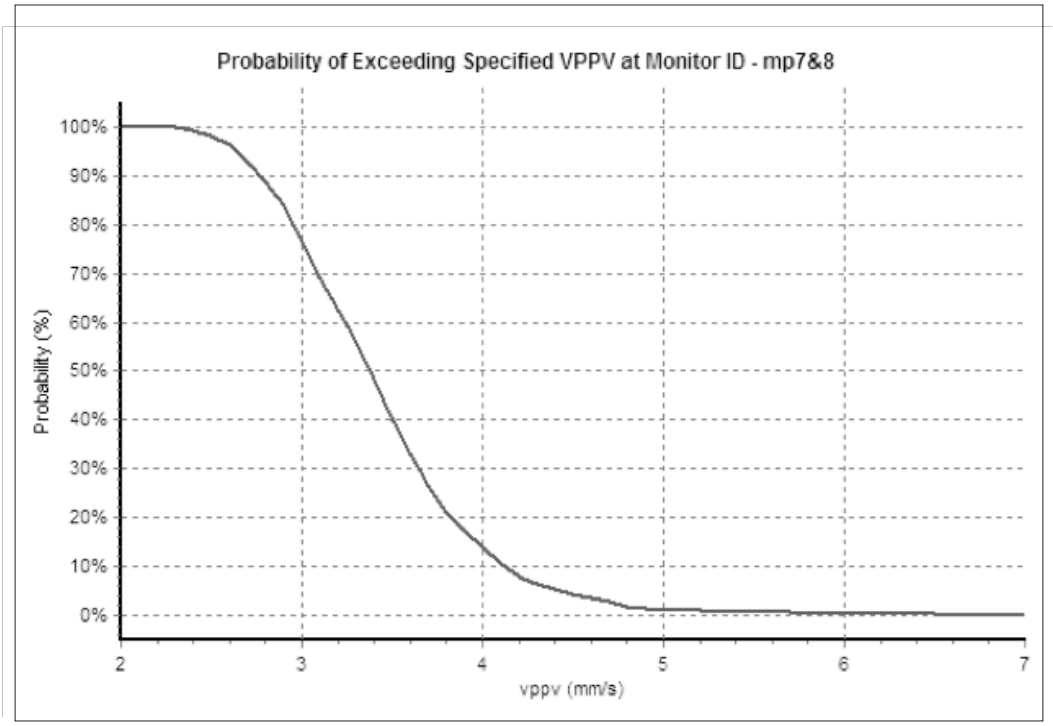

Figure 30. Mp 7 & 8, 255m distance. The risk of exceeding 4 mm/s is 13 %, average value 3.4 mm/s (Nonel detonators).

In a comparison between the I-kon and Nonel blast we can see that in this case the difference is quite small. The vibration level goes up from 3.2 to 3.4 mm/s (average) and the risk of exceeding 4 mm/s increases from 8 % to 13 %. It's unlikely that this improvement will make it meaningful to use electronic detonators in this case. However with larger blasts and more complicated initiation plans the difference between the two systems may justify the use of the I-kon system.

6.5 Decked charges

If it's not possible to move the blast backwards in order to decrease vibration levels the alternative is to reduce the charge weight per delay. This can be achieved by several methods but the method suggested here is by decked charges. The way this method is performed is by dividing the charge in each hole by putting a distance of stemming material in the middle of the hole having charges below and above this stemming (see Figure 31). In this way we divide the charge in the hole into two separate charges which can (if the stemming length is enough) be shot separately.

In order to be successful with decked charges electronic detonators are a necessity; the precision of electronic detonators is highly beneficial in this case.

A blast with decked charges was simulated and is shown in Figure 31. The conclusion is that decking can be a powerful tool to reduce vibrations. In this case we simulate the same blast as was presented in Figure 27 where the risk of exceeding 4 mm/s was 70 %. In the example with decked charges we reduce this risk down to 1 % (Figure 32).

Two of the calibration blasts in this project were shot with decked charges (no 4 and 5). The tests with decked charges were successful in the way that the monitored result was close to that predicted in both blasts.

What generally should be noticed is the importance in keeping a precise delay time between the decks. This is highlighted by modelling which shows that if the delay is increased from 17 ms to 35 ms the mean peak vibration level is reduced from 1.5 mm/s to 1.3 mm/s. This should be compared to the fully charged blast with a calculated vibration level of 1.8 mm/s.

7. THE MONTE CARLO MODEL VS CHARGE WEIGHT SCALING LAW EQUATION

It could also be of interest to examine how the Monte Carlo model relates to the more conventional method to do vibration predictions, i.e. the charge weight scaling law equation achieved from regression analysis. It's important to remember that the Monte Carlo model partly is a regression analysis model. The method has been briefly described earlier in the paper but commonly this part is the only used for predictions.

In order to compare the two methods we can

Figure 31. Deck charging. The bore plan is identical to excavation direction 2 (Figure 25) but the charge is divided into two decks.

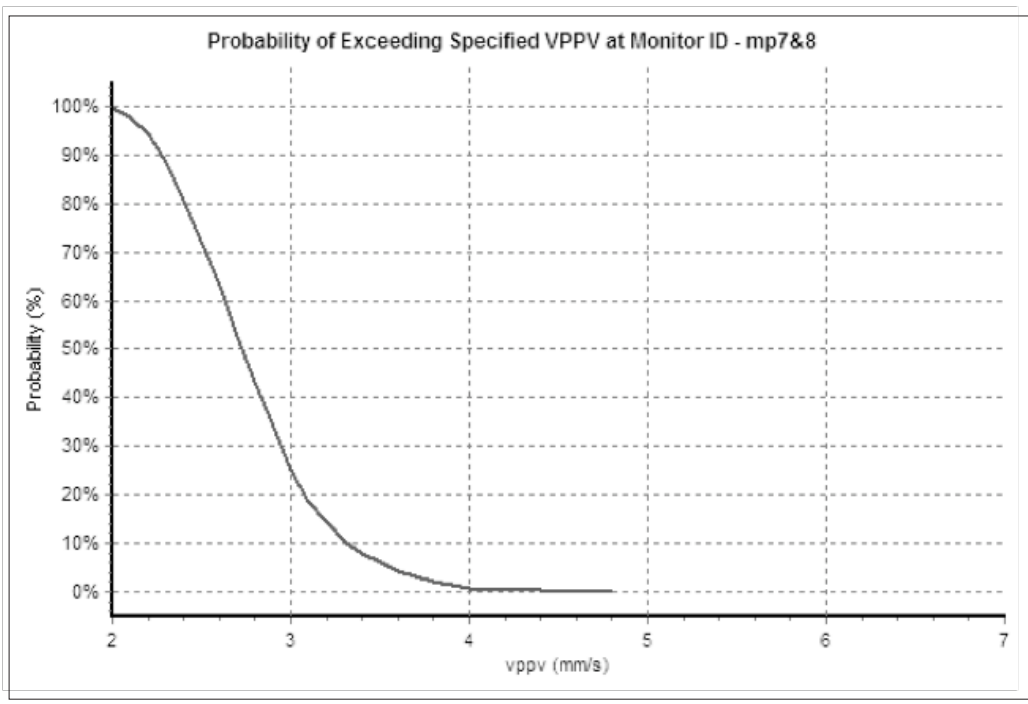

Figure 32. Mp 7and mp 8, approx. 1% risk to be above 4 mm/s. Average value: 2.8 mm/s. Delay times: 70 ms between holes and 35 ms between decks.

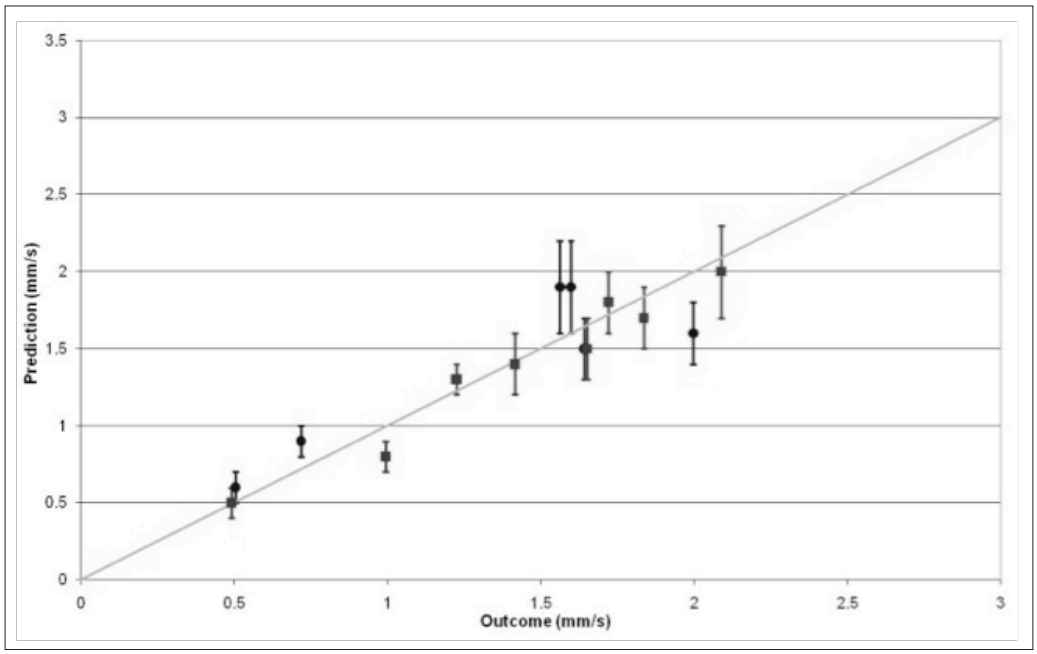

Figure 33. Outcome from the Monte Carlo model.

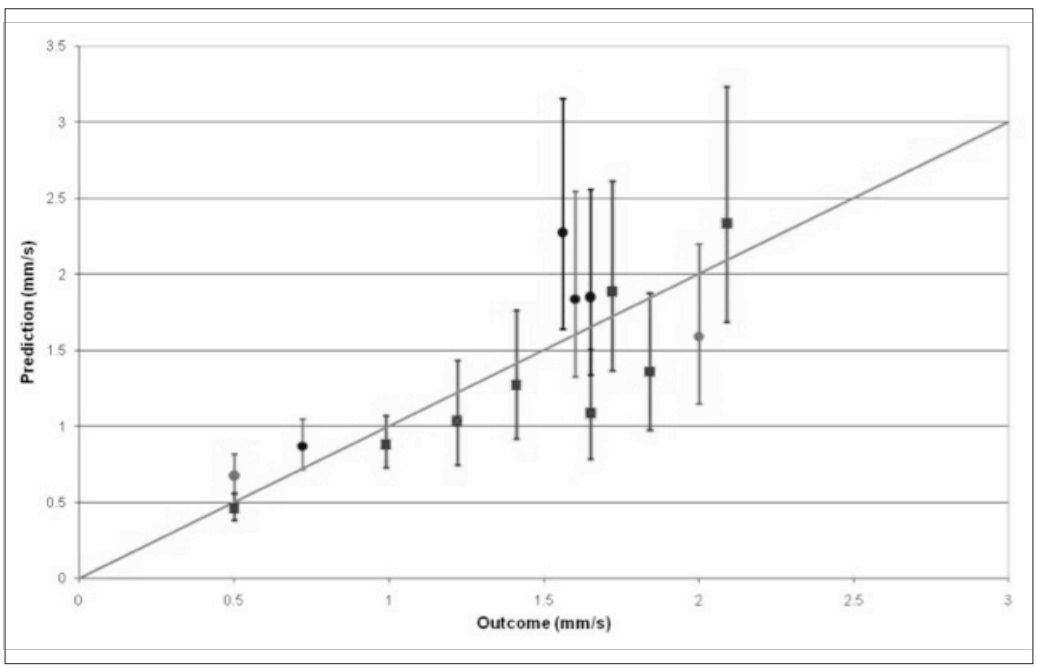

Figure 34. Outcome from the charge weight scaling law equation model only.

plot the result from the regression analysis in the same way as we previously plotted the result from the Monte Carlo model. What can be seen is that both models seem to work fine, below the results are compared, Figures 33 and 34.

However we can see that the calculated uncertainty (standard deviation), is considerably bigger in the charge weight scaling law equation model, this is mainly due to the fact that fewer parameters are calculated compared to the Monte Carlo model, i.e. delay, time, screening, blast design and delay scatter.

8. CONCLUSIONS

The Monte Carlo model has proven to be a powerful tool when it comes to predicting vibrations from blasting.

The model provides an opportunity to model the vibration waveform from blasting, not only regarding charge and distance but also regarding initiation plan, initiation system and screening/ direction of excavation.

When comparing the model to the more conventional method (charge weight scaling law equation only), the model presents a smaller standard deviation in the calculations or more directly written: more accurate vibration predictions.

9. ACKNOWLEDGEMENTS

The author is thankful to Nordkalk AB for the opportunity to publish this material and to Anders Jonsson Nordkalk AB who initiated the project, Niclas Nilsson (Forcit Sverige AB) who acted as project manager for the project and Roger Dahlbeck (Nitro Consult, Gothenburg) who was in charge of the vibration monitoring during the test blast. The group that did the drilling and charging from Nybergs and Orica Mining Services should also be remembered for a project well done. Valuable comments and advice during the project has come from Alex Spathis and Michael Noy, Orica Mining Services, Australia.

REFERENCES

Anderson, D.A. 2008. Signature Hole Blast Vibration Control – Twenty Years Hence and Beyond. *Proc of the annual conf. of Explosives and Blasting Technique.* V 34(2): 27-38.

Blair, D.P. 1999. Statistical models for ground vibration and airblast. *Fragblast, The International Journal for Blasting and Fragmentation,* V 3: 335-364.

Blair, D.P. & Armstrong L.W. 2001. The Influence of Burden on Blast Vibration. *Fragblast, The International Journal for Blasting and Fragmentation.* V 5: 108-129.

Blair, D.P. 2004. Charge Weight Scaling Laws and the Superposition of Blast Vibration Waves. *Fragblast, The International Journal for Blasting and Fragmentation.* V 8: 221 – 239.

Blair, D.P. 2007. Non-Linear superposition models of blast vibration. *Int. J. of Rock Mechanics and Mining Sciences.* V 45: 235-247.

Persson, P-A. , Holmberg, R. & Lee, J. 1993. Rock Blasting and Explosives Engineering. CRC Press.

Spathis , A.T. 2009. A brief review of the measurement, modelling and management of vibrations produced by blasting *Workshop on vibrations from blasting* 12-13 September 2009 Granada, Spain: 1-11.

Swedish Standard SS 460 48 66 Vibration and shock – Guidance levels for blasting induced vibration in buildings (1991).
vibration and airblast. *Fragblast, The International Journal for Blasting and Fragmentation,* V 3: 335-364.

Blair, D.P. & Armstrong L.W. 2001. The Influence of Burden on Blast Vibration. *Fragblast, The International Journal for Blasting and Fragmentation.* V 5: 108-129.

Blair, D.P. 2004. Charge Weight Scaling Laws and the Superposition of Blast Vibration Waves. *Fragblast, The International Journal for Blasting and Fragmentation.* V 8: 221 – 239.

Blair, D.P. 2007. Non-Linear superposition models of blast vibration. *Int. J. of Rock Mechanics and Mining Sciences.* V 45: 235-247.

Persson, P-A. , Holmberg, R. & Lee, J. 1993. Rock Blasting and Explosives Engineering. CRC Press.

Spathis, A.T. 2009. A brief review of the measurement, modelling and management of vibrations produced by blasting *Workshop on vibrations from blasting* 12-13 September 2009 Granada, Spain: 1-11.

Swedish Standard SS 460 48 66 Vibration and shock – Guidance levels for blasting induced vibration in buildings (1991).